CLUSTER ALGEBRAS AND DISCRETE INTEGRABLE SYSTEMS

BY

PANUPONG VICHITKUNAKORN

DISSERTATION

Submitted in partial fulfillment of the requirements
for the degree of Doctor of Philosophy in Mathematics
in the Graduate College of the
University of Illinois at Urbana-Champaign, 2017

Urbana, Illinois

Doctoral Committee:

Associate Professor Maarten Bergvelt, Chair
Professor Rinat Kedem, Director of Research
Professor Philippe Di Francesco, Director of Research
Professor Alexander Yong

Abstract

This dissertation presents connections between cluster algebras and discrete integrable systems, especially T-systems and their specializations/generalizations.

We give connections between the T-system or the octahedron relation, and the pentagram map and its various generalizations. A solution to the T-system with quasi-periodic boundary conditions gives rise to a solution to a higher pentagram map. In order to obtain all the solutions of higher pentagram map, we define T-systems with principal coefficients from cluster algebra aspect. Combinatorial solutions of the T-systems with principal coefficients with respect to any valid initial condition are shown to be partition functions of perfect matchings, non-intersecting paths and networks. This also provides a solution to other systems with various choices of coefficients on T-systems including Speyer's octahedron recurrence (Speyer 2007), generalized lambda-determinants (Di Francesco 2013) and (higher) pentagram maps (Schwartz 1992, Ovsienko et al. 2010, Glick 2011, Gekhtman et al. 2016).

We study a discrete dynamic on weighted bipartite graphs on a torus, analogous to dimer integrable systems of Goncharov and Kenyon 2013. We show that all Hamiltonians, partition functions of all weighted perfect matchings with a common homology class, are invariant under a move on the weighted graph. This move coincides with a cluster mutation, analog to Y-seed mutation in dimer integrable systems. Q-systems are reductions of T-systems by forgetting one of the parameters. We construct graphs for Q-systems of type A and B and show that the Hamiltonians are conserved quantities of the systems. The conserved quantities can be written as partition functions of hard particles on a certain graph. For type A, they Poisson commute under a nondegenerate Poisson bracket.

Acknowledgments

This dissertation would not have been completed without the support of many people. I would like to thank my advisors, Rinat Kedem and Philippe Di Francesco, who provide a lot of guidance and support during the past several years. Also thanks to my committee members, Maarten Bergvelt and Alexander Yong, who offered useful comments. And finally, thanks to my family and friends, who always offer love and support. My research was supported in part by Gertrude and Morris Fine foundation, NSF grants DMS-1301636, DMS-1100929, DMS-1404988, DMS-1643027 and the Institut Henri Poincaré.

Table of Contents

Chapter 1

Introduction

The broad theme of this dissertation lies between cluster algebras and discrete integrable systems, focusing mainly on T-systems and their specializations/generalizations.

A cluster algebra [FZ02] is an algebra over a semifield with a distinguished set of basis. There is a map called a mutation which sends one set of basis to another. By restricting the study to such mutations on the sets of basis, one can consider discrete dynamical systems obtained from a cluster algebra.

A classical Liouville integrable system is a Hamiltonian system on a manifold equipped with a nondegenerate Poisson bracket together with the maximum number (half of the dimension of the phase space) of independent Poisson-commuting functions (see for example [BBT03]). A notion of discrete Liouville integrability was introduced in the context of integrability of a Poisson map [Mae87, Ves91]. A discrete dynamical system is said to be Liouville integrable if the evolution is a Poisson map and there exist the maximum number of independent Poisson-commuting functions invariant under the map (see for example [For14, Section 3]).

There are numerous researches on integrability of discrete dynamical systems obtained from cluster mutations such as the (higher) pentagram maps [OST10, Gli11, GSTV12, GSTV16], Coxeter-Toda flows [GSV11], recurrence relation from periodic quivers [FM11, For11, FH11, FH14], dimer models [GK13, FM16], T-systems, Y-systems and Q-systems [DFK10, HI14, Wil15].

T-systems are recurrence relations which can be realized as mutations in a certain cluster algebra [DFK09]. In various integrable systems obtained from cluster algebras, we notice some connections to T-systems. In particular, in Chapter 2 we study connections between T-systems and (higher) pentagram maps through Y-systems. Conserved quantities of Q-systems, the systems which can be obtained as a specialization of T-systems, are studied in Chapter 4. And we give combinatorial solutions to T-systems with principal coefficients in Chapter 3.

The results in Chapters 2 and 3 are from [KV15] and [Vic16], respectively.

Throughout the text, we use the following notations:

$$[x]_+ = \max(0, x),\ [m, n] = \{m, m+1, \ldots, n\},\ \operatorname{sgn}(x) = \begin{cases} x/|x|, & x \neq 0, \\ 0, & x = 0. \end{cases}$$

1.1 Cluster algebras

In this section, we quote some basic definitions and important results in the theory of cluster algebras mainly from [FZ02, FZ07].

1.1.1 Finite rank cluster algebras

Let $(\mathbb{P}, \oplus, \cdot)$ be a semifield, i.e., $(\mathbb{P}, \cdot)$ is an abelian group, and $\oplus$ is an auxiliary addition: commutative, associative and distributive with respect to the multiplication. The following are two important examples of semifields.

Definition 1.1 (Universal semifield)**.** For a set of labels J, the *universal semifield* on the set of variables $\{y_j \mid j \in J\}$ denoted by $\mathbb{Q}_{sf}(y_j : j \in J) := (\mathbb{Q}_{sf}(y_j : j \in J), +, \cdot)$ is the set of all subtraction-free expressions of rational functions in independent variables $\{y_j \mid j \in J\}$ over $\mathbb{Q}$ with the usual addition and multiplication.

Definition 1.2 (Tropical semifield)**.** For a set of labels J, the *tropical semifield* on the set of variables $\{y_j \mid j \in J\}$ denoted by $\operatorname{Trop}(y_j : j \in J)$ is the free multiplicative abelian group generated by $\{y_j \mid j \in J\}$ with the auxiliary addition defined by:

$$\prod_j y_j^{a_j} \oplus \prod_j y_j^{b_j} = \prod_j y_j^{\min(a_j, b_j)}.$$

Let $n \in \mathbb{N}$, we now state the main definitions of cluster algebras of rank n. Let $\mathbb{P}$ be a semifield, $\mathcal{F} = \mathbb{QP}(x_1, \ldots, x_n)$ an ambient field, $\mathbb{T}_n$ the $n-$regular tree whose n edges incident to each vertex have different labels from 1 to n.

Definition 1.3 (Cluster patterns and Y-patterns)**.** A *cluster pattern* (resp. *Y-pattern*) is an assignment $t \mapsto (\mathbf{x}_t, \mathbf{y}_t, B_t)$ (resp. $t \mapsto (\mathbf{y}_t, B_t)$) of any vertex $t \in \mathbb{T}_n$ to a *labeled seed* (resp. *labeled*

Y-seed) such that:

- The *cluster* tuple $\mathbf{x_t} = (x_{1;t}, \ldots, x_{n;t})$ is an $n-$tuple of elements of $\mathcal{F}$ forming a free generating set.
- The *y-variable* (a.k.a *coefficient*) tuple $\mathbf{y_t} = (y_{1;t}, \ldots, y_{n;t})$ is an $n-$tuple in $\mathbb{P}$.
- The *exchange matrix* $B_t = (b_{ij}^{(t)}) \in M_{n\times n}(\mathbb{Z})$ is a skew-symmetrizable matrix.
- $t \overset{k}{\sim} t'$ in $\mathbb{T}_n$ if and only if $(\mathbf{x}_t, \mathbf{y}_t, B_t) \overset{\mu_k}{\longleftrightarrow} (\mathbf{x}_{t'}, \mathbf{y}_{t'}, B_{t'})$, where μ_k is the *seed mutation* in direction k defined by:
  - $B_{t'} = (b_{ij}^{(t')})$ where

$$b_{ij}^{(t')} = \begin{cases} -b_{ij}^{(t)}, & i = k \text{ or } j = k, \\ b_{ij}^{(t)} + \operatorname{sgn}(b_{ik}^{(t)})[b_{ik}^{(t)} b_{kj}^{(t)}]_+, & \text{otherwise.} \end{cases}$$

  - $\mathbf{y}_{t'} = (y_{1,t'}, \ldots, y_{n,t'})$ where

$$y_{j,t'} = \begin{cases} y_{k,t}^{-1}, & j = k, \\ y_{j,t}(y_{k;t}^{+})^{[b_{kj}^{(t)}]_+}(y_{k;t}^{-})^{-[-b_{kj}^{(t)}]_+}, & j \neq k. \end{cases}$$

  - $\mathbf{x}_{t'} = (x_{1;t'}, \ldots, x_{n;t'})$ where

$$x_{j;t'} = \begin{cases} x_{k,t}^{-1}\left(y_{k;t}^{+}\prod_{i=1}^{n} x_{i;t}^{[b_{ik}^{(t)}]_+} + y_{k;t}^{-}\prod_{i=1}^{n} x_{i;t}^{[-b_{ik}^{(t)}]_+}\right), & j = k, \\ x_{j;t}, & j \neq k, \end{cases}$$

  where $y_{k;t}^{+} = \dfrac{y_{k;t}}{(y_{k;t} \oplus 1)}$ and $y_{k;t}^{-} = \dfrac{1}{(y_{k;t} \oplus 1)}$.

Definition 1.4 (Cluster algebra)**.** The *cluster algebra* $\mathcal{A}$ associated with a cluster pattern $t \mapsto (\mathbf{x}_t, \mathbf{y}_t, B_t)$ for $t \in \mathbb{T}_n$ is defined to be the $\mathbb{ZP}$-algebra generated by all cluster variables, i.e.

$$\mathcal{A} := \mathbb{ZP}[x_{i,t} : t \in \mathbb{T}_n, i \in [1, n]].$$

We will only consider cluster algebras with skew-symmetric exchange matrix. In this case, we can think of the cluster mutation as a combinatorial rule performing on a quiver.

Definition 1.5 (The quiver associated with a skew-symmetric B)**.** When the exchange matrix $B = (b_{ij})_{i,j\in[1,n]}$ is skew-symmetric, we define $\mathcal{Q}_B$, the *quiver* associated with B, to be a directed graph with vertices $1, \ldots, n$. There are b_{ij} arrows from i to j if and only if $b_{ij} > 0$.

All the information of the exchange matrix B, skew-symmetric, is encoded in the quiver $\mathcal{Q}_B$. The mutation μ_k will then act on $\mathcal{Q}_B$ by the following process:

1. For every pair of arrows $i \to k$ and $k \to j$, add an arrow $i \to j$.
2. Reverse all the arrows incident to k.
3. Remove all oriented 2-cycles one by one.

One can easily check that $\mu_k(\mathcal{Q}_B) = \mathcal{Q}_{\mu_k(B)}$. The following is an example of the quiver associated with an exchange matrix and the quiver mutation.

$$\begin{bmatrix} 0 & 1 & 0 & -1 \\ -1 & 0 & 1 & 0 \\ 0 & -1 & 0 & 1 \\ 1 & 0 & -1 & 0 \end{bmatrix} \overset{\mu_1}{\longleftrightarrow} \begin{bmatrix} 0 & -1 & 0 & 1 \\ 1 & 0 & 1 & -1 \\ 0 & -1 & 0 & 1 \\ -1 & 1 & -1 & 0 \end{bmatrix} \overset{\mu_3}{\longleftrightarrow} \begin{bmatrix} 0 & -1 & 0 & 1 \\ 1 & 0 & -1 & 0 \\ 0 & 1 & 0 & -1 \\ -1 & 0 & 1 & 0 \end{bmatrix}$$

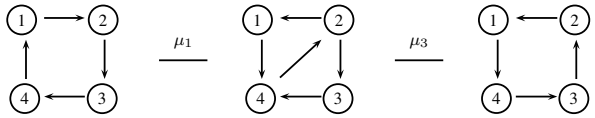

Fixing $t_0 \in \mathbb{T}_n$, we can express variables $x_{1;t}, \ldots, x_{n;t}, y_{1,t}, \ldots, y_{n;t}$ of the labeled seed at arbitrary $t \in \mathbb{T}_n$ in terms of variables $x_{1;t_0}, \ldots, x_{n;t_0}, y_{1,t_0}, \ldots, y_{n;t_0}$ at t_0. We will then call the labeled seed (resp. labeled Y-seed) at t_0 an *initial labeled seed* (resp. *initial labeled Y-seed*) and assign a simpler notations:

$$\mathbf{x} = \mathbf{x}_{t_0},\ \mathbf{y} = \mathbf{y}_{t_0},\ B = B_{t_0}$$

where

$$x_i = x_{i;t_0},\ y_i = y_{i,t_0},\ b_{ij} = b_{ij}^{(t_0)} \quad (i, j \in [1, n]).$$

Unless stated otherwise, the initial labeled seed $(\mathbf{x}, \mathbf{y}, B)$ is always at t_0 and we denote $\mathcal{A}(\mathbf{x}, \mathbf{y}, B)$ the cluster algebra with an initial labeled seed $(\mathbf{x}, \mathbf{y}, B)$. Clearly, a cluster pattern (resp. Y-pattern)

is completely determined by its initial labeled seed (resp. initial labeled Y-seed). In addition, a cluster variable is a Laurent polynomial in the initial variables, as stated in the following theorem.

Theorem 1.6 (Laurent phenomenon [FZ07, Theorem 3.7])**.** *The algebra $\mathcal{A}(\mathbf{x}, \mathbf{y}, B)$ is contained in the Laurent polynomial ring $\mathbb{ZP}[\mathbf{x}^{\pm 1}]$, i.e. every cluster variable is a Laurent polynomial over $\mathbb{ZP}$ in the initial cluster seed $x_1, \ldots, x_n$.*

When $\mathbb{P}$ is trivial, we have $y_{i,t} = 1$ for all $i \in [1, n], t \in \mathbb{T}_n$. We call $\mathcal{A}$ a *coefficient-free* cluster algebra, and write just $(\mathbf{x}_t, B_t)$ for for its labeled seeds.

Definition 1.7 (Frozen variables)**.** For a cluster algebra (resp. cluster pattern) of rank m with initial seed $(\mathbf{x}, \mathbf{y}, B)$, we consider a subpattern $t \in \mathbb{T}_n \subseteq \mathbb{T}_m \mapsto (\mathbf{x}_t, \mathbf{y}_t, B_t)$. It is the pattern obtained by $\mu_1, \ldots, \mu_n$. That means the directions $n+1, \ldots, m$ are not mutated. We call it a cluster algebra (resp. cluster pattern) of rank n with *frozen variables* $x_{n+1}, \ldots, x_m$.

Remark 1.8. In the cluster algebra of rank n with frozen variables $x_{n+1}, \ldots, x_m$, the cluster seeds are not mutated in directions $n+1, \ldots, m$. So, the necessary information in the $m \times m$ matrix B for mutations are only the columns 1 to n. Hence we often use a *reduced exchange matrix* $\tilde{B}$ instead of the full exchange matrix B, where $\tilde{B}$ is the $m \times n$ submatrix of B obtained by deleting columns $n+1$ to m.

Definition 1.9 (Geometric type)**.** A cluster algebra (or cluster pattern, or Y-pattern) is of *geometric type* if $\mathbb{P}$ is a tropical semifield.

Remark 1.10 (Geometric type and Frozen variables)**.** For a cluster algebra or cluster pattern of geometric type, the notion of coefficients and frozen variables are interchangeable. Let $t \in \mathbb{T}_n \mapsto (\mathbf{x}_t, \mathbf{y}_t, B_t)$ be a cluster pattern of geometric type of rank n where $\mathbb{P} = \mathrm{Trop}(x_{n+1}, \ldots, x_m)$. Since $x_{n+1}, \ldots, x_m$ generate $\mathbb{P}$, we can choose the initial seed coefficients to be $y_j = \prod_{i=n+1}^{m} x_i^{b_{ij}}$ for all $j \in [1, n]$. Then the pattern is equivalent to a coefficient-free cluster pattern: $t \in \mathbb{T}_m \mapsto ((x_{1;t}, \ldots, x_{m;t}), \tilde{B}_t)$ with frozen variables $x_{n+1}, \ldots, x_m$, where $\tilde{B} = (b_{ij})_{m \times n}$.

Example 1.11. Consider a semifield $\mathbb{P} = \mathrm{Trop}(x_5, x_6)$ and a rank 4 cluster algebra of geometric type with an initial seed $(\mathbf{x}, \mathbf{y}, B)$ where

$$\mathbf{x} = (x_1, x_2, x_3, x_4), \quad \mathbf{y} = \left(\frac{x_6}{x_5}, \frac{1}{x_6}, 1, 1\right), \quad B = \begin{pmatrix} 0 & 1 & 0 & -1 \\ -1 & 0 & 1 & 0 \\ 0 & -1 & 0 & 1 \\ 1 & 0 & -1 & 0 \end{pmatrix}.$$

We have $y_1^+ = x_6$ and $y_1^- = x_5$. After the seed mutation μ_1 (Definition 1.3), we have

$$\mathbf{x}' = \left(\frac{x_6x_4 + x_5x_2}{x_1}, x_2, x_3, \ldots, x_6\right), \quad \mathbf{y}' = \left(\frac{x_5}{x_2}, 1, 1, \frac{1}{x_5}\right).$$

On the other hand, by Remark 1.10, we can think of x_5, x_6 as frozen variables and transform our cluster algebra with coefficients to the coefficient-free cluster algebra of rank 6 with the following cluster variables and reduced exchange matrix.

$$\mathbf{x} = (x_1, x_2, \ldots, x_6), \quad \tilde{B} = \begin{bmatrix} 0 & 1 & 0 & -1 \\ -1 & 0 & 1 & 0 \\ 0 & -1 & 0 & 1 \\ 1 & 0 & -1 & 0 \\ -1 & 0 & 0 & 0 \\ 1 & -1 & 0 & 0 \end{bmatrix}.$$

The mutation μ_1 gives the new cluster tuple $\mathbf{x}' = \left(\frac{x_4x_6 + x_2x_5}{x_1}, x_2, x_3, \ldots, x_6\right)$ and the following quiver mutation.

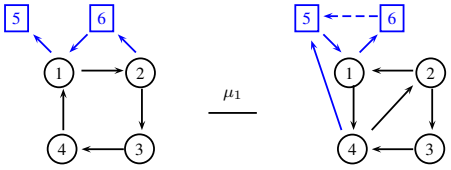

We see that the mutated quiver encodes the information of $\mathbf{y}' = \left(\frac{x_5}{x_2}, 1, 1, \frac{1}{x_5}\right)$. Also notice that we can omit arrows between frozen variables because they will not effect any mutations at non-frozen variables.

Definition 1.12 (Principal coefficient)**.** A cluster algebra (or cluster pattern, or Y-pattern) has a *principal coefficients* at $t_0 \in \mathbb{T}_n$ if $\mathbb{P} = \mathrm{Trop}(y_1, \ldots, y_n)$ where the initial coefficient tuple is $y_{t_0} = (y_1, \ldots, y_n)$. We denote $\mathcal{A}_\bullet(B)$ for the cluster algebra with principal coefficients.

Remark 1.13 (Principal coefficients and Frozen variables)**.** From Remark 1.10, a cluster algebra with principal coefficients of rank n with initial seed $(\mathbf{x}, \mathbf{y}, B)$ where $\mathbf{x} = (x_1, \ldots, x_n)$ and $\mathbf{y} = (y_1, \ldots, y_n)$ can be identified with a coefficient-free cluster algebra of rank $2n$ with an initial seed

$$((x_1, \ldots, x_n, y_1, \ldots, y_n), \tilde{B}) \quad \text{where } \tilde{B} = \begin{bmatrix} B \\ I_n \end{bmatrix}.$$

The quiver $\mathcal{Q}_{\tilde{B}}$ is obtained from $\mathcal{Q}_B$ by adding one vertex i' and an arrow $i' \to i$ for any vertex i in the quiver Q_B. The new $\mathcal{Q}_{\tilde{B}}$ is called the *coframed quiver* associated with $\mathcal{Q}_B$.

Definition 1.14 (The functions $X_{l;t}^{(B)}$ and $F_{l;t}^{(B)}$)**.** Given an exchange matrix B, we consider the unique (up to isomorphism) cluster pattern $t \mapsto (\mathbf{X}_t, \mathbf{Y}_t, B_t)$ with principal coefficients at t_0 and an initial seed $(\mathbf{X}, \mathbf{Y}, B)$. For $l \in [1, n]$ and $t \in \mathbb{T}_n$, we let

$$X_{l;t}^{(B)} \in \mathbb{Q}_{sf}(X_1, \ldots, X_n; Y_1, \ldots, Y_n)$$

be the l-th component of the cluster tuple at t, and

$$F_{l;t}^{(B)} := X_{l;t}^{(B)}(1, \ldots, 1; Y_1, \ldots, Y_n) \in \mathbb{Z}[Y_1, \ldots, Y_n].$$

In short, $X_{l;t}^{(B)}$ is a cluster variable in the cluster algebra with principal coefficients. For a fixed B, we often view it as a function on the initial variables X_i and Y_i for $i \in [1, n]$. The function $F_{l;t}^{(B)}$ is a specialization of $X_{l;t}^{(B)}$ when $X_i = 1$ for $i \in [1, n]$.

The next theorem states that cluster variables of any cluster pattern can be written in terms of the functions $X_{l;t}^{(B)}$ and $F_{l;t}^{(B)}$ with some restriction.

Theorem 1.15 (Separation formula [FZ07, Theorem 3.7])**.** *Let $t \mapsto (\mathbf{x}_t, \mathbf{y}_t, B_t)$ be a cluster pattern over a semifield $\mathbb{P}$ with an initial seed $(\mathbf{x}, \mathbf{y}, B)$. Then*

$$x_{l;t} = \frac{X_{l;t}^{(B)}(x_1, \ldots, x_n; y_1, \ldots, y_n)}{F_{l;t}^{(B)}|_{\mathbb{P}}(y_1, \ldots, y_n)}.$$

The notation $F_{l;t}^{(B)}|_{\mathbb{P}}(y_1, \ldots, y_n)$ means that we compute $F_{l;t}^{(B)}(y_1, \ldots, y_n)$ in $\mathbb{P}$ by changing $+$ to $\oplus$.

Example 1.16. Consider the cluster algebra with principal coefficients with the same exchange matrix as in Example 1.11. Let $\mathbb{P} = \mathrm{Trop}(Y_1, Y_2, Y_3, Y_4)$, we can write an initial seed as $(\mathbf{X}, \mathbf{Y}, B)$ where

$$\mathbf{X} = (X_1, X_2, X_3, X_4), \quad \mathbf{Y} = (Y_1, Y_2, Y_3, Y_4).$$

By Remark 1.13, we think of Y_i's as frozen variables and get a coefficient-free cluster algebra of rank 8 with the following quiver and exchange matrix, where Y_i is the cluster variable on the vertex $i+4$.

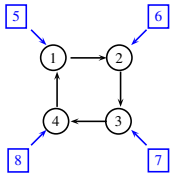

$$\begin{bmatrix} 0 & 1 & 0 & -1 \\ -1 & 0 & 1 & 0 \\ 0 & -1 & 0 & 1 \\ 1 & 0 & -1 & 0 \\ 1 & 0 & 0 & 0 \\ 0 & 1 & 0 & 0 \\ 0 & 0 & 1 & 0 \\ 0 & 0 & 0 & 1 \end{bmatrix}$$

Then the mutation μ_1 gives

$$X_1' = \frac{Y_1X_4 + X_2}{X_1}.$$

Let us try to compute x_1' in Example 1.11 using the separation formula. From the formula, we think of X_1' as a function $(X_1, \ldots, X_4; Y_1, \ldots, Y_4) \mapsto \dfrac{Y_1X_4 + X_2}{X_1}$. Then

$$\begin{aligned} x_1' &= \frac{X_1'\left(x_1, x_2, x_3, x_4; \frac{x_6}{x_5}, \frac{1}{x_6}, 1, 1\right)}{X_1'\left(1,1,1,1; \frac{x_6}{x_5}, \frac{1}{x_6}, 1, 1\right)\big|_{\mathrm{Trop}(x_5,x_6)}} \\ &= \frac{(\frac{x_6}{x_5}x_4 + x_2)/x_1}{(\frac{x_6}{x_5} \oplus 1)/1} = \frac{(\frac{x_6}{x_5}x_4 + x_2)/x_1}{1/x_5} = \frac{x_4x_6 + x_2x_5}{x_1}. \end{aligned}$$

Definition 1.17 (The functions $Y_{l,t}^{(B)}$)**.** Given an exchange matrix B, we consider the unique (up to isomorphism) Y-pattern $t \mapsto (\mathbf{Y}_t, B_t)$ having an initial seed $(\mathbf{Y}, B)$ in the semifield $\mathbb{Q}_{sf}(Y_1, \ldots, Y_n)$. Let $Y_{l;t}^{(B)} \in \mathbb{Q}_{sf}(Y_1, \ldots, Y_n)$ be the l-th component in the coefficient tuple at t.

Again, we think of $Y_{l;t}^{(B)}$ as a function on $Y_1, \ldots, Y_n$. The next theorem gives an expression of the function $Y_{j,t}^{(B)}$ in terms of the polynomials $F_{i,t}^{(B)}$.

Theorem 1.18 ([FZ07, Proposition 3.13])**.** *Given an exchange matrix B and a semifield $\mathbb{P} = \mathrm{Trop}(y_1, \ldots, y_n)$, we get*

$$Y_{j;t}^{(B)}(y_1, \ldots, y_n) = Y_{j;t}^{(B)}\big|_{\mathbb{P}}(y_1, \ldots, y_n) \prod_{i=1}^{n} \left(F_{i;t}^{(B)}(y_1, \ldots, y_n)\right)^{b_{ij}^{(t)}}.$$

where $Y_{j;t}^{(B)}|_{\mathbb{P}}(y_1, \ldots, y_n)$ can be interpreted as a cluster coefficient in the Y-pattern with principal coefficients with an initial coefficient tuple $(y_1, \ldots, y_n)$.

Example 1.19. Consider the Y-pattern with the following quiver and the initial coefficient tuple

(y_1, y_2, y_3, y_4) in $\mathbb{P} = \mathbb{Q}_{sf}(y_1, y_2, y_3, y_4)$.

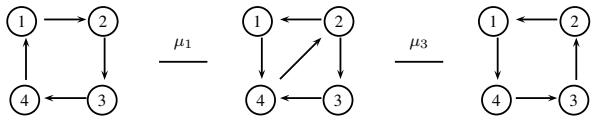

$$\begin{aligned} \mathbf{y} = (y_1,\, y_2,\, y_3,\, y_4) \quad &\underline{\quad\mu_1\quad} \quad \mathbf{y}' = \left(\frac{1}{y_1},\, y_2\frac{y_1}{1+y_1},\, y_3,\, y_4(1+y_1)\right) \\ &\underline{\quad\mu_3\quad} \quad \mathbf{y}'' = \left(\frac{1}{y_1},\, y_2y_1\frac{1+y_3}{1+y_1},\, \frac{1}{y_3},\, y_4y_3\frac{1+y_1}{1+y_3}\right) \end{aligned} \tag{1.1}$$

Consider a different Y-pattern with the same quiver but with principal coefficients. So with the same initial coefficients, we set $\mathbb{P} = \mathrm{Trop}(Y_1, Y_2, Y_3, Y_4)$. Using Remark 1.10, we can realize the coefficients as frozen variables.

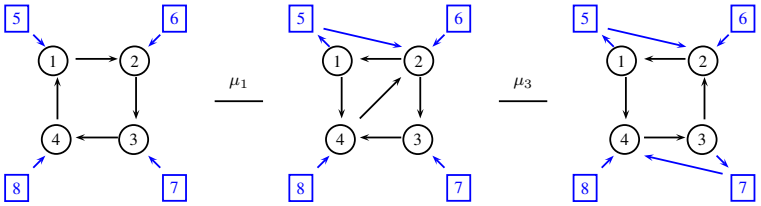

$$\begin{aligned} \mathbf{Y} = (Y_1,\, Y_2,\, Y_3,\, Y_4) \quad &\underline{\quad\mu_1\quad} \quad \mathbf{Y}' = \left(\frac{1}{Y_1},\, Y_2Y_1,\, Y_3,\, Y_4(1+Y_1)\right) \\ &\underline{\quad\mu_3\quad} \quad \mathbf{Y}'' = \left(\frac{1}{Y_1},\, Y_2Y_1,\, \frac{1}{Y_3},\, Y_4Y_3\right). \end{aligned}$$

In order to apply Theorem 1.18, we also need to compute the cluster variables of the cluster algebra with principal coefficients of the same quiver. Let (X_1, X_2, X_3, X_4) be the initial cluster tuple, we then get the following.

$$\begin{aligned} \mathbf{X} = (X_1,\, X_2,\, X_3,\, X_4) \quad &\underline{\quad\mu_1\quad} \quad \mathbf{X}' = \left(\frac{Y_1X_4 + X_2}{X_1},\, X_2,\, X_3,\, X_4\right) \\ &\underline{\quad\mu_3\quad} \quad \mathbf{X}'' = \left(\frac{Y_1X_4 + X_2}{X_1},\, X_2,\, \frac{Y_3X_2 + X_4}{X_3},\, X_4\right) \end{aligned}$$

We consider $\mathbf{Y}_2''$, $\mathbf{X}_1''$ and $\mathbf{X}_3''$ as functions on X_i's and Y_i's. By Theorem 1.18 we have

$$y_2'' = \mathbf{Y}_2''(y_1, y_2, y_3, y_4)\frac{\mathbf{X}_3''(1,1,1,1; y_1, y_2, y_3, y_4)}{\mathbf{X}_1''(1,1,1,1; y_1, y_2, y_3, y_4)} = y_2y_1\frac{y_3+1}{y_1+1}.$$

This is the same result as we computed directly in (1.1).

Definition 1.20 (τ-coordinates [GSV03])**.** Let $(\mathbf{x}, B)$ be a coefficient-free cluster seed. There is a map τ sending $(\mathbf{x}, B)$ to a Y-seed $(\mathbf{y}, B)$ in $\mathbb{Q}_{sf}(y_j : j \in [1, n])$ where

$$y_j := \prod_i x_i^{B_{ij}}.$$

The map τ commutes with the mutations [FZ07, Proposition 3.9]. In particular,

$$\tau(\mu_k(\Sigma)) = \mu_k(\tau(\Sigma)).$$

The mutation on the left of the equation is a cluster mutation, while the mutation on the right is a Y-seed mutation. So τ is extended to a map sending a coefficient-free cluster pattern $t \mapsto (\mathbf{x}_t, B_t)$ to a Y-pattern $t \mapsto (\mathbf{y}_t, B_t)$.

1.1.2 Infinite rank cluster algebras

We define infinite rank cluster algebras in a similar way. The cluster tuple, coefficient tuple and the exchange matrix now are infinite dimensional. For the mutation to make sense, we only need the condition: For each j, $b_{ij} = 0$ for all but finitely many i. If B is also skew-symmetric, this condition is equivalent to saying that an infinite quiver $\mathcal{Q}_B$ has only finitely many arrows incident to each of its non-frozen vertex.

For the cluster pattern, although we think of it as an assignment from the infinite tree $\mathbb{T}$, we usually restrict the study to only those seeds obtainable from the initial seed by finitely many mutations.

1.2 The octahedron relation and T-systems

1.2.1 A bilinear recursion relation

Let T be a function defined on the vertices of the lattice $\mathbb{Z}^3$. The octahedron relation is a recursion relation between the values of the function T on a sublattice of $\mathbb{Z}^3$:

$$T_{i,j,k+1}T_{i,j,k-1} = T_{i,j+1,k}T_{i,j-1,k} + T_{i+1,j,k}T_{i-1,j,k}. \tag{1.2}$$

For each choice of integers (i, j, k), this is a relation between the values of T on the vertices of an octahedron in $\mathbb{Z}^3$ centered at (i, j, k). It relates even and odd vertices in $\mathbb{Z}^3$ separately, that is, those with $i + j + k = 0 \bmod 2$ or $1 \bmod 2$. Without loss of generality, we may concentrate on the sublattice with odd parity.

We consider the octahedron relation to be a discrete evolution. Given a set of initial data on a valid initial data surface $\mathbf{k} = (i, j, k(i, j))$, the function T is determined everywhere else in $\mathbb{Z}^3$. By a valid initial data surface we mean one where $|k(i, j) - k(i \pm 1, j)| = 1$ and $|k(i, j) - k(i, j \pm 1)| = 1$ for all $i, j \in \mathbb{Z}$. An example of a valid initial data surface is $(i, j, i + j + 1 \bmod 2)$.

1.2.2 Cluster algebra structure

All values T are determined by the initial data $T_{i,j,i+j+1 \bmod 2}$ for $i, j \in \mathbb{Z}$. Application of the octahedron relation give all other values of T. If we write $x_{i,j} = T_{i,j,i+j+1 \bmod 2}$ then for each j, k, the mutation

$$\mu_{i,j}(x_{i,j}) = x'_{i,j} = \frac{x_{i,j+1}x_{i,j-1} + x_{i+1,j}x_{i-1,j}}{x_{i,j}}$$

is encoded by the exchange matrix

$$B_{i,j}^{i',j'} = (-1)^{i+j}(\delta_{i,i'}\delta_{j,j'\pm 1} - \delta_{j,j'}\delta_{i,i'\pm 1}). \tag{1.3}$$

We illustrate the quiver associated with the initial exchange matrix B in Figure 1.1.

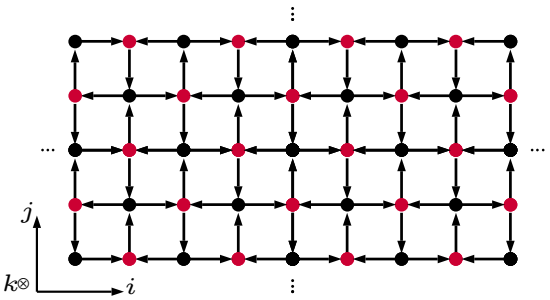

Figure 1.1: The quiver associated with the exchange matrix B of the octahedron relation for the initial data $T_{i,j,i+j+1 \bmod 2}$. The red dots correspond to the $k = 0$ plane and the black ones to the $k = 1$ plane. The quiver is infinite in the i and j directions.

All this just means that the octahedron relation is written as

$$x'_{i,j}x_{i,j} = \prod_{i',j'} x_{i',j'}^{[B_{i,j}^{i',j'}]_+} + \prod_{i',j'} x_{i',j'}^{[-B_{i,j}^{i',j'}]_+},$$

where $[n]_+$ is the positive part of n. We interpret the new variable $x'_{i,j}$ to be $T_{i,j,2}$ if $i + j$ is odd, or $T_{i,j,-1}$ if $i + j$ is even.

The theorem [DFK09] is as follows:

Theorem 1.21. *The octahedron relations are mutations in a cluster algebra which contains the initial cluster consisting of the cluster variables* $\{T_{i,j,i+j+1 \bmod 2} : i, j \in \mathbb{Z}\}$ *and the exchange matrix* B *of Equation* (1.3).

The subset of mutations among all cluster algebra mutations which correspond to one of the octahedron relations correspond to a mutation at a vertex of the quiver which has two incoming and two outgoing arrows. Mutations of the quiver itself create other types of vertices but repeated applications of the octahedron relations locally restore the original quiver.

1.3 Q-systems

1.3.1 Recursion relations

Q-systems first appeared in an analysis of Bethe ansatz of generalized Heisenberg spin chains. They were first introduced in [KR87] for the classical algebras and later generalized for exceptional algebras [HKO$^+$99], twisted quantum affine algebras [HKO$^+$02] and double affine algebras [Her10].

We refer to [KNS11] for a review on the subject. A normalized version of Q-systems has been studied in [Ked08, DFK09], and we will use it as the definition of the *Q-systems*.

Let $\mathfrak{g}$ be a simple Lie algebra with Cartan matrix C. We denote a simple root α by its corresponding integer in $[1, r]$. The Q-system associated with $\mathfrak{g}$ is defined to be the following recurrence relation on a set of variables $\{Q_{\alpha,k} \mid \alpha \in [1, r], k \in \mathbb{Z}\}$:

$$Q_{\alpha,k+1}Q_{\alpha,k-1} = Q_{\alpha,k}^2 + \prod_{\beta \sim \alpha} \prod_{i=0}^{|C_{\alpha,b}|-1} Q_{\beta,\left\lfloor \frac{t_\beta k+i}{t_\alpha} \right\rfloor}, \tag{1.4}$$

where t_α are the integers which symmetrize the Cartan matrix. That is, $t_r = 2$ for B_r, $t_\alpha = 2\,(\alpha < r)$ for C_r, $t_3 = t_4 = 2$ for F_4, $t_2 = 3$ for G_2, and $t_\alpha = 1$ otherwise.

We note that the *T-system* associated with a simple Lie algebra $\mathfrak{g}$ can be defined in a similar manner to (1.4):

$$T_{\alpha,j,k+1}T_{\alpha,j,k-1} = T_{\alpha,j+1,k}T_{\alpha,j-1,k} + \prod_{\beta \sim \alpha} \prod_{i=0}^{|C_{\alpha,b}|-1} T_{\beta,j,\left\lfloor \frac{t_\beta k+i}{t_\alpha} \right\rfloor}. \tag{1.5}$$

We refer the reader to [KNS11] for the details. We see that the octahedron recurrence (1.2) can be thought as the limit of A_r T-systems as $r \to \infty$. It is also called the *A_∞ T-system* [DFK13]. The Q-systems associated with $\mathfrak{g}$ can be also viewed as a specialization of the T-system associated with $\mathfrak{g}$ by ignoring the parameter j.

The Q-system recursions (1.4) for type A and B explicitly read:

$$A_r: \quad Q_{\alpha,k+1}Q_{\alpha,k-1} = Q_{\alpha,k}^2 + Q_{\alpha+1,k}Q_{\alpha-1,k} \quad (\alpha = 1, \dots, r), \tag{1.6}$$

$$Q_{\alpha,k+1}Q_{\alpha,k-1} = Q_{\alpha,k}^2 + Q_{\alpha+1,k}Q_{\alpha-1,k} \quad (\alpha = 1, \dots, r-2),$$

$$B_r: \quad Q_{r-1,k+1}Q_{r-1,k-1} = Q_{r-1,k}^2 + Q_{r-2,k}Q_{r,2k}, \tag{1.7}$$

$$Q_{r,k+1}Q_{r,k-1} = Q_{r,k}^2 + Q_{r-1,\lfloor \frac{k}{2} \rfloor}Q_{r-1,\lfloor \frac{k+1}{2} \rfloor},$$

with boundary conditions $Q_{0,k} = Q_{r+1,k} = 1$ for $k \in \mathbb{Z}$.

Given a valid set of initial values $\{Q_{\alpha,0} = q_{\alpha,0}, Q_{\alpha,1} = q_{\alpha,1} \mid \alpha \in [1, r]\}$ for $q_{\alpha,0}, q_{\alpha,1} \in \mathbb{C}^*$, we can solve for $Q_{\alpha,k}$ which satisfies the Q-system for any $\alpha \in [1, r]$ and $k \in \mathbb{Z}$ in terms of the initial values. So Q-systems can be interpreted a discrete dynamical system on the phase space

$\mathcal{X} = (\mathbb{C}^*)^{2r}$ where the (forward) evolution is

$$\begin{aligned}\varphi : (Q_{1,t_1k}, \dots, Q_{r,t_rk}, Q_{1,t_1k+1}, \dots, Q_{r,t_rk+1}) \\ \mapsto (Q_{1,t_1k+t_1}, \dots, Q_{r,t_rk+t_r}, Q_{1,t_1k+t_1+1}, \dots, Q_{r,t_rk+t_r+1}).\end{aligned}$$

A *conserved quantity* of a discrete dynamical system is a function $H : \mathcal{X} \to \mathbb{C}$ on the phase space $\mathcal{X}$ which is invariant under the evolution of the system. So a conserved quantity for a Q-system is a function H such that

$$\varphi^* H = H.$$

In Chapter 4, we will compute conserved quantities of the Q-systems of type A and B.

1.3.2 Cluster algebra structure

We review the results of [Ked08, DFK09] on the formulations of Q-systems as cluster mutations for simple Lie algebras.

Theorem 1.22 ([DFK09, Theorem 3.1])**.** *Let C be the Cartan matrix of an underlying simple Lie algebra. The Q-system relation (1.4) can be realized as cluster mutations. There is a sequence of mutations such that every Q-system variable appears as a cluster variable.*

The sequence of mutations in the theorem is explicitly described in terms of the root system of the underling Lie algebra. We translate it into a sequence of mutation together with relabeling of indices as follows.

Let C be a Cartan matrix of rank r, we let $\Sigma_k := (\mathbf{A}_k, B)$ be cluster seeds of rank $2r$ where

$$B = \begin{bmatrix} C & -C^T \\ -C & 0 \end{bmatrix} \begin{bmatrix} C^T \\ 0 \end{bmatrix}. \tag{1.8}$$

There exists a sequence of mutations μ and a permutation $\sigma \in \mathfrak{S}_{2r}$ such that

$$\cdots \xleftarrow{\sigma\mu} \Sigma_2 \xleftarrow{\sigma\mu} \Sigma_1 \xleftarrow{\sigma\mu} \Sigma_0 \xleftarrow{\sigma\mu} \cdots \tag{1.9}$$

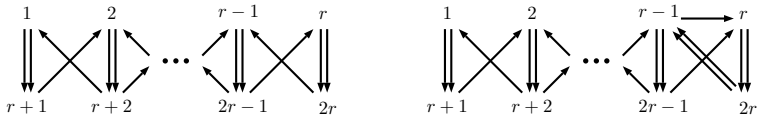

Figure 1.2: The quivers for A_r Q-system (left) and B_r Q-system (right).

The cluster tuple $\mathbf{A}_k$, the permutation σ and the sequence of mutations μ are defined according to the type of the Cartan matrix C. The following are their definitions for type A and B.

- For type A_r we have $\mu := \prod_{i=1}^{r} \mu_i$,

$$A_{i,k} := \begin{cases} Q_{i,k}, & i \in [1, r], \\ Q_{i-r,k+1}, & i \in [r+1, 2r], \end{cases} \qquad \sigma(i) := i + r \bmod 2r. \tag{1.10}$$

- For type B_r we have $\mu := \mu_{2r}(\prod_{i=1}^{r-1} \mu_i)\mu_r$,

$$A_{i,k} := \begin{cases} Q_{i,k}, & i \in [1, r-1], \\ Q_{r,2k}, & i = r, \\ Q_{i-r,k+1}, & i \in [r+1, 2r-1], \\ Q_{r,2k+1}, & i = 2r, \end{cases} \qquad \sigma(i) := \begin{cases} i, & i = r \text{ or } 2r, \\ i + r \bmod 2r, & \text{otherwise.} \end{cases} \tag{1.11}$$

The quivers associated to the matrices B for type A and B are shown in Figure 1.2. We also note that the mutations μ_i in the product $\prod_i \mu_i$ in equations (1.10) and (1.11) commute, so the product makes sense.

Chapter 2

T-systems and the pentagram map

2.1 Introduction

The material in this chapter is a joint work with Rinat Kedem and has been published under the title "T-systems and the pentagram map" in *J. Geom. Phys.*, 87:233–247, 2015.

The purpose of this chapter is to summarize two connections between (generalized) pentagram maps and the octahedron relation with special boundary conditions, also known as the T-system. The first connection is essentially the one found by Glick [Gli11] and by Gekhtman et. al. [GSTV12, GSTV16] in the two-dimensional case, and we clarify here the exact relation between the variables of octahedron relation and the various coordinates used in describing the pentagram maps. Essentially the pentagram map is the Y-system corresponding to the usual octahedron relation with initial conditions wrapped on a torus. We show how to unfold the Y-system so that the result is a quasi-periodic T-system on the same torus. The discrete dynamics of the pentagram map is inherited from the usual octahedron map.

The second connection to T-systems is related to the Zamolodchikov (quasi-) periodicity phenomenon for the A_d T-systems. It relates the solutions of the T-system exhibiting the Zamolodchikov periodicity phenomenon to the lift of the projective coordinates of the polyhedron in projective d-space. It gives a new interpretation to the coefficients appearing in the linear recursion relation satisfied by the lifted coordinates in terms of generalized q-characters of $U_q(\widehat{\mathfrak{sl}}_{d+1})$.

The chapter is organized as follows. In Section 2.2, we recall the octahedron relation (the T-system with no boundary conditions) and the solutions using networks found in [DFK13]. In Section 2.3 we introduce the generalized pentagram maps [GSTV12, GSTV16] and show how this map is related to the octahedron relation with quasi-periodic initial data, or its related Y-system with initial data wrapped on a torus. We also introduce the linear recursion relation satisfied by

the lifted coordinates of the n-gon in projective d-space. In Section 2.4, we return to this linear recursion relation, and relate its coefficients as conserved quantities of the A-type T-system with wall type boundary conditions. Periodicity of the coefficients is a direct result of Zamolodchikov periodicity.

2.2 Octahedron relation and T-systems

Recall the definition and results on octahedron relations from Section 1.2. In this section we review a solution of the octahedron relations via network matrices from [DF13]. We also discuss the Y-system associated to the octahedron relation. The connection between the Y-systems and the higher pentagram maps will be discussed in Section 2.3.

2.2.1 Solutions of the octahedron relations via network matrices

Solving the octahedron relation means providing an explicit expression for any variable $T_{i',j',k}$ (assume without loss of generality that $i'+j'+k \equiv 1 \bmod 2$) in terms of the variables of the initial data $\mathbf{x}_0 = \{T_{i,j,i+j+1 \bmod 2} : i,j \in \mathbb{Z}\}$. In fact, since the octahedron relation is a mutation in a cluster algebra, the solutions are all cluster variables and hence are Laurent polynomials (instead of just rational functions) [FZ02] of a finite subset of the initial data variables in $\mathbf{x}_0$.

Moreover, by explicitly solving the system, we can show that its coefficients are non-negative integers [DFK13], in line with the general positivity conjecture of cluster algebras.

We give an expression for the explicit solution in the particularly simple case we consider here. This version of the solution is found in [DF13] and we do refer the reader to that resource for the details of this solution.

Assume $k > 1$ (for $k < 0$, a symmetric argument holds). Then we can visualize the point i', j', k as a point in a plane above the initial data plane $\{i, j, i+j+1 \bmod 2, i, j \in \mathbb{Z}\}$. The initial data surface is in bijection with a weighted network, whose edge weights are monomials in the initial data, as follows: The edge weights are given in terms of the face variables as follows: The point i, j, k with $i+j+k$ odd is situated above the point $i, j, i+j+1 \bmod 2$ on the initial data plane. Consider a diamond-shaped subset of the initial data plane centered at this point, with sides of length k, and its corresponding weighted network.

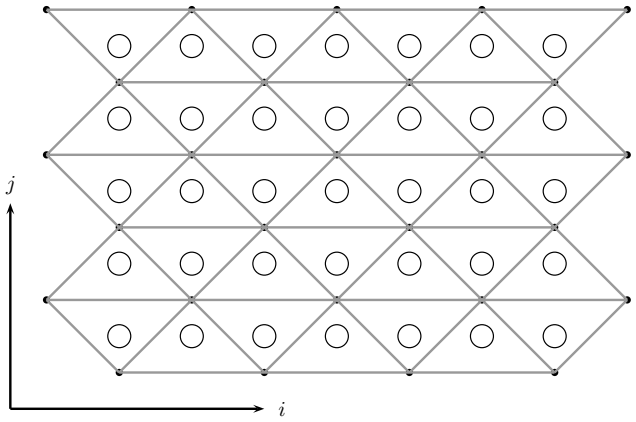

Figure 2.1: The network corresponding to the initial data surface. The initial data $T_{i,j,i+j+1 \bmod 2}$ is situated at the white circles on the lattice faces. The network is the triangular lattice, where all edges are assumed to be oriented from left to right. Its weights are given in terms of the face variables.

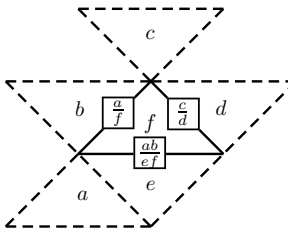

Figure 2.2: The edge weights of the network in terms of the face variables. The variables a, b, c etc. are the initial data $T_{i,j,i+j \bmod 2}$ and the weights are positive Laurent monomials in these variables.

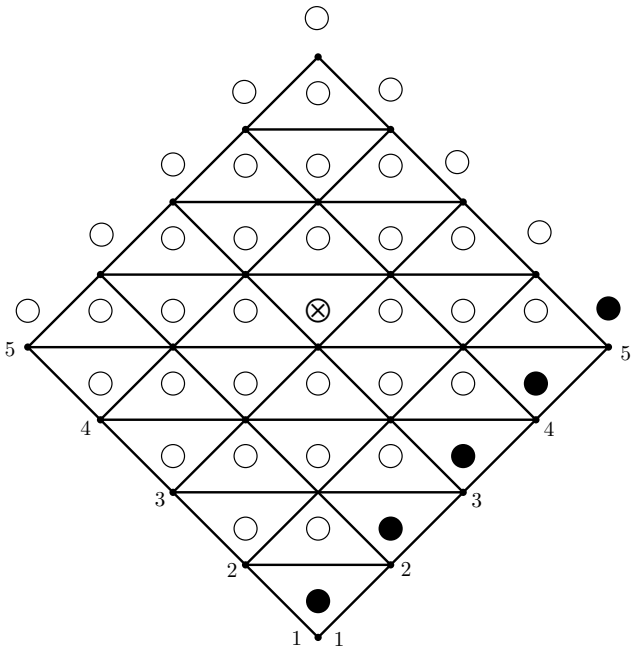

Figure 2.3: The network which contributes to the expression $T_{i,j,5}$ a distance $k = 5$ above the initial data surface. The marked circle at the center is the point i, j on the surface in the i-j-plane.

The network matrix of size $k \times k$, $N_k(i,j)$, is the matrix whose a,b entry is the partition function of paths on the weighted matrix from point a on the left of the network in Figure 2.3 to point b on the right. The determinant of this matrix is the partition function of k non-intersecting paths on the network from the points $(1,...,k)$ on the left to the points $(1,...,k)$ on the right [GV85]. The partition function is just the sum of products of edge weights, hence a positive Laurent polynomial in the initial data.

Finally the variable $T_{i,j,k}$ is the determinant of $N_k(i,j)$, multiplied by the k variables denoted by black dots along the southeast edge of the diamond in Figure 2.3.

2.2.2 Associated Y-system

There is a closely related discrete evolution to the T-system or the octahedron relation called the Y-system. It was originally encountered in the context of thermedynamic Bethe ansatz in the 80's [Zam91] as a relation among the fugacities of quasiparticles in conformal field theories. It can be obtained directly from the T-system as follows [KNS94].

Define the variables

$$Y_{i,j,k} = \frac{T_{i+1,j,k}T_{i-1,j,k}}{T_{i,j+1,k}T_{i,j-1,k}}.$$

Dividing both sides of the octahedron relation (1.2) by $T_{i+1,j,k}T_{i-1,j,k}$ and multiplying the resulting equations for two separate values of (i,j,k), we get a so-called Y-system:

$$Y_{i,j,k+1}Y_{i,j,k-1} = \frac{(1+Y_{i+1,j,k})(1+Y_{i-1,j,k})}{(1+Y^{-1}_{i,j+1,k})(1+Y^{-1}_{i,j-1,k})}. \tag{2.1}$$

Remark 2.1. The original Y-system associated with the Lie algebra A_d has a restricted set of values for i with the appropriate boundary conditions, that is $1 \leq i \leq d$. The system (2.1) is again a recursion relation in $\mathbb{Z}^3$.

The Y-system (2.1) is identified with the mutation relation for *coefficients* (Y-variables in the language of [FZ02] or x-variables in the laguage of [FG06].) The exchange matrix B or the quiver associated with it are the same as for the T-system. The birational expression for Y in terms of the T-variables means that the map between the two sets of variables is not bijective but projective. Therefore, given a Y-system, there are many choices of "unfolding" it back into a T-system. We

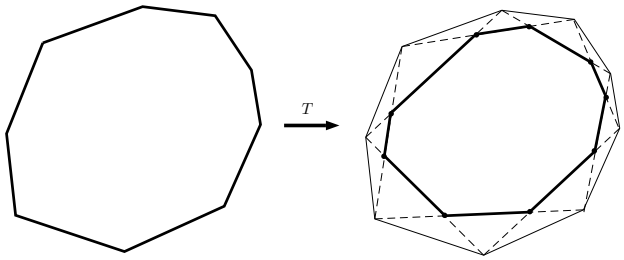

Figure 2.4: The pentagram map on a closed polygon

will give explicit formulas for sufficiently general such unfoldings in Chapter 2.

2.3 The higher pentagram map: coordinates, cluster algebra and Y-system

2.3.1 The (higher) pentagram map

The pentagram map is a discrete evolution equation acting on points in $\mathbb{RP}^2$. In its original version it was introduced by Richard Schwartz in series of papers [Sch92, Sch01, Sch08]. See also [OST10] for a concise review. This map acts on a (twisted) polygon with n vertices to give another twisted n-gon, whose vertices are the intersections of the short diagonals of the original polygon (connecting next-nearest neighbor vertices modulo n). See Fig. 2.4 for an example.

A twisted $n-$gon is a sequence of vertices $(v_i)_{i\in\mathbb{Z}}$ in $\mathbb{RP}^2$ together with a monodromy M, a projective automorphism, such that $v_{i+n} = M \circ v_i$ for all $i \in \mathbb{Z}$. Denote by $\mathcal{P}_n$ the space of projective equivalence classes of twisted $n-$gons, and let $T : \mathcal{P}_n \to \mathcal{P}_n$ denote the pentagram map. The i-th vertex of the image, $T(v_i)$, is then defined to be the intersection of the two diagonals $\overline{v_{i-1}v_{i+1}}$ and $\overline{v_i v_{i+2}}$, i.e.,

$$T(v_i) = \overline{v_{i-1}v_{i+1}} \cap \overline{v_i v_{i+2}}.$$

as in Fig. 2.5.

More recently, Ovsienko, Schwartz and Tabachnikov proved integrability of the pentagram map for the space of twisted polygons [OST10] with the help of a pentagram-invariant Poisson structure, and for the space of closed polygons [OST13].

There also is a sequence of generalizations of the pentagram map in $\mathbb{RP}^2$ called "higher penta-

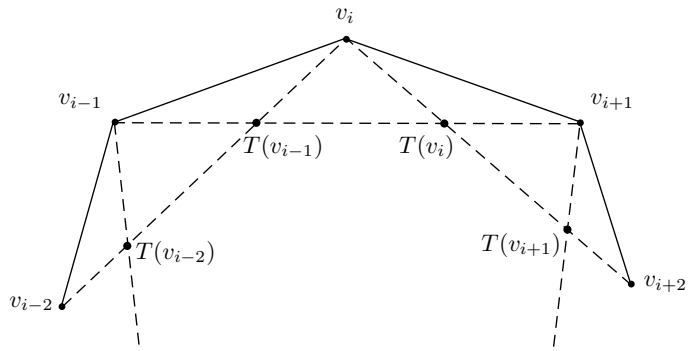

Figure 2.5: The image of v_i under the pentagram map

gram maps" [GSTV12, GSTV16]. This generalization was inspired by the cluster algebra structure of the Schwartz pentagram map, first described by Glick [Gli11]. The higher pentagram maps correspond to using intersections of longer diagonals of the n-gon to map $\mathcal{P}_n$ to itself. For a given integer $\kappa \geq 3$, the generalized pentagram map T_κ constructs a new polygon using $(\kappa-1)^{th}-$diagonals (connecting vertex i to vertex $i+\kappa-1$) instead of the shortest diagonals. Using the Poisson structure compatible with the cluster algebra structure the authors were also able to show the integrability of the higher pentagram maps [GSTV12, GSTV16].

Let us introduce two integers $r = \lfloor \frac{\kappa-2}{2} \rfloor$ and $r' = \lceil \frac{\kappa-2}{2} \rceil$, such that

$$r + r' + 2 = \kappa, \qquad r' = \begin{cases} r & \kappa \text{ even} \\ r+1 & \kappa \text{ odd.} \end{cases}$$

The higher pentagram map can be expressed in terms the projective invariants p, q of the twisted polygon A, defined as follows:

$$\begin{aligned} p_i(A) &= -\chi(v_{i-r'}, \overline{v_{i-r'-1}v_{i+r}} \cap L, L \cap \overline{v_{i-r'+1}v_{i+r+2}}, v_{i+r+1})^{-1}, \\ q_i(A) &= -\chi(\overline{v_{i-\kappa+1}v_{i-\kappa+2}} \cap \overline{v_i v_{i+1}}, v_i, v_{i+1}, \overline{v_i v_{i+1}} \cap \overline{v_{i+\kappa-1}v_{i+\kappa}}) \,. \end{aligned}$$

Here,

$$\chi(a,b,c,d) = \frac{(a-b)(c-d)}{(a-c)(b-d)}.$$

and $L = \overline{v_{i-r'}v_{i+r+1}}$. Note that p_i and q_i are periodic with period n. The higher pentagram

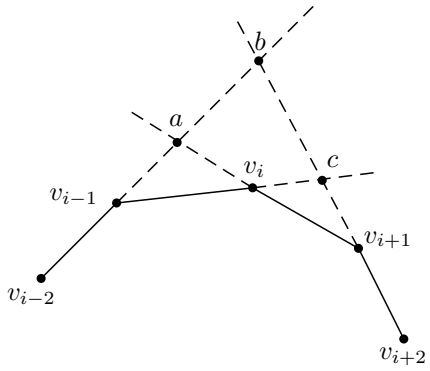

Figure 2.6: Corner invariants: $X_i = \chi(v_{i-2}, v_{i-1}, a, b),\ Y_i = \chi(b, c, v_{i+1}, v_{i+2})$

transformation $A \to T_\kappa(A)$ reads[1]:

$$q_i(T_\kappa(A)) = p_{i+r'-r}(A)^{-1} \qquad p_i(T_\kappa(A)) = q_i(A)\frac{(1+p_{i-r}(A))(1+p_{i+r'}(A))}{(1+p_{i-r-1}(A)^{-1})(1+p_{i+r'+1}(A)^{-1})} \tag{2.3}$$

This map was shown by [OST10, GSTV12, GSTV16, Sol13] to be integrable. In particular, there are two useful conserved quantities:

$$O_n(A) = \prod_{i=1}^{n} p_i(A) \qquad \text{and} \qquad E_n(A) = \prod_{i=1}^{n} q_i(A) \tag{2.4}$$

namely such that $O_n(T_\kappa(A)) = O_n(A)$ and $E_n(T_\kappa(A)) = E_n(A)$.

2.3.2 The Schwartz pentagram map: cluster algebra structure

Note that the transformation (2.3) reduces to the ordinary [Sch92] pentagram map $T \equiv T_3$ of Fig. 2.5 when $\kappa = 3$, i.e. $r = 0$ and $r' = 1$.

In his original construction, Schwartz introduced for any twisted n-gon $A = (v_i)_{i\in\mathbb{Z}}$ a set of

[1]Eq. 2.3 is in fact the inverse of the transformation defined in [GSTV12, GSTV16], up to the interchange of the p and q invariants. The latter reads $(p_i, q_i) \mapsto (p_i^*, q_i^*)$, with:

$$q_i^* = p_{i+r-r'}^{-1} \qquad p_i^* = q_i\frac{(1+p_{i-r'-1})(1+p_{i+r+1})}{(1+p_{i-r'}^{-1})(1+p_{i+r}^{-1})} \tag{2.2}$$

coordinates $(X_i, Y_i)_{i=1}^n$ called *corner invariants*, and defined as:

$$\begin{aligned} X_i(A) &= \chi(v_{i-2}, v_{i-1}, \overline{v_{i-2}v_{i-1}} \cap \overline{v_i v_{i+1}}, \overline{v_{i-2}v_{i-1}} \cap \overline{v_{i+1}v_{i+2}}), \\ Y_i(A) &= \chi(\overline{v_{i-2}v_{i-1}} \cap \overline{v_{i+1}v_{i+2}}, \overline{v_{i-1}v_i} \cap \overline{v_{i+1}v_{i+2}}, v_{i+1}, v_{i+2}). \end{aligned}$$

These are illustrated in Figure 2.6. The corner invariants are related to the p, q invariants via:

$$p_i(A) = -\left(X_i(A)Y_i(A)\right)^{-1}, \quad q_i(A) = -Y_i(A)X_{i+1}(A)\,. \tag{2.5}$$

Now we can formally relate the pentagram map evolution of y-coordinates and the cluster algebra mutation. For a twisted $n-$gon A parameterized by y-parameters $(p_i, q_i)_{i=1}^n$, we define a labeled Y-seed corresponding to A to be $(\mathbf{y}, B)$ where

$$\mathbf{y} = (p_1(A), \ldots, p_n(A), q_1(A), \ldots, q_n(A))\,, \quad B = \begin{pmatrix} \mathbf{0} & C \\ -C^\top & \mathbf{0} \end{pmatrix} \tag{2.6}$$

where $C = (c_{ij})$ is an $n \times n$ matrix defined by $c_{ij} = \delta_{i,j-1} - \delta_{i,j} - \delta_{i,j+1} + \delta_{i,j+2}$ where the indices are read modulo n. Equivalently, the quiver corresponding to the exchange matrix B is a bipartite graph with $2n$ vertices labeled by $p_1, \ldots, p_n, q_1, \ldots, q_n$. There are four arrows adjacent to each q_i: two outgoing arrows from q_i to p_i and p_{i+1}, two incoming arrows from p_{i-1} and p_{i+2} to q_i. See an example in Fig. 2.7.

The pentagram map is then a composition of a sequence of mutations on all the p_i-vertices followed by a relabeling $\{p_i \mapsto q_{i+1}, q_i \mapsto p_i\}$[Gli11]. This maps the coefficients($y-$parameters) $(p_i(A), q_i(A))$ to $(p_i(T(A)), q_i(T(A)))$, and the quiver B to ifself. See an example in Fig. 2.8.

2.3.3 Higher pentagram maps: cluster algebra structure

Similarly to the case $\kappa = 3$, the evolution (2.3) can be identified with a cluster algebra mutation. For a twisted $n-$gon A having $(\mathbf{p}, \mathbf{q})-$parameters $(p_i, q_i)_{i=1}^n$, we define a labeled $Y-$seed corresponding to A to be $(\mathbf{y}, B)$ as in (2.6) except that the matrix $C = (c_{ij})$ is defined to be $c_{ij} = \delta_{i,j-r-1} - \delta_{i,j-r} - \delta_{i,j+r'} + \delta_{i,j+r'+1}$ with indices read modulo n. In other word, the quiver corresponding to the exchange matrix B is a bipartite graph with $2n$ vertices labeled by $p_1, \ldots, p_n, q_1, \ldots, q_n$. There are

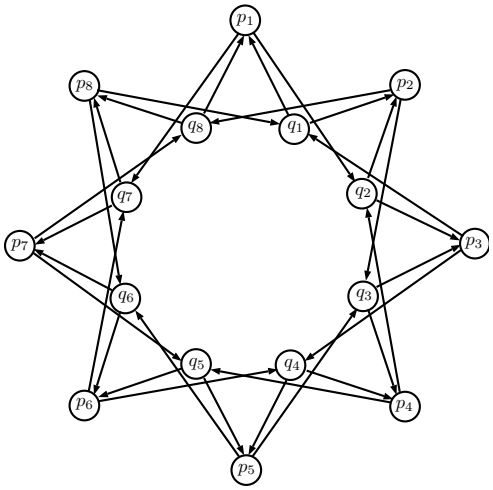

Figure 2.7: Glick's quiver for $n = 8$

four arrows adjacent to each q_i: two outgoing arrows from q_i to p_{i-r} and $p_{i+r'}$, two incoming arrows from p_{i-r-1} and $p_{i+r'+1}$ to q_i. This is called a *generalized Glick's quiver* $\mathcal{Q}_{k,n}$, see Figure 2.9. The higher pentagram map T_κ is then a composition of a sequence of mutations on all the p_i-vertices and a relabeling $\{p_i \mapsto q_{i+r'-r}, q_i \mapsto p_i\}$[GSTV12, GSTV16].

2.3.4 Higher pentagram maps and Y-systems

We now use the wrapping of the generalized Glick's quiver $\mathcal{Q}_{\kappa,n}$ around a torus, interpreted in [DFK13] as the "octahedron" quiver with vertices in $\mathbb{Z}^2$ of Fig. 1.1, and with suitable identification of vertices, along the two periods of the torus: $(i, j) \equiv (i + \kappa, j + 2 - \kappa)$ and $(i, j) \equiv (i + n, j - n)$. We show a sample of such a wrapping in Fig. 2.10 for $\kappa = 3$ and $n = 5$.

Having established this connection, upon carefully comparing the transformation (2.3) with the Y-system evolution (2.1) , it is now easy to interpret the p, q coordinates of the higher pentagram map in terms of Y-system solutions. We arrive at the following:

Proposition 2.2. *Let A be a twisted $n-$gon in $\mathbb{RP}^{\kappa-1}$ with p, q coordinates $(p_i(A), q_i(A))_{i\in[1,n]}$. Let $\{Y_{i,j,k} : i, j, k \in \mathbb{Z}, i + j + k \equiv 0 \bmod 2\}$ be the $Y-$system solution subject to the initial conditions:*

$$\begin{aligned} Y_{i,j,-1} &= \left(q_{(((\kappa-2)i+\kappa j+r-r')/2}(A)\right)^{-1} && (i, j \in \mathbb{Z}; i + j = 1 \bmod 2) \\ Y_{i,j,0} &= p_{((\kappa-2)i+\kappa j)/2}(A) && (i, j \in \mathbb{Z}; i + j = 0 \bmod 2), \end{aligned} \tag{2.7}$$

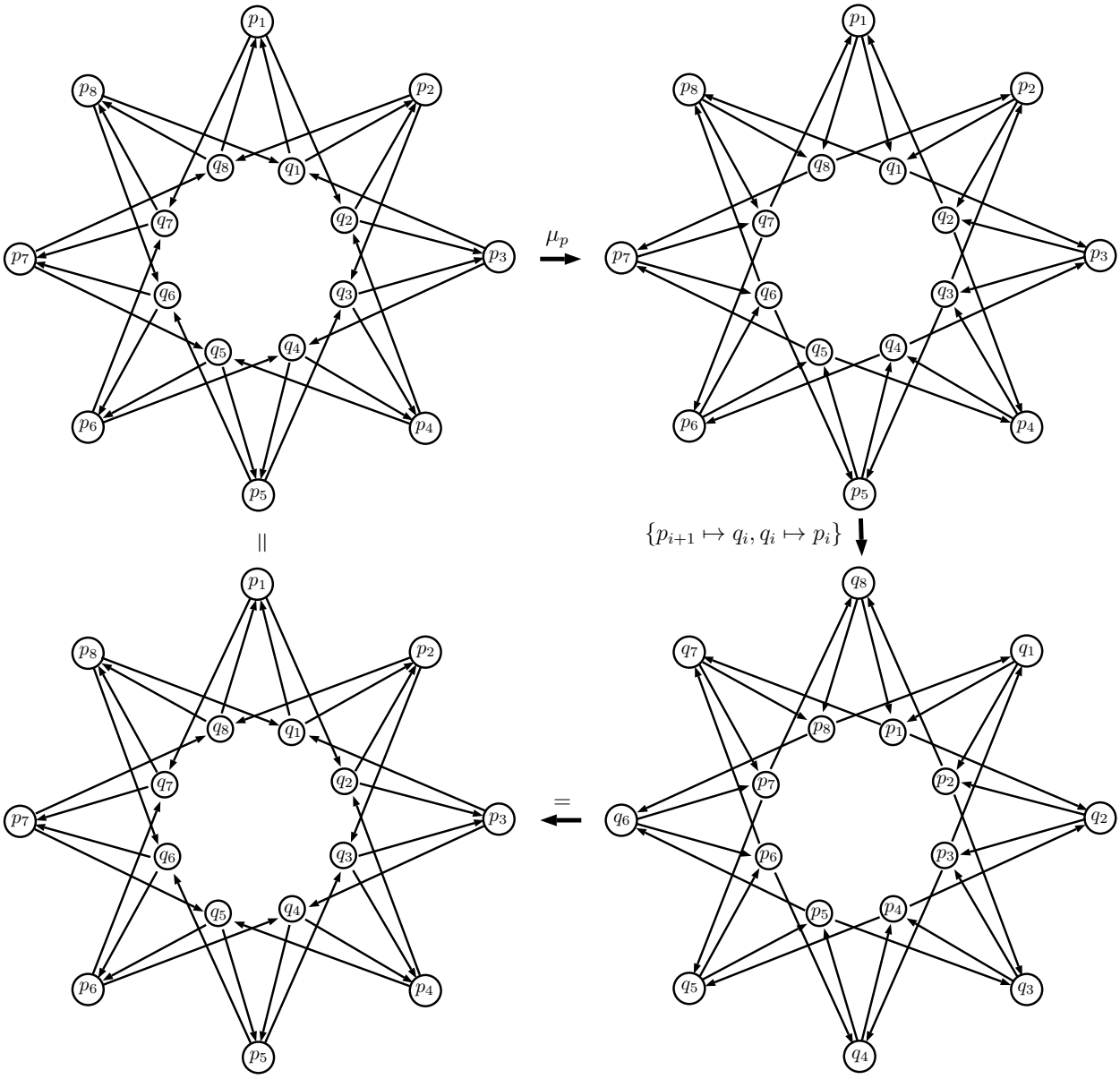

Figure 2.8: The Glick's quiver ($n = 8$) after a sequence of mutations on all $p - vertices$ and a relabelling $\{p_{i+1} \mapsto q_i, q_i \mapsto p_i\}$.

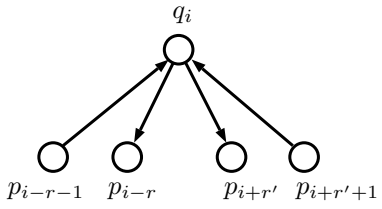

Figure 2.9: The quiver $\mathcal{Q}_{\kappa,n}$ at q_i

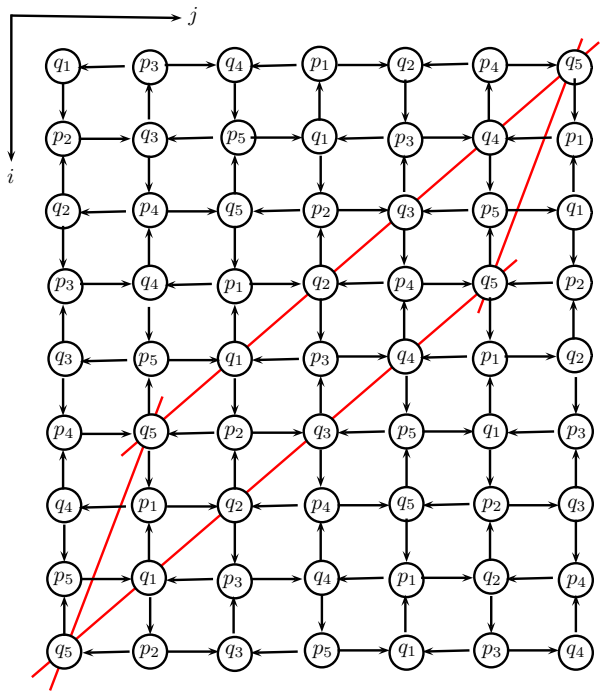

Figure 2.10: Glick's quiver for the pentagram map, viewed as a torus-wrapped octahedron quiver for $\kappa = 3$ and $n = 5$. We have represented a fundamental domain by solid lines, along the two periods $(3, -1)$ and $(5, -5)$.

Then, the p, q coordinates of the k-th iterate T_κ^k of the higher pentagram map on the polygon A read:

$$p_{((\kappa-2)i+\kappa j+k(r-r'))/2}\Big(T_\kappa^k(A)\Big) = Y_{i,j,k},\ \ q_{((\kappa-2)i+\kappa j+(k+1)(r-r'))/2}\Big(T_\kappa^k(A)\Big) = Y^{-1}_{i,j,k-1}$$

for any $i, j, k \in \mathbb{Z}$ with respectively $i + j + k \equiv 0 \bmod 2$ and $i + j + k - 1 \equiv 0 \bmod 2$.

Recalling that the coordinates $p_i(A)$ and $q_i(A)$ are periodic with period n, so are $p_i\Big(T_\kappa^k(A)\Big)$ and $q_i\Big(T_\kappa^k(A)\Big)$. We deduce the following:

Corollary 2.3. *The $Y-$system solution in Proposition 2.2 has double periodicity $(\kappa, 2-\kappa, 0)$ and $(n, -n, 0)$, i.e.,*

$$Y_{i,j,k} = Y_{(i,j,k)+\alpha(\kappa,2-\kappa,0)+\beta(n,-n,0)} \tag{2.8}$$

for $i + j + k \equiv 0 \bmod 2$ and $\alpha, \beta \in \mathbb{Z}$.

2.3.5 From periodic Y-systems to quasi-periodic solutions of the octahedron relation

We now unfold the Y-system solution of the previous section into a solution of the octahedron relation with suitable "quasi-periodic" boundary conditions. The latter will be explicitly functions of the conserved quantities (2.4). The main problem here is the "inversion" of the relations

$$Y_{i,j,k} = \frac{T_{i+1,j,k}T_{i-1,j,k}}{T_{i,j+1,k}T_{i,j-1,k}} \tag{2.9}$$

namely find T's for given Y's. Writing as before the simplest initial data for the octahedron relation in the form $T_{i,j,i+j+1 \bmod 2} = x_{i,j}$, we want to find conditions on the variables $x_{i,j}$ which guarantee that the Y variables (2.9), expressed in terms of the octahedron solution $T_{i,j,k}$, actually encode the p, q invariants of twisted polygons and their iterated images under the higher pentagram map.

We saw in previous section that the corresponding Y variables must satisfy the double periodicity conditions of Corollary 2.3. Conversely, given any solution of the Y-system with such periodicity conditions, let us define p, q invariants of a twisted polygon A by (2.7). We may then interpret the p and q invariants of the k-th iterate of the higher pentagram map on A in terms of the solution $Y_{i,j,k}$ and $Y^{-1}_{i,j,k-1}$.

We have the following:

Theorem 2.4. *Let $T_{i,j,k}$, $i+j+k = 1$ mod 2, be the solution of the octahedron relation (1.2) with initial conditions $T_{i,j,i+j+1 \bmod 2} = x_{i,j}$ for $i, j \in \mathbb{Z}$. Assuming that*

$$\begin{aligned} x_{i+\kappa,j+2-\kappa} &= x_{i,j} \qquad (i,j \in \mathbb{Z}) \\ x_{i+n,i-n} &= x_{i,j} \times \begin{cases} \lambda^{(\kappa-2)i+\kappa j} & \text{if } i+j = 1 \bmod 2 \\ \mu^{(\kappa-2)i+\kappa j} & \text{if } i+j = 0 \bmod 2 \end{cases} \end{aligned} \tag{2.10}$$

then the solution $T_{i,j,k}$ with $i+j+k = 1$ mod 2 satisfies the same properties, namely $T_{i+\kappa,j+2-\kappa,k} = T_{i,j,k}$ and

$$T_{i+n,j-n,k} = T_{i,j,k} \times \begin{cases} \lambda^{(\kappa-2)i+\kappa j} & \text{if } k = 0 \bmod 2 \\ \mu^{(\kappa-2)i+\kappa j} & \text{if } k = 1 \bmod 2 \end{cases} \tag{2.11}$$

and the corresponding $Y_{i,j,k}$ of eq.(2.9) is doubly periodic as in (2.8). Moreover, the two integrals of motion O_n and E_n of eq. (2.4) are given by: $O_n = \lambda^{2\kappa-2}$ and $E_n = \mu^{2-2\kappa}$.

Proof. We must choose a fundamental domain of the integer plane $\mathbb{Z}^2$ under translations by $(\kappa, 2-\kappa)$ and $(n, -n)$. Let us pick two parallel lines $P_n = \{(i, -i), (i+1, -i)\}_{i\in[0,n-1]}$, and consider the periodicity condition in Y that identifies $i \equiv i+n$ (see Figure 2.10 for an illustration: the two parallel lines are made of vertices $q_1, q_2, ..., q_5$ and $p_1, p_2, ..., p_5$ respectively). Using the relation (2.9), we see that the initial data for the Y-system now satisfy: $Y_{i+n,-i-n,k} = Y_{i,-i,k}$ and $Y_{i+\kappa,j+2-\kappa,k} = Y_{i,j,k}$ for $k = 0, 1$ by direct substitution of (2.10), and moreover we can compute:

$$\prod_{i=0}^{n-1} Y_{i,-i,0} = \prod_{i=0}^{n-1} \frac{x_{i+1,-i}x_{i-1,-i}}{x_{i,-i+1}x_{i,-i-1}} = \frac{x_{-1,0}x_{n,-n+1}}{x_{0,1}x_{n-1,-n}} = \lambda^{2\kappa-2} \tag{2.12}$$

$$\prod_{i=0}^{n-1} Y^{-1}_{i+1,-i,1} = \prod_{i=0}^{n-1} \frac{x_{i+1,-i+1}x_{i+1,-i-1}}{x_{i+2,-i}x_{i,-i}} = \frac{x_{1,1}x_{n,-n}}{x_{0,0}x_{n+1,-n+1}} = \mu^{2-2\kappa} \tag{2.13}$$

The equation (2.11) follows immediately by induction, using the octahedron equation, and the double periodicity of the $Y_{i,j,k}$ follows by direct substitution. Finally, we recover that the products of even Y's and that of odd Y's are separately conserved modulo the octahedron equation, which confirms the two conserved quantities (2.4). Their values are given by (2.12-2.13). □

Remark 2.5. As noted in [GSTV12, GSTV16], the ordinary pentagram case studied by Glick has the two conserved quantities O_n, E_n related via $O_nE_n = 1$, which would correspond here to choosing λ, μ such that $\lambda = \mu$. However, in general, the two conserved quantities can have arbitrary values.

2.3.6 Higher dimensional generalizations of the pentagram map

The higher pentagram maps of [GSTV12, GSTV16] are to be distinguished from the higher dimensional generalizations of the pentagram maps, which are maps on n-gons in d-dimensional projective space [KS12]. These maps are also integrable in the continuous limit, and in some cases are shown to be Adler-Gelfand-Dickii flows. Integrability is shown in these cases by presenting Lax representations with a spectral parameter [KS12, KS13, MB13, MB15].

A twisted $n-$gon in $\mathbb{RP}^d$ is a sequence $(v_j)_{j\in\mathbb{Z}}$ in $\mathbb{RP}^d$ together with a monodromy matrix

$M \in PSL_{d+1}(\mathbb{R})$ such that $v_{j+n} = M \circ v_j$ for all $j \in \mathbb{Z}$. We can lift it to a sequence $(V_j)_{j\in\mathbb{Z}}$ in $\mathbb{R}^d$ satisfying $\det(V_j V_{j-1} \dots V_{j-(d-1)}) = 1$ for all $j \in \mathbb{Z}$. This implies a linear relation of the form

$$V_j = a_{j,1}V_{j+1} + a_{j,2}V_{j+2} + \cdots + a_{j,d}V_{j+d} + (-1)^d V_{j+d+1},\ j \in \mathbb{Z}, \tag{2.14}$$

The coefficients $a_{j,i}$ are periodic: $a_{j+n,i} = a_{j,i}$ for some $a_{j,l} \in \mathbb{R}$. In the next section we will connect the coefficients of this equation with the T-system with special boundary conditions. The periodicity of the coefficients in the linear recursion relation will turn out to be a manifestation of the Zamolodchikov periodicity phenomonon for the q-characters of the Lie algebra A_d.

2.4 The T-system with special boundary conditions

2.4.1 The T-system of type A

The octahedron relation (1.2) is a relation between variables on $\mathbb{Z}^3$. There are several important examples of interesting boundary conditions for this equation. The first one comes from the representation theory of the quantum affine algebra $U_q(\widehat{sl}_{d+1})$.

The q-characters [FR99] of $U_q(\widehat{\mathfrak{sl}}_{d+1})$ form a commutative algebra which generalizes that satisfied by the characters of $\mathfrak{sl}_{d+1}$. These q-characters satisfy the A_d T-system with special initial data [Nak03]. (This initial data does not play a role in the context of this chapter, so we sometimes refer to q-characters as the solutions of the A_d T-system absent the specialized initial data.) We therefore refer to the A_d T-system as the octahedron relation (1.2) subject to the following boundary conditions:

$$T_{0,j,k} = T_{d+1,j',k'} = 1, \qquad j, j', k, k' \in \mathbb{Z}. \tag{2.15}$$

It is immediate from Equation (1.2) that this implies that $T_{-1,j,k} = T_{d+2,j,k} = 0$ for all j, k. The T-system is an therefore a discrete evolution equation which takes place in in a subset of $\mathbb{Z}^3$ consisting of a strip, defined by $0 \le i \le d+1$ and $j, k \in \mathbb{Z}$.

Remark 2.6. The meaning of the indices (i, j, k) in the representation theory of the quantum affine algebra is as follows. The index i corresponds to one of the r simple roots of $\mathfrak{sl}_{d+1}$. The index k is related to the shift in the spectral parameter carried by finite-dimensional $U_q(\widehat{\mathfrak{sl}}_{d+1})$-modules.

The q-character of $T_{i,j,k}$ is that of the Kirillov-Reshetikhin module which, in the classical limit, has highest weight $j\omega_i$ and spectral paramater zq^{2k} for a fixed non-zero complex number z.

2.4.2 Plücker relations and conserved quantities

The A_d T-system is a special Plücker relation called the Desnanot-Jacobi relation or Dodgson condensation. This is a relation which gives the determinant of an $n \times n$ matrix in terms of determinants of $(n-1) \times (n-1)$ and $(n-2) \times (n-2)$ matrices.

Let M be an $n \times n$ matrix and let $M^{j_1,...,j_k}_{i_1,...,i_k}$ be the $(n-k) \times (n-k)$ minor obtained be *deleting* the rows $i_1, ..., i_k$ and columns $j_1, ..., j_k$. Then the relation is that

$$|M||M^{1,n}_{1,n}| = |M^1_1||M^n_n| - |M^n_1||M^1_n|. \tag{2.16}$$

This is a discrete recursion with the natural initial data that the 0×0 determinant is 1 and that the 1×1 determinant is the single entry in the 1×1 matrix.

If $T_{0,j,k} = 1$, then this relation is satisfied by solutions of the A_d T-system. To see this, write an arbitrary $(i+1) \times (i+1)$ matrix $M^{(i+1)}_{j,k}$ with the following notation:

$$M^{(i+1)}_{j,k} = \begin{pmatrix} x_{j,k-i} & x_{j+1,k-i+1} & \cdots & x_{j+i,k} \\ x_{j-1,k-i+1} & x_{j,k-i+2} & \cdots & x_{j+i-1,k+1} \\ \vdots & & \ddots & \vdots \\ x_{j-i,k} & x_{j-i+1,k+1} & \cdots & x_{j,k+i} \end{pmatrix} \tag{2.17}$$

where for economy of space we use the variables $x_{j,k} = T_{1,j,k}$.

With this notation, we can make the identification of the minors of $M = M^{(i+1)}_{j,k}$: are (with $n = i+1$)

$$M^{1,n}_{1,n} = M^{(i-1)}_{j,k}, \qquad M^1_1 = M^{(i)}_{j,k+1}, \qquad M^n_n = M^{(i)}_{j,k-1},$$
$$M^n_1 = M^{(i)}_{j-1,k}, \qquad M^1_n = M^{(i)}_{j+1,k}.$$

With the boundary condition that $T_{0,j,k} = 1$ we conclude that $T_{i,j,k} = M^{(i)}_{j,k}$ satisfies the T-system when $i \geq 0$. Therefore we conclude that $T_{i,j,k}$ is determinant of a matrix of size i, $M^{(i)}_{j,k}$.

In the A_d T-system, we impose the additional boundary condition that $T_{d+1,j,k} = 1$, which, upon inspection, implies that $T_{d+2,j,k} = 0$. This last condition means that a determinant of a matrix of size $d+2$ vanishes. When we expand this matrix along a row or a column, we get two linear recursion relations for the variables $T_{1,*,*}$ with $d+2$ terms along the two directions $j+k$ and $k-j$. We claim these the coefficients in these recursion relations are the discrete integrals of the motion in the two directions of the discrete evolution, $j+k$ and $j-k$.

In one direction, consider the two matrices with determinant 1, $M^{(d+1)}_{j,k}$ and $M^{(d+1)}_{j+1,k+1}$. These two matrices have d columns in common with each other: Only the first column of $M^{(d+1)}_{j,k}$ does not appear among the columns of $M^{(d+1)}_{j+1,k+1}$, and only the last column of the latter does not appear among the columns of the first.

Let V_a be the $d+1$-dimensional vector making up the first column of the matrix $M^{(d+1)}_{j,k}$. Here, $a = \lfloor \frac{j+k}{2} \rfloor - d$ is determined by the sum of the two indices of the variables in the first columns: This sum is a constant along each column. That is, $V_a = (x_{j,k-d}, x_{j-1,k-d+1}, \cdots, x_{j-d,k})^t$.

With this notation,

$$M^{(d+1)}_{j,k} = (V_a, V_{a+1}, \cdots, V_{a+d}), \qquad M^{(d+1)}_{j+1,k+1} = (V_{a+1}, V_{a+2}, \cdots, V_{a+d+1}).$$

Therefore,

$$\begin{aligned} |M^{(d+1)}_{j+1,k+1}| &= 1 = |(V_{a+1}, V_{a+2}, \cdots, V_{a+d+1})| \\ &= (-1)^d |(V_{a+d+1}, V_{a+1}, V_{a+2}, \cdots, V_{a+d})|. \end{aligned}$$

Taking the difference between the two determinants:

$$\begin{aligned} 0 &= 1 - 1 = |M^{(d+1)}_{j,k}| - |M^{(d+1)}_{j+1,k+1}| \\ &= |(V_a, V_{a+1}, \cdots, V_{a+d})| - (-1)^d |(V_{a+d+1}, V_{a+1}, V_{a+2}, \cdots, V_{a+d})| \\ &= |(V_a - (-1)^d V_{a+d+1}, V_{a+1}, \cdots, V_{a+d})|, \end{aligned}$$

where in the last line we use the linearity property of the determinant in its columns.

We conclude that there is a linear relation between the columns of the matrix in the last line.

Theorem 2.7. *The columns of an arbitrary $(d+1)\times(d+1)$ matrix of determinant 0, such that each of its solid minors has determinant 1, satisfy the linear recursion relation*

$$0 = V_a + \sum_{i=1}^{d} (-1)^i \alpha_{a,i} V_{a+i} - (-1)^d V_{a+d+1}. \tag{2.18}$$

We note the similarity of this relation to Equation (2.14). The difference so far is the fact that there is no periodicity of the coefficients $\alpha_{a,i}$. We will add this in the following sections, interpreting the various ingredients in terms of the T-system.

We conclude that an ordered sequence of points in $\mathbb{PR}^d$, lifted to $\mathbb{R}^{d+1}$ under the the restriction that every $(d+1)\times(d+1)$ determinant of the vectors corresponding to neighboring points is equal to 1, is given by the columns of $M^{(d+1)}_{j,k}$ and satisfy a linear recursion relation of the form (2.18). Moreover the components of these vectors correspond to solutions $T_{1,j,k}$ for various j,k of the A_d T-system.

Before doing so, let us consider the question of discrete integrability of the T-system which follows from these recursion relations. On the other hand we can consider this as a relation between the components of the vectors V_b, that is, the entries of the matrix M. The relation holds for each of the rows of the vectors. The $(b+1)$-st component of the relation is

$$0 = x_{j-b,k-d+b} + \sum_{i=1}^{d} (-1)^i \alpha_{a,i} x_{j-b+i,k+b+i-d} - (-1)^d x_{j-b+d+1,k+b+1}, \quad 0 \le b \le d, \tag{2.19}$$

where *the coefficients $\alpha_{a,i}$ are independent of the row b*, that is, they are independent of $j-k$.

To summarize, for any j,k we have

Lemma 2.8. *There is a linear recursion relation satisfied by entries of the matrix M:*

$$0 = x_{j,k-d} + \sum_{i=1}^{d} (-1)^i c_i(j+k) x_{j+i,k+i-d} - (-1)^d x_{j+d+1,k+1}, \tag{2.20}$$

where the coefficients $c_i(j+k)$ are independent of the difference $j-k$.

Similarly, if we compare the matrices $M^{(r+1)}_{j,k}$ and $M^{(r+1)}_{j-1,k+1}$ we will see they differ by one row, and we will find another relation between the $x_{j,k}$'s with coefficients which are independent of $j+k$. That is,

Lemma 2.9. *There is a linear recursion relation satisfied by entries of the matrix M:*

$$0 = x_{j,k-d} + \sum_{i=1}^{d} (-1)^i d_i(j-k) x_{j-i,k+i-d} - (-1)^d x_{j-d-1,k+1},$$

where the coefficients $d_i(j-k)$ are independent of the sum $j+k$.

The coefficients c and d therefore have the interpretation of constants of the motion in the direction $j-k$ and $j+k$, respectively. The A_d T-system is a discrete integrable system.

2.4.3 Wall boundary conditions

In this section, we consider only the A_d T-system, that is, the octahedron relation with the boundary conditions (2.15) imposed on it. We now consider the effects of further boundary conditions, in a perpendicular direction, on the solutions of the A_d T-system. We call these "wall" boundary condition. First, we impose the following conditions:

$$T_{i,0,k} = 1, \qquad i,k \in \mathbb{Z}. \tag{2.21}$$

Remark 2.10. There is now a question of compatibility of boundary conditions here: In fact, one can show [DFK13] that simply setting initial data $T_{i,0,1} = T_{i,0,0} = 1$ implies the relation (2.22) for all k. This statement as well as the Theorems quoted below are all proved using the network solution of the octahedron relation.

From the octahedron relation (1.2) it is immediate that (2.21) implies that $T_{i,-1,k} = 0$ for all i,k. Moreover, although it is not immediately obvious from the T-system itself, it was shown in [DFK13] that

Theorem 2.11. *The solutions of the equation (1.2) with boundary conditions (2.15) and (2.21) satisfy*

$$T_{i,-j,k} = 0, \qquad 0 \le j \le d, \ \ i,k \in \mathbb{Z}. \tag{2.22}$$

Furthermore, there is a "mirroring" phenomenon [DFK13]:

Theorem 2.12. *The variables on one side of the "wall of 1's" are determined by the variables on*

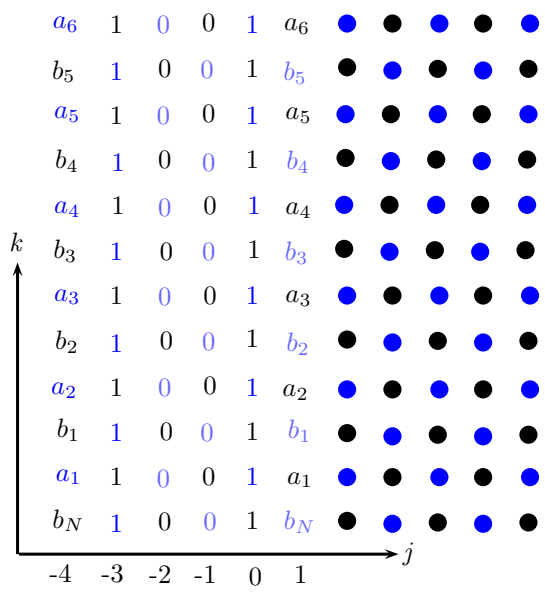

Figure 2.11: An illustration of the mirroring phenomenon for $d = 2$. The circles denote the variables $T_{i,j,k}$ where $i \in \{1, 2\}$ and $j > 0$.

the other side as follows:

$$T_{i,j,k} = (-1)^{di} T_{d+1-i,-j-d-1,k}. \tag{2.23}$$

An illustration of this for $\mathfrak{sl}_3$ is shown in Figure 2.11. In this case, we can see the $i = 1$ and $i = 2$ planes in $\mathbb{Z}^3$ can be viewed as projected to the same plane, as $j + k \in 2\mathbb{Z} + 1$ for $i = 1$ and $j + k \in 2\mathbb{Z}$ for $i = 2$, so they cover complementary sublattices in $\mathbb{Z}^2$. Since $d = 2$, the minus sign from Equation (2.23) does not contribute to the variables on the left of the picture.

Remark 2.13. Note that this is consistent with the linear recursion relations of Lemmas 2.20 when we interpret it as a recursion relation for $T_{1,j,k}$:

$$0 = T_{1,j,k} + \sum_{i=1}^{d} (-1)^i c_i (j + k) T_{1,j+i,k+i} - (-1)^d T_{1,j+d+1,k+d+1}, \quad j + k \in 2\mathbb{Z} + 1, \tag{2.24}$$

which has $d+2$ terms, with the first coefficient equal to 1 and the last coefficient equal to $(-1)^{d+1}$. When $j = -d-1$, for any k and $i = 1$, all the entries in the sum in the middle vanish, and we have $(-1)^d - (-1)^d = 0$.

2.4.4 Identification of conserved quantities with solutions of the T-system with wall boundary conditions

We will now show that, under the "wall" boundary conditions (2.21), the conserved quantities $c_i(j+k)$ in Equation (2.20) are in fact solutions of the A_d T-system, in particular, those with $j=1$.

Theorem 2.14. *The coefficients $c_i(j+k)$ are equal to the values of $T_{i',1,k'}$ along the boundary $j=1$, with $i'=d+1-i$ and $k'=k+d+i$.*

Proof. Consider the $(d+2)\times(d+2)$ matrix $M^{(d+2)}_{1,k+d+1}$ under the boundary conditions (2.21). Due to Theorem 2.22 about the vanishing of the solutions when $-d-1<j<0$ this matrix has the following form:

$$M := M^{(d+2)}_{1,k+d+1} = \begin{pmatrix} x_{1,k} & x_{2,k+1} & x_{3,k+2} & x_{4,k+3} & \cdots & x_{d+2,k+d+1} \\ 1 & x_{1,k+2} & x_{2,k+3} & x_{3,k+4} & \cdots & x_{d+1,k+d+2} \\ 0 & 1 & x_{1,k+4} & x_{2,k+5} & \cdots & x_{d,k+d+3} \\ 0 & 0 & 1 & x_{1,k+6} & \cdots & x_{d-1,k+d+4} \\ \cdots & & & \ddots & \cdots & \\ 0 & 0 & \cdots & 0 & 1 & x_{1,k+2(d+1)} \end{pmatrix} \tag{2.25}$$

where we denoted $x_{j,k}=T_{1,j,k}$. The determinant of this matrix is $T_{d+2,1,k+d+1}=0$ so it vanishes. Moreover it has a one-dimensional kernel, by definition of the A_d T-system (the determinants of any of the solid $(d+1)\times(d+1)$ minors are equal to 1). We solve the nullspace equation

$$M\vec{a}=\vec{0}$$

for $\vec{a}=(a_0,a_1,...,a_{d+1})$. On the one hand, the entries of this vector are the coefficients (up to normaliation) of the linear recursion relation:

$$\sum_{i=0}^{d+1} a_i x_{i+1,k+i}=0$$

so we may identify $a_i=(-1)^i c_i(k+d+1)$.

On the other hand, expanding the determinant along the first row, we get $a_i = (-1)^i |M_1^{(d+i-1)}|$. The determinant of the minor is particularly simple to compute. It is equal to the determinant of the $(d+1-i) \times (d+1-i)$-matrix $M^{(d+1-i)}_{1,k+d+i+2}$, which is, by definition, $T_{d+1-i,1,k+d+i+2}$.

□

2.4.5 Linear recursion relations under Zamolodchikov periodicity

We have now identified the coefficients in the linear recursion relation (2.14) as solutions of the T-system, as long as we do not require them to be periodic. To see how periodicity enters the picture in the context of T-systems, we refer to the Zamolodchikov periodicity phenomenon.

We must impose one final additional boundary condition on the A_d T-system, of the form of a second "wall of 1's" of the same form as (2.21), but positioned at $j = \ell + 1$ where $\ell \geq 2$. That is, we look at the octahedron equation restricted to the A_d slice with boundary conditions (2.15), together with the wall boundary conditions at $j = 0$ (2.21) and

$$T_{i,\ell+1,k} = 1. \tag{2.26}$$

There remains an evolution of the T-system under these boundary conditions in the k-direction, taking place in a tube with walls at $j = 0, \ell+1$ and $i = 0, d+1$. A valid initial data for this system are the values of the function T in the finite set of points ($d \times \ell$ of these) $\{(i, j, i + j \bmod 2 : 1 \leq i \leq d, 1 \leq j \leq \ell\}$. All other values of T are positive Laurent polynomials in this initial data, due to the Laurent property of cluster algebras.

An important result about these boundary conditions, originally conjectured by Zamolodchikov [Zam91] and later proven in various contexts [DFK13, IIK+13], is that there is a periodicity phenomenon:

Theorem 2.15. *The solutions of the A_d T-system $T_{i,j,k}$ under the boundary conditions (2.21) and (2.26) satisfy a periodicity phenomonon:*

$$T_{i,j,k+p} = T_{d+1-i,\ell+1-j,k}, \qquad p = \ell + d + 2 \tag{2.27}$$

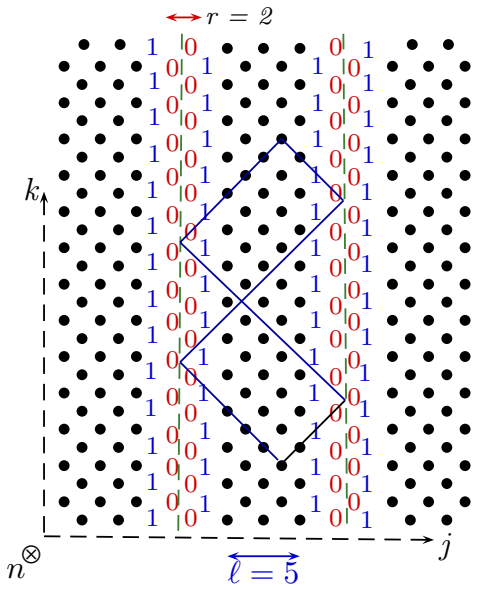

Figure 2.12: An illustration of the how the mirroring along two lines implies periodicity for $d = 2$, $\ell = 5$. The T-variable at the bottom has two lines emanating from it, in the $j - k$ and $j + k$ directions, and these are mirrored a the dashed "mirror" lines. Where they intersect at the top, the T-variable is equal to the original one at the bottom of the picture.

so that

$$T_{i,j,k+2p} = T_{i,j,k}. \tag{2.28}$$

This can be visualized as a mirroring along the line $j = -(d+1)/2$ (as implied by Equation (2.23)) as well as $j = \ell + 1 + (d+1)/2$, by symmetry. See [DFK13] for a detailed analysis using the network formulation.

In this situation, for fixed ℓ and d, we have a periodicity of the coefficients $c_i(j+k)$. We have identified the coefficients $\alpha_{a,i}$ in Equation (2.18) with $T_{i',1,k}$, with $a = \lfloor \frac{j+k}{2} \rfloor - d$. Therefore we have

$$\alpha_{a+p,i} = \alpha_{a,i}, \qquad p = \ell + d + 2.$$

Thus, the integrals of the motion in the case with wall boundary conditions are also periodic. The number of integrals $\alpha_{a,i}$ is $p \times d = (\ell + d + 2)d$. However these integrals are not algebraically independent in the periodic case, because they are determined by the set of initial data, which contains $\ell \times d$ indepenent data. Therefore, there are $d(d+2)$ relations between the variables $\alpha_{a,i}$.

The vectors V_a are also periodic in this case: $V_{a+p} = (-1)^d V_a$. They can be visualized as the collection of variables along a diagonal connecting $d + 1$ points from NW to SE on the lattice of

$T_{1,j,k}$'s. Then the set of such collections, translated with respect to each other by the vector $(1,1)$ in the (j,k) direction, is periodic with period p (recall that $a \sim (j+k)/2$). We can therefore interpret the vectors V_a as the lifts of the vertices of a closed n-gon in projective space.

Remark 2.16. There is a more general quasi-periodicity phenomonon corresponding to n-gons with monodromy for T-systems. This can be seen indirectly from the fact that (a) it is always possible to unfold the Y-variables corresponding to an arbitrary T-system such that periodic Y-systems unfold to quasi-periodic T-systems (as in Section 2.3) and (b) Zamolodchikov periodicity for Y-systems has been proven [Kel13].

2.5 Conclusion and discussion

In this chapter, our interest was to exhibit two seemingly unrelated relations between the T-system and the various versions of the pentagram maps, which are all discrete integrable systems. The first relation, discussed in Section 2.3, shows that the (generalized) pentagram map in projective 2-space is in fact the octahedron relation with special, quasi-periodic boundary conditions. Therefore integrability follows from the fact that the octahedron relation is known to be integrable. Integrability was proved in general for this map by [GSTV12, GSTV16] by more classical means.

The second relation is simply the identification of the invariants which are the periodic coefficients of the lifted coordinates of the n-gon in projective d-space for general d are solutions of the A_d T-system, that the fact that they are not algebraically independent follows from the evolution of this T-system, and that their periodicity is directly related to the Zamolodchikov periodicity phenomenon.

The pentagram map is more generally defined for polygons with a monodromy, not necessarily closed polygons corresponding to periodicity. It would be interesting to see if there are compatible boundary conditions for the T-system which reflect this more general type of periodicity.

Moreover, the pentagrm map acts on projective variables, which are related to ratios of solutions of the T-system. These satisfy the Y-system. To get the most general type of Y-system solutions, one must introduce coefficients into the T-system in a sufficiently generic fashion. In the next chapter, we consider T-systems with principal coefficients. This choice of coefficients gives a general solution to the Y-system.

Chapter 3

Solutions to the T-systems with principal coefficients

3.1 Introduction

The material in this chapter is published in "Solutions to the T-systems with principal coefficients.", *Electron. J. Combin.*, 23(2):Paper 2.44, 56, 2016.

We recall the octahedron relation (1.2), which will be refered to as the *A_∞ T-system* or just *T-system* in this chapter. Several combinatorial solutions have been considered including solutions in terms of alternating sign matrices [RR86], domino tilings [RR86, EKLP92], perfect matchings [Spe07] and networks [DFK13].

One can also consider cluster algebras with coefficients [FZ07]. For cluster algebras of geometric type, this is equivalent to adding frozen vertices to the quiver. A quite general type of coefficients are principal coefficients. It corresponds to adding one frozen vertex for each quiver vertex and an arrow pointing from it to the quiver vertex. In some literature, this new quiver is called the coframed quiver associated with the octahedron quiver. The reason why the principal coefficients are very important is due to the separation formula [FZ07, Theorem 3.7], stating that a cluster algebras with any coefficients can be written in terms of one with principal coefficients.

Some generalizations of T-systems with coefficients have been suggested by Speyer in his work on Speyer's octahedron recurrence [Spe07] and by Di Francesco in his work on the generalized lambda determinant [DF13]. In this chapter, we consider A_∞ T-systems with principal coefficients using cluster algebras definition. We then give combinatorial solutions in terms of perfect matchings, non-intersecting paths and networks.

This chapter is organized as follows. In Section 1.1, we review some basic definitions and results in cluster algebras from [FZ02, FZ07]. In Section 3.2, we define the T-system with principal coefficients, whose initial condition is in the form of initial data on a stepped surface.

The goal is to find, for an arbitrary point (i_0, j_0, k_0) and a stepped surface $\mathbf{k}$, an expression of T_{i_0,j_0,k_0} in terms of initial data on $\mathbf{k}$. Laurent phenomenon for cluster variables [FZ02, Theorem 3.1] guarantees that the expression is indeed a Laurent polynomial in the initial data and coefficients. We give explicit combinatorial expressions of T_{i_0,j_0,k_0} in terms of initial data when the point (i_0, j_0, k_0) is above $\mathbf{k}$ and $\mathbf{k}$ is above the fundamental stepped surface $\mathbf{fund} : (i, j) \mapsto (i + j \bmod 2) - 1$. Some other cases will be discussed in Section 3.8.

Section 3.3 is devoted to a perfect matching solution. Following the construction in [Spe07], we first construct a finite bipartite graph with open faces G depending on both (i_0, j_0, k_0) and $\mathbf{k}$, then construct face-weight w_f and pairing-weight w_p on perfect matchings of G. This leads to the perfect-matching solution (Theorem 3.13):

$$T_{i_0,j_0,k_0} = \sum_M w_p(M) w_f(M)$$

where the sum runs over all perfect matchings of G. The weight $w_p(M)$ is a monomial in the cluster coefficients, while $w_f(M)$ is a Laurent monomial in the initial data (cluster variables).

In Section 3.4, we define the closure $\overline{G}$ of the graph G and transform our previous two weights to the edge-weight w_e. This gives another form of the perfect-matching solution (Theorem 3.22):

$$T_{i_0,j_0,k_0} = \sum_{\overline{M}} w_e(\overline{M}) \Big/ w_e(\overline{M}_0)\big|_{c_{i,j}=1}.$$

The sum runs over all perfect matchings of $\overline{G}$ with a certain boundary condition, see Definition 3.20.

In Section 3.5, we orient all the edges of G and $\overline{G}$ and give an explicit bijection between perfect matchings of G and non-intersecting paths on G with certain sources and sinks. This bijection can also be extended to $\overline{G}$. Using the modified edge-weight w'_e obtaining from w_e together with the bijection, the perfect-matching solution for $\overline{G}$ gives the nonintersecting-path solution (Theorem 3.40):

$$T_{i_0,j_0,k_0} = \sum_{\overline{P}} w'_e(\overline{P}) \Big/ \prod_{\circ\!-\!\bullet\, b \in \overline{M}_0} \bar{p}_b$$

where the sum runs over all non-intersecting paths on $\overline{G}$ with certain sources and sinks, see Theorem

3.40.

In Section 3.6, we first consider the network N, studied in [DF10, DFK13] associated with (i_0, j_0, k_0) and $\mathbf{k}$. It is obtained from the shadow of the point (i_0, j_0, k_0) on the lozenge covering on $\mathbf{k}$. We point out that it can also be obtained from the graph $\overline{G}$ by tilting all the diagonal edges of $\overline{G}$ so that they become horizontal. This allows us to pass the modified edge-weight w'_e on $\overline{G}$ to a weight on the network N. Paths on $\overline{G}$ then become paths on N. From Theorem 3.40, we get the network solution (Theorem 3.43) as a partition function of weighted non-intersecting paths on the network N, which can also be written as a certain minor of the network matrices (Theorem 3.48).

In Section 3.7, we discuss other types of coefficients of the T-system related to Speyer's octahedron recurrence [Spe07], generalized lambda-determinants [DF13] and (higher) pentagram maps [Sch92, OST10, Gli11, GSTV12, GSTV16].

3.2 T-systems

3.2.1 T-systems without coefficients

We first recall the definition of the T-system in Equation (1.2). A *stepped surface* is a subset $\{(i, j, \mathbf{k}(i, j)) \mid i, j \in \mathbb{Z}\} \subset \mathbb{Z}^3_{\text{odd}}$ defined by a function $\mathbf{k} : \mathbb{Z} \times \mathbb{Z} \to \mathbb{Z}$ satisfying:

$$|\mathbf{k}(i, j) - \mathbf{k}(i', j')| = 1 \quad \text{when} \quad |i - i'| + |j - j'| = 1.$$

We will also denote this surface by the function $\mathbf{k}$. The condition $|i - i'| + |j - j'| = 1$ is referred to as (i, j) and (i', j') are *lattice-adjacent*, and $\mathbf{k}(i, j)$ is called the *height* of (i, j) with respect to $\mathbf{k}$. There are three important stepped surfaces which we will use throughout the chapter. We define

$$\begin{aligned} \mathbf{fund} &: (i, j) \mapsto (i + j \bmod 2) - 1, \\ \mathbf{proj}_{(i',j',k')} &: (i, j) \mapsto k' - |i - i'| - |j - j'|, \\ \mathbf{k}_p &: (i, j) \mapsto \min\left(\mathbf{k}(i, j), \mathbf{proj}_p(i, j)\right), \end{aligned} \tag{3.1}$$

and call them the *fundamental stepped surface*, the *stepped surface projected from a point* (i', j', k') and the *adjusted stepped surface* associated with a surface $\mathbf{k}$ and a point p, respectively. See Figure

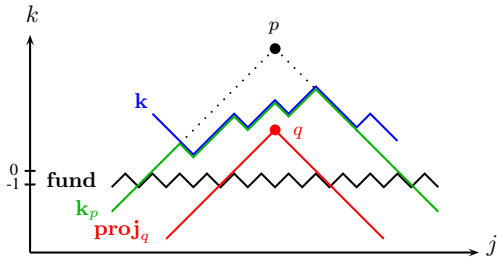

Figure 3.1: The surfaces **fund**, $\mathbf{proj}_q$ and $\mathbf{k}_p$ associated with a surface $\mathbf{k}$ in the section $i = i_0$ of the 3-dimensional lattice.

3.1 for examples.

To each $\mathbf{k}$, we can attach an *initial condition* $X_{\mathbf{k}}(\mathbf{t}) : \{T_{i,j,\mathbf{k}(i,j)} = t_{i,j} \mid i, j \in \mathbb{Z}\}$ for some formal variables $\mathbf{t} = \{t_{i,j} \mid i, j \in \mathbb{Z}\}$, to which we refer as *initial data/values* along the stepped surface $\mathbf{k}$.

It is worth pointing out that for a point $(i_0, j_0, k_0) \in \mathbb{Z}^3_{\text{odd}}$, not every initial data gives a finite solution to T_{i_0,j_0,k_0}. In other words, an expression of T_{i_0,j_0,k_0} in terms of $t_{i,j}$'s may not be finite. We call an initial data on $\mathbf{k}$ that gives a finite expression for T_{i_0,j_0,k_0} an *admissible initial data* with respect to (i_0, j_0, k_0).

Example 3.1. The fundamental stepped surface is always admissible with respect to any point in $\mathbb{Z}^3_{\text{odd}}$. The stepped surface $\mathbf{proj}_{(0,0,m)}$ is not admissible with respect to a point $(0, 0, n)$ when $n > m$.

Recall that the T-system can also be interpreted as an infinite-rank coefficient-free cluster algebra [DFK09]. Using $\mathbb{Z}^2$ as the index set, the initial seed is $(\mathbf{x}, B) = \left((x_{i,j})_{(i,j)\in\mathbb{Z}^2}, (b_{(i',j'),(i,j)})\right)$ where

$$x_{i,j} = T_{i,j,\mathbf{fund}(i,j)} \quad \text{and} \quad b_{(i',j'),(i,j)} = (-1)^{i+j}\left(\delta_{i',i\pm1}\delta_{j',j} - \delta_{i',i}\delta_{j',j\pm1}\right).$$

The quiver $\mathcal{Q}_B$ associated with B, the octahedron quiver, is shown in Figure 3.2. We embed the vertices of the quiver into the 3-dimensional lattice $\mathbb{Z}^3_{\text{odd}}$ so that they lie on the fundamental stepped surface, i.e. the vertex (i, j) of the octahedron quiver lies at the point $(i, j, \mathbf{fund}(i, j)) \in \mathbb{Z}^3_{\text{odd}}$. The reason for picking this choice is to associate it to the index of the initial cluster variables $T_{i,j,\mathbf{fund}(i,j)}$ at (i, j) for $(i, j) \in \mathbb{Z}^2$.

We then allow mutations only on vertices (i, j, k) having the property that there are exactly two incoming and two outgoing arrows incident to (i, j, k). This property is equivalent to saying

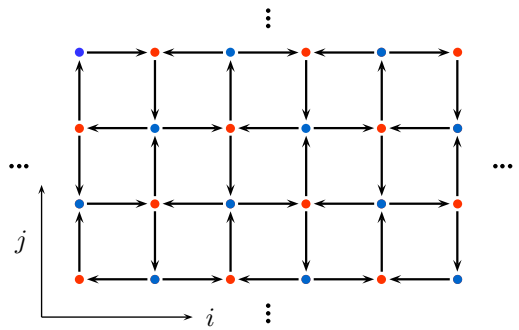

Figure 3.2: The octahedron quiver. The red dots correspond to indices (i, j) where $i + j$ is even, and the blue to the odd $i + j$. The quiver is infinite in both i and j directions.

that all four neighbors of (i, j, k) have the same third coordinate in $\mathbb{Z}^3_{\text{odd}}$, i.e., the four neighbors are all either $(i \pm 1, j \pm 1, k - 1)$ or $(i \pm 1, j \pm 1, k + 1)$.

If the neighbors are $(i \pm 1, j \pm 1, k - 1)$, after the mutation at (i, j, k), we move the vertex that used to be at (i, j, k) to $(i, j, k - 2)$ and call the new cluster variable obtained by the mutation $T_{i,j,k-2}$. We call this mutation a *downward mutation*. On the other hand, when the neighbors are $(i \pm 1, j \pm 1, k + 1)$, (i, j, k) is moved to $(i, j, k + 2)$ and the new cluster variable is called $T_{i,j,k+2}$. We call it an *upward mutation*.

The set of vertices of a quiver $\mathcal{Q}$ obtained from the octahedron quiver by allowed mutations forms a stepped surface, denoted by $\mathbf{k}_{\mathcal{Q}}$. On the other hand, we can create a quiver from a stepped surface by reading the arrangement of the quiver arrows from Table 3.1, and call this quiver $\mathcal{Q}_{\mathbf{k}}$. We notice that the quiver mutation at (i, j) corresponds to moving $(i, j, \mathbf{k}(i, j))$ to $(i, j, \mathbf{k}(i, j) \pm 2)$, depending on the height of its neighbors as discussed above. We say that $\mathbf{k}'$ is obtained from $\mathbf{k}$ by a *mutation* at (i, j) if $\mathcal{Q}_{\mathbf{k}'} = \mu_{(i,j)}(\mathcal{Q}_{\mathbf{k}})$.

3.2.2 T-systems with principal coefficients

We define the *T-systems with principal coefficients* from the cluster algebra setting. Instead of the coefficient-free cluster algebra with the octahedron quiver, we consider the cluster algebra with principal coefficients (Definition 1.12) on the same quiver, where the initial coefficient at (i, j) is $c_{i,j}$. Due to Remark 1.13, it is the same as the coefficient-free cluster algebras on the coframed octahedron quiver, where the variables $c_{i,j}$ on the added vertices are frozen, see Figure 3.3. We

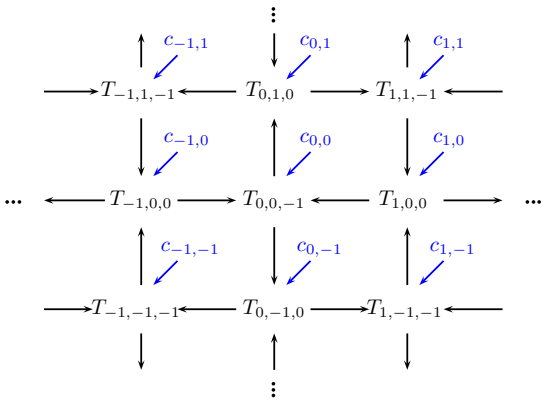

Figure 3.3: A portion of the infinite framed octahedron quiver and its cluster variables including frozen variables $c_{i,j}$.

show that the cluster variables satisfy the recurrence relation (3.2) on $\{T_{i,j,k} \mid (i,j,k) \in \mathbb{Z}^3_{\text{odd}}\}$ with an extra set of coefficients $\{c_{i,j} \mid (i,j) \in \mathbb{Z}^2\}$. We will use this recursion as an alternative definition of the T-system with principal coefficients.

Theorem 3.2. *Let $\{T_{i,j,k} \mid (i,j,k) \in \mathbb{Z}^3_{\text{odd}}\}$ be the set of cluster variables obtained from the T-system with principal coefficients. Then*

$$T_{i,j,k-1}T_{i,j,k+1} = J_{i,j,k}T_{i-1,j,k}T_{i+1,j,k} + I_{i,j,k}T_{i,j-1,k}T_{i,j+1,k} \tag{3.2}$$

where

$$I_{i,j,k} = \begin{cases} \prod_{a=k+1}^{-(k+1)} c_{i+a,j}, & k < 0, \\ 1, & k \geq 0, \end{cases} \quad \text{and} \quad J_{i,j,k} = \begin{cases} 1, & k < 0, \\ \prod_{a=-k}^{k} c_{i,j+a}, & k \geq 0. \end{cases} \tag{3.3}$$

We call the relation (3.2) the *octahedron recurrence with principal coefficients*. The pictorial representation of I and J are shown in Figure 3.4.

In order to prove Theorem 3.2, we first compute the coefficients at the vertices in any quiver obtained by the octahedron quiver. We note that unlike cluster variables, a coefficient at (i,j) on a stepped surface $\mathbf{k}$ depends on the height of (i,j) and its neighbors $(i \pm 1, j \pm 1)$.

Proposition 3.3. *Consider the T-system with principal coefficients. Let $\mathbf{k}$ be a stepped surface obtained from* **fund** *by a finite number of allowed mutations. Let $y_{(i,j),\mathbf{k}}$ be the coefficient at the*

vertex (i,j) *in* $\mathcal{Q}_{\mathbf{k}}$. *Then*

$$y_{(i,j),\mathbf{k}} = \frac{I_{i,j,k-1} J_{i,j-1,k}^{[\epsilon_1]_+} J_{i,j+1,k}^{[\epsilon_2]_+}}{J_{i,j,k-1} I_{i-1,j,k}^{[\epsilon_3]_+} I_{i+1,j,k}^{[\epsilon_4]_+}} = \frac{J_{i,j,k+1} I_{i-1,j,k}^{[-\epsilon_3]_+} I_{i+1,j,k}^{[-\epsilon_4]_+}}{I_{i,j,k+1} J_{i,j-1,k}^{[-\epsilon_1]_+} J_{i,j+1,k}^{[-\epsilon_2]_+}}, \tag{3.4}$$

when $\mathbf{k}(i,j) = k$, $\mathbf{k}(i,j-1) = k+\epsilon_1$, $\mathbf{k}(i,j+1) = k+\epsilon_2$, $\mathbf{k}(i-1,j) = k+\epsilon_3$ *and* $\mathbf{k}(i+1,j) = k+\epsilon_4$ *where* $\epsilon_\ell \in \{-1,1\}$, *as described as follows:*

$$(i, j+1, k+\epsilon_2)$$

$$(i-1, j, k+\epsilon_3) \qquad (i,j,k) \qquad (i+1, j, k+\epsilon_4)$$

$$(i, j-1, k+\epsilon_1)$$

Example 3.4. Consider a stepped surface $\mathbf{k}$ having height as the following.

$$(i, j+1, k+1)$$

$$(i-1, j, k+1) \qquad (i,j,k) \qquad (i+1, j, k-1)$$

$$(i, j-1, k-1)$$

The coefficient at the vertex (i,j), $y_{(i,j),\mathbf{k}}$, computed by Proposition 3.3 is

$$y_{(i,j),\mathbf{k}} = \frac{I_{i,j,k-1} J_{i,j+1,k}}{J_{i,j,k-1} I_{i-1,j,k}} = \frac{J_{i,j,k+1} I_{i+1,j,k}}{I_{i,j,k+1} J_{i,j-1,k}}.$$

Proof of Proposition 3.3. We fist show the second equality in (3.4). Notice that $[\epsilon_i]_+ + [-\epsilon_i]_+ = 1$ for all i. So we only need to show

$$\frac{I_{i,j,k-1} J_{i,j-1,k} J_{i,j+1,k}}{J_{i,j,k-1} I_{i-1,j,k} I_{i+1,j,k}} = \frac{J_{i,j,k+1}}{I_{i,j,k+1}},$$

which can be easily derived from the definition of I and J in (3.3).

We will then prove the proposition by induction on the number of mutations from the funda-

mental stepped surface. On **fund**, the vertices are in the forms $(i,j,-1)$ or $(i,j,0)$ depending on the parity of $i+j$, and $y_{(i,j),\mathbf{fund}} = c_{i,j}$ for all (i,j). When $i+j \equiv 0 \bmod 2$, $\mathbf{fund}(i,j) = -1$ and the neighbors of $(i,j,-1)$ are $(i\pm1, j\pm1, 0)$. So $\epsilon_\ell = 1$ for all ℓ at (i,j). We also have

$$y_{(i,j),\mathbf{k}} = c_{i,j} = \frac{J_{i,j,0}}{I_{i,j,0}}.$$

When $i+j \equiv 1 \bmod 2$, $\mathbf{fund}(i,j) = 0$ and the neighbors of $(i,j,0)$ are $(i\pm1, j\pm1, -1)$. So $\epsilon_\ell = -1$ for all ℓ. We have

$$y_{(i,j),\mathbf{k}} = c_{i,j} = \frac{I_{i,j,-1}}{J_{i,j,-1}}.$$

Hence the proposition holds for the fundamental stepped surface.

Next we assume that the proposition holds for a stepped surface $\mathbf{k}$. Consider a stepped surface $\mathbf{k}'$ obtained from $\mathbf{k}$ by a mutation at (i,j). Then $\mathbf{k} = \mathbf{k}'$ on every point except at (i,j). Also $y_{(a,b),\mathbf{k}} = y_{(a,b),\mathbf{k}'}$ for all (a,b) but at most five points: (i,j), $(i\pm1, j\pm1,)$. So we only need to consider the coefficients at these five points.

Let us assume that $\mathbf{k}(i,j) = k$. Since $\mathbf{k}$ is mutable at (i,j), we have two cases: $\mathbf{k}(i\pm1, j\pm1) = k-1$ or $\mathbf{k}(i\pm1, j\pm1) = k+1$, as shown in the following pictures.

$$\begin{array}{ccccc} & & (i,j+1,k-1) & & \\ & & \downarrow & & \\ (i-1,j,k-1) & \longleftarrow & (i,j,k) & \longrightarrow & (i+1,j,k-1) \\ & & \uparrow & & \\ & & (i,j-1,k-1) & & \end{array} \quad . \qquad \begin{array}{ccccc} & & (i,j+1,k+1) & & \\ & & \uparrow & & \\ (i-1,j,k+1) & \longrightarrow & (i,j,k) & \longleftarrow & (i+1,j,k+1) \\ & & \downarrow & & \\ & & (i,j-1,k+1) & & \end{array} \quad .$$

Case 1 We know that $y_{(i,j),\mathbf{k}} = I_{i,j,k-1}/J_{i,j,k-1}$ by the induction hypothesis. After the mutation at (i,j), the point (i,j,k) becomes $(i,j,k-2)$. So on $\mathbf{k}'$, $\epsilon_i = 1$ for all i. We also get

$$y_{(i,j),\mathbf{k}'} = \left(\frac{I_{i,j,k-1}}{J_{i,j,k-1}}\right)^{-1} = \frac{J_{i,j,k'+1}}{I_{i,j,k'+1}} = \frac{J_{i,j,k'+1} I_{i-1,j,k'}^{[-1]_+} I_{i+1,j,k'}^{[-1]_+}}{I_{i,j,k'+1} J_{i,j-1,k'}^{[-1]_+} J_{i,j+1,k'}^{[-1]_+}}$$

where $k' = k-2$. Hence the expression of $y_{(i,j),\mathbf{k}'}$ agrees with the proposition.

At $(i, j+1, k-1)$, the induction hypothesis gives

$$y_{(i,j+1),\mathbf{k}} = \frac{I_{i,j+1,k-2} J_{i,j,k-1}^{[1]_+} J_{i,j+2,k-1}^{[\epsilon_2]_+}}{J_{i,j+1,k-2} I_{i-1,j+1,k-1}^{[\epsilon_3]_+} I_{i+1,j+1,k-1}^{[\epsilon_4]_+}}$$
$$= \frac{I_{i,j+1,k-2} J_{i,j,k-1} J_{i,j+2,k-1}^{[\epsilon_2]_+}}{J_{i,j+1,k-2} I_{i-1,j+1,k-1}^{[\epsilon_3]_+} I_{i+1,j+1,k-1}^{[\epsilon_4]_+}}.$$

We know that $\epsilon_1 = 1$ since $\mathbf{k}(i,j) = k = \mathbf{k}(i,j+1) + 1$. Then the mutation at (i,j) gives

$$\begin{aligned} y_{(i,j+1),\mathbf{k}'} &= y_{(i,j+1),\mathbf{k}}(1 \oplus y_{(i,j),\mathbf{k}}) \\ &= y_{(i,j+1),\mathbf{k}} \frac{1}{J_{i,j,k-1}} \\ &= \frac{I_{i,j+1,k-2} J_{i,j,k-1}^{[-1]_+} J_{i,j+2,k-1}^{[\epsilon_2]_+}}{J_{i,j+1,k-2} I_{i-1,j+1,k-1}^{[\epsilon_3]_+} I_{i+1,j+1,k-1}^{[\epsilon_4]_+}}, \end{aligned}$$

which agrees to the proposition. By the similar argument, we can show that all four of the $y_{(i\pm1,j\pm1),\mathbf{k}'}$ agree to the proposition.

Case 2 We know that $y_{(i,j),\mathbf{k}} = J_{i,j,k+1}/I_{i,j,k+1}$ by the induction hypothesis. After the mutation at (i,j), the point (i,j,k) becomes $(i,j,k+2)$. So on $\mathbf{k}'$, $\epsilon_i = -1$ for all i. We also get

$$y_{(i,j),\mathbf{k}'} = \left(\frac{J_{i,j,k+1}}{I_{i,j,k+1}}\right)^{-1} = \frac{I_{i,j,k'-1}}{J_{i,j,k'-1}} = \frac{I_{i,j,k'-1} J_{i,j-1,k'}^{[-1]_+} J_{i,j+1,k'}^{[-1]_+}}{J_{i,j,k'-1} I_{i-1,j,k'}^{[-1]_+} I_{i+1,j,k'}^{[-1]_+}}$$

when $k' = k+2$. Hence the expression of $y_{(i,j),\mathbf{k}'}$ agrees with the proposition.

At $(i, j+1, k-1)$, the induction hypothesis gives

$$y_{(i,j+1),\mathbf{k}} = \frac{I_{i,j+1,k-2} J_{i,j,k-1}^{[-1]_+} J_{i,j+2,k-1}^{[\epsilon_2]_+}}{J_{i,j+1,k-2} I_{i-1,j+1,k-1}^{[\epsilon_3]_+} I_{i+1,j+1,k-1}^{[\epsilon_4]_+}}$$
$$= \frac{I_{i,j+1,k-2} J_{i,j,k-1} J_{i,j+2,k-1}^{[\epsilon_2]_+}}{J_{i,j+1,k-2} I_{i-1,j+1,k-1}^{[\epsilon_3]_+} I_{i+1,j+1,k-1}^{[\epsilon_4]_+}}.$$

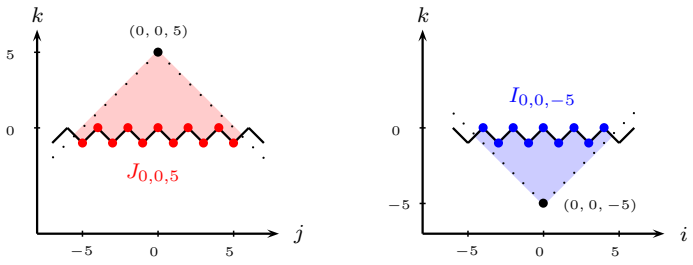

Figure 3.4: $J_{0,0,5} = c_{0,-5}c_{0,-4}\dots c_{0,5}$ can be realized as a shadow shaded down from $(0,0,5)$ as depicted by the red dots in the section $i = 0$. $I_{0,0,-5} = c_{-4,0}c_{-3,0}\dots c_{4,0}$ can be realized as a shadow shaded up from $(0,0,-5)$ as depicted by the blue dots in the section $j = 0$.

We know that $\epsilon_1 = -1$ since $\mathbf{k}(i,j) = k = \mathbf{k}(i,j+1) - 1$. Then the mutation at (i,j) gives

$$\begin{aligned} y_{(i,j+1),\mathbf{k}'} &= y_{(i,j+1),\mathbf{k}} \frac{y_{(i,j),\mathbf{k}}}{(1 \oplus y_{(i,j),\mathbf{k}})} \\ &= y_{(i,j+1),\mathbf{k}} J_{i,j,k-1} \\ &= \frac{I_{i,j+1,k-2} J_{i,j,k-1}^{[1]_+} J_{i,j+2,k-1}^{[\epsilon_2]_+}}{J_{i,j+1,k-2} I_{i-1,j+1,k-1}^{[\epsilon_3]_+} I_{i+1,j+1,k-1}^{[\epsilon_4]_+}}, \end{aligned}$$

which agrees to the proposition. By the similar argument, we can show that all four of the $y_{(i\pm1,j\pm1),\mathbf{k}'}$ agree to the proposition.

By both cases, we proved the proposition. □

Proof of Theorem 3.2. To show (3.2), it is enough to show that it is the mutation rule at $(i,j,k-1)$ on $\mathbf{k}$ such that $\mathbf{k}(i\pm1,j\pm1) = k$ and $\mathbf{k}(i,j) = k-1$. The quiver at (i,j) will look like the following:

$$\begin{array}{ccccc} & & (i,j+1,k) & & \\ & & \uparrow & & \\ (i-1,j,k) & \to & (i,j,k-1) & \leftarrow & (i+1,j,k) \\ & & \downarrow & & \\ & & (i,j-1,k) & & \end{array}$$

So it is equivalent to show that $y_{(i,j),\mathbf{k}} = J_{i,j,k}/I_{i,j,k}$, which comes from Proposition 3.3. □

Due to Theorem 3.2, we view the T-system with principal coefficients as a recurrence relation on $T_{i,j,k}$, $(i,j,k) \in \mathbb{Z}^3_{\text{odd}}$ with extra coefficient variables $c_{i,j}$, $(i,j) \in \mathbb{Z}^2$. Fixing a point $p = (i_0,j_0,k_0) \in \mathbb{Z}^3_{\text{odd}}$ and an admissible initial data on a stepped surface $\mathbf{k}$, Theorem 1.6 guarantees that the

expression of T_{i_0,j_0,k_0} is a Laurent polynomial in the initial data $\{t_{i,j} = T_{i,j,\mathbf{k}(i,j)} \mid (i,j) \in \mathbb{Z}^2\}$ and coefficients $\{c_{i,j} \mid (i,j) \in \mathbb{Z}^2\}$. The goal is to give combinatorial interpretation for this expression. In this chapter, we study the case when p is above the $\mathbf{k}$ and $\mathbf{k}$ is above $\mathbf{fund}$, i.e.

$$k_0 \geq \mathbf{k}(i_0, j_0) \quad \text{and} \quad \mathbf{k}(i,j) \geq \mathbf{fund}(i,j) = (i + j \bmod 2) - 1. \tag{3.5}$$

In this case, we have explicit combinatorial solutions in terms of perfect matchings in Sections 3.3 and 3.4, non-intersecting paths in Section 3.5 and networks in Section 3.6.

3.3 Perfect-matching solution

The goal of this section is to give an expression of T_{i_0,j_0,k_0} in terms of a partition function of weighted perfect matchings of a certain graph. There are previous works [Spe07, MS10, JMZ13] on expressing cluster variables by using perfect matchings of certain weighted graphs. Regarding only cluster variables, the weight studied in [Spe07] coincides with the "face-weight" in Definition 3.9, while the weight in [MS10, JMZ13] coincides with the "edge-weight" in Definition 3.19. The height function in [JMZ13] is also another interpretation of the "pairing-weight" in Definition 3.10.

3.3.1 Graphs from stepped surfaces

We fix a point $p = (i_0, j_0, k_0) \in \mathbb{Z}^3_{\text{odd}}$, an admissible stepped surface $\mathbf{k}$ and an initial data $X_{\mathbf{k}}(\mathbf{t}) : \{T_{i,j,\mathbf{k}(i,j)} = t_{i,j} \mid i,j \in \mathbb{Z}\}$ on $\mathbf{k}$. Also assume that $k_0 \geq \mathbf{k}(i_0, j_0)$ and $\mathbf{k} \geq \mathbf{fund}$, i.e. $\mathbf{k}(i,j) \geq \mathbf{fund}(i,j)$ for all $(i,j) \in \mathbb{Z}^2$.

From the stepped surface $\mathbf{k}$, we follow the construction in [Spe07] and define, using Table 3.1, an infinite bipartite graph $G_{\mathbf{k}}$ associated with $\mathbf{k}$. This graph can also be realized as the dual of the quiver $\mathcal{Q}_{\mathbf{k}}$ associated with $\mathbf{k}$ with vertex bi-coloring, see the end of Section 3.2.1. Faces of $\mathcal{Q}_{\mathbf{k}}$ become vertices of $G_{\mathbf{k}}$. Since all faces of $\mathcal{Q}_k$ are always oriented, we color a vertex of the graph in white if the arrows around its corresponding face of the quiver are oriented counter-clockwise and black if they are oriented clockwise. Vertices of $\mathcal{Q}_{\mathbf{k}}$ become faces of $G_{\mathbf{k}}$. Since the vertices of the quiver are indexed by $\mathbb{Z}^2$, we will use $(i,j) \in \mathbb{Z}^2$ to represent a face of the graph. Arrows of $\mathcal{Q}_{\mathbf{k}}$ give edges of $G_{\mathbf{k}}$. There are three types of edges in the graphs: horizontal, vertical and diagonal,

$\mathbf{k}(D)$ $\mathbf{k}(C)$ $\mathbf{k}(A)$ $\mathbf{k}(B)$	A part in $\mathcal{Q}_{\mathbf{k}}$	A part in $G_{\mathbf{k}}$
k $k+1$ $k+1$ k	$D \leftarrow C$ $\downarrow \quad \uparrow$ $A \rightarrow B$	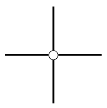
$k+1$ k k $k+1$	$D \rightarrow C$ $\uparrow \quad \downarrow$ $A \leftarrow B$	
$k-1$ k k $k+1$	$D \leftarrow C$ $\downarrow \nearrow \downarrow$ $A \leftarrow B$	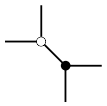
$k+1$ k k $k-1$	$D \rightarrow C$ $\uparrow \swarrow \uparrow$ $A \rightarrow B$	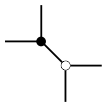
k $k+1$ $k-1$ k	$D \leftarrow C$ $\uparrow \searrow \uparrow$ $A \leftarrow B$	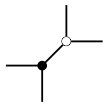
k $k-1$ $k+1$ k	$D \rightarrow C$ $\downarrow \nwarrow \downarrow$ $A \rightarrow B$	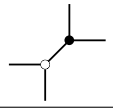

Table 3.1: All six local pictures of $\mathcal{Q}_{\mathbf{k}}$ and $G_{\mathbf{k}}$ for four points $A = (i, j)$, $B = (i + 1, j)$, $C = (i + 1, j + 1)$, and $D = (i, j + 1)$ on a stepped surface $\mathbf{k}$.

which came from vertical, horizontal and diagonal arrows of the quiver, respectively. See Figure 3.5 for an example.

If $\mathbf{k}'$ is obtained from $\mathbf{k}$ by a mutation at (i, j), then we can see from Table 3.1 that the face (i, j) in G_k must be a square. In addition, $G_{\mathbf{k}'}$ can be obtained [Ciu03, Spe07] from $G_{\mathbf{k}}$ by the following steps.

1. Apply *urban renewal* at the face (i, j), see Figure 3.6.

2. *Collapse* any degree-2 vertices created by the previous step, see Figure 3.7.

We use the notations $F(G)$, $V(G)$ and $E(G)$ for the set of faces, vertices and edges of a graph G, respectively. We then define two subsets $\mathring{F} = \mathring{F}(p, G_{\mathbf{k}})$ and $\partial F = \partial F(p, G_{\mathbf{k}})$ of $F(G_{\mathbf{k}}) = \mathbb{Z}^2$

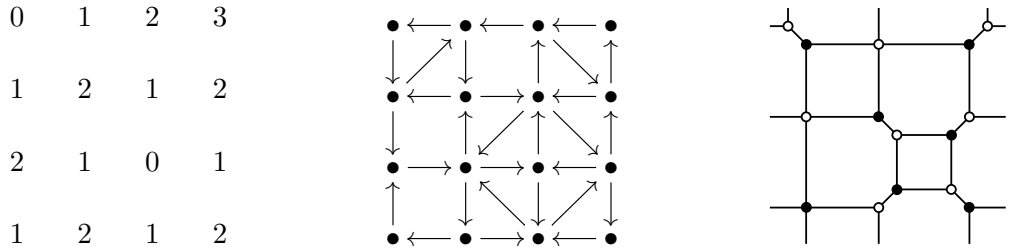

(a) A portion of $\mathbf{k}$ (b) A portion of $\mathcal{Q}_{\mathbf{k}}$ (c) A portion of $G_{\mathbf{k}}$

Figure 3.5: An example of $\mathbf{k}$ and its corresponding $\mathcal{Q}_k$ and $G_{\mathbf{k}}$.

Figure 3.6: The urban renewal at the face (i, j).

depending on p and $\mathbf{k}$ as follows.

$$\begin{aligned} \mathring{F} &= \left\{(i,j) \in \mathbb{Z}^2 \;\middle|\; |i-i_0| + |j-j_0| < k_0 - \mathbf{k}(i,j)\right\}, \\ \partial F &= \left\{(i',j') \in \mathbb{Z}^2 \setminus \mathring{F} \;\middle|\; |i'-i| + |j'-j| = 1 \text{ for some } (i,j) \in \mathring{F}\right\}. \end{aligned} \tag{3.6}$$

We also assume that $\partial F = \{(i_0, j_0)\}$ when $k_0 = \mathbf{k}(i_0, j_0)$. The set $\mathring{F}$ can be illustrated as the set of points inside (excluding boundary) the shadow projecting from p onto $\mathbf{k}$, while ∂F is the boundary of the projection. The following example shows elements of $\mathring{F}$ in blue and elements of ∂F in red when $p = (0, 0, 3)$ and $\mathbf{k} : (i, j) \mapsto |i + j| - 1$.

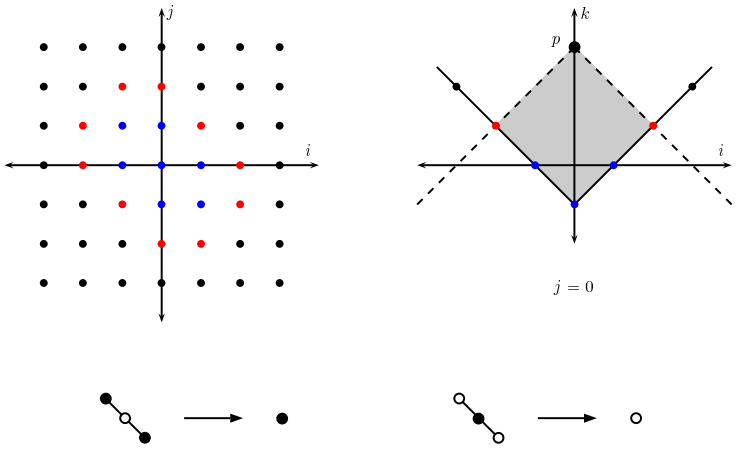

Figure 3.7: A degree-2 vertex and its two adjacent vertices collapse into one vertex.

The picture on the left shows the faces on (i, j)-plane, discarding the k-direction. The picture on the right shows the projection in the section $j = 0$ of the whole 3-dimensional space.

We will see later from the solution to the T-system (Theorem 3.13) that the expression of T_{i_0,j_0,k_0} depends only on $t_{i,j}$'s where $(i, j) \in \mathring{F} \cup \partial F$. Due to this reason, we will work on a finite subgraph $G_{p,\mathbf{k}}$ of $G_{\mathbf{k}}$ generated by the faces in $\mathring{F}$, while considering faces in ∂F as "open faces" as in the following definition.

Definition 3.5 (Graph with open faces [Spe07, Section 2.2])**.** The *graph with open faces* associated with p and $\mathbf{k}$ is defined to be a pair $(G, \partial F(G))$ where $G := G_{p,\mathbf{k}}$ is a finite subgraph of $G_{\mathbf{k}}$ generated by the faces in $\mathring{F}$, and $\partial F(G) := \partial F$ is the set of *open faces*.

Since we can always determine $\partial F(G)$ from $F(G)$, we will omit $\partial F(G)$ by writing just G instead of $(G, \partial F(G))$. The faces in $F(G) = \mathring{F}$ are called *closed faces*, while the faces in $\partial F(G) = \partial F$ are called *open faces*.

Later in the chapter, some other solutions to the T-systems with principal coefficients will look nicer if written in terms of the "closure" of G instead of G. This will be a graph with no open faces.

Definition 3.6 (The closure $\overline{G}$ of G)**.** For a point p and a surface $\mathbf{k}$, let $\mathbf{k}_p$ be the adjusted stepped surface associated with $\mathbf{k}$ and p defined in (3.1) and $G_\infty := G_{\mathbf{k}_p}$ be the graph associated to $\mathbf{k}_p$. We define the closure $\overline{G}$ of G to be the finite subgraph of G_∞ generated by $\mathring{F} \cup \partial F$, and we think of it as a graph with no open face.

We note that $\mathbf{k}(i, j) = \mathbf{k}_p(i, j)$ for all $(i, j) \in F(G) \cup \partial F(G)$. So the graphs with open faces $G_{p,\mathbf{k}}$ and $G_{p,\mathbf{k}_p}$ are exactly the same except for the shape of the open faces. Due to the following proposition, we can obtain $\overline{G}$ directly from G by closing all the open faces of G in a certain way.

Proposition 3.7. *All 16 types of the faces of $\overline{G}$ in $F(\overline{G}) \setminus F(G) = \partial F$ are shown in Figure 3.8 where dotted lines indicate edges in $E(\overline{G}) \setminus E(G)$.*

Proof. At each open face of G, we consider the height of its neighboring faces. The shape of the faces are obtained from Table 3.1. The proposition then easily follows. □

Example 3.8. Let $\mathbf{k}(i, j) = |i + j| - 1$ and $p = (0, 0, 3)$. Then the infinite graphs $G_{\mathbf{k}}$, $G_\infty = G_{\mathbf{k}_p}$ and the finite graphs $G = G_{p,\mathbf{k}}$, $\overline{G}$ are shown in Figure 3.9.

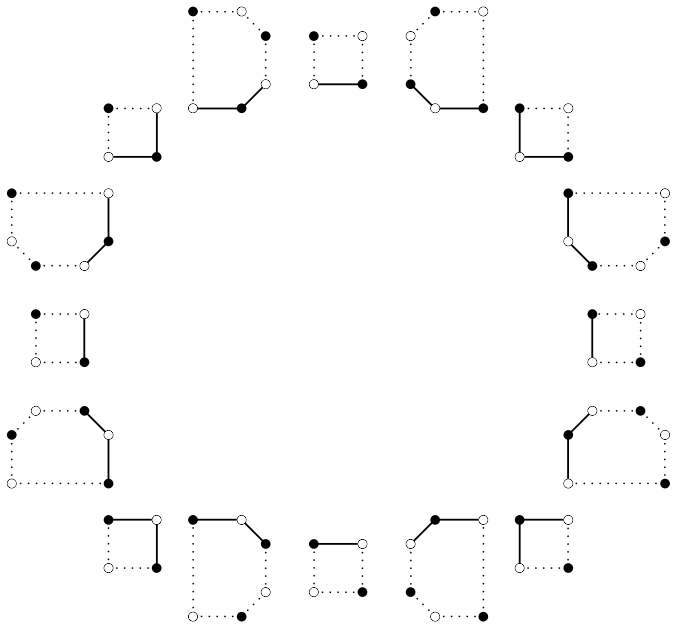

Figure 3.8: Faces in $F(\overline{G}) \setminus F(G) = \partial F$ of $\overline{G}$.

3.3.2 Face-weight and pairing-weight

From this point onward, we let $G := G_{p,\mathbf{k}}$ as a graph with open faces. Let $\mathcal{M}$ be a set of all perfect matchings, a.k.a. dimer configurations, of G. We recall that a perfect matching of G is a subset $M \subseteq E(G)$ such that each $v \in V(G)$ is incident to exactly one edge in M.

We define the face-weight w_f and the pairing-weight w_p on G, which contribute cluster variables/initial data $t_{i,j}$'s and coefficients $c_{i,j}$'s, respectively, to the expression of T_{i_0,j_0,k_0}.

Definition 3.9. For a face $(i,j) \in \mathring{F} \cup \partial F$, we define the *face-weight* depending on a perfect matching M of G as:

$$w_f(M) := \prod_{x \in \mathring{F} \cup \partial F} w_f(x),$$

where a contribution of a face to the product is defined as:

$$w_f(i,j) := \begin{cases} t_{i,j}^{\lceil \frac{b-a}{2} \rceil - 1}, & (i,j) \in \mathring{F}, \\ t_{i,j}^{\lceil \frac{b-a}{2} \rceil}, & (i,j) \in \partial F, \end{cases}$$

where a is the number of sides of (i,j) in the matching M and b the number of sides in $E(G) \setminus M$.

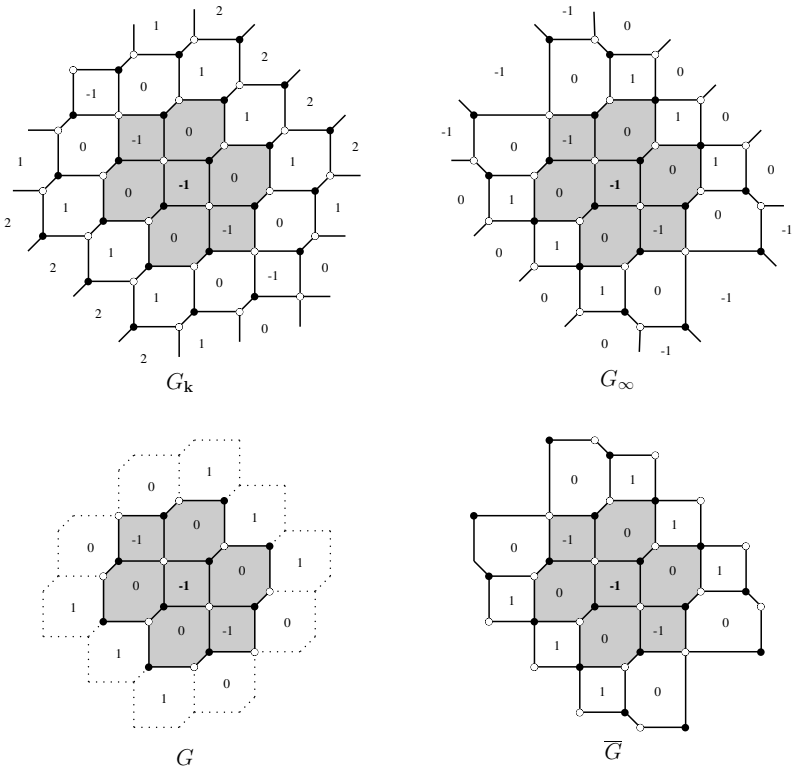

Figure 3.9: $G_{\mathbf{k}}$, G_∞, G and $\overline{G}$ when $\mathbf{k}(i,j) = |i+j| - 1$ and $p = (0,0,3)$. The shaded faces are the faces in $\mathring{F}$.

The pairing-weight will be defined on pairs of horizontal edges in M. We first note that there are exactly two types of horizontal edges in G as follows.

$N(i,j) :=$ 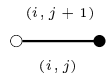

$S(i,j) :=$ 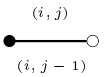

- a *white-black* horizontal edge, an edge joining a white vertex on the left and a black vertex on the right. We will call it $N(i,j)$, indexing by the face (i,j) below it (the north side of the face (i,j)).
- a *black-white* horizontal edge, an edge joining a black vertex on the left and a white vertex on the right. We will call it $S(i,j)$, indexing by the face (i,j) above it (the south side of the face (i,j)).

Let an *allowed pair* be a pair of $S(i,j_1)$ and $N(i,j_2)$ when $j_1 \leq j_2$ in the same column of the graph. In the other words, an allowed pair is a pair of a white-black horizontal edge above a black-white horizontal edge in the same column. We denote $\binom{N(i,j_2)}{S(i,j_1)}$ for an allowed pair. Since $F(G) \subset \mathbb{Z}^2$, for each i we can consider a subgraph of G generated by the faces in $F(G) \cap (\{i\} \times \mathbb{Z})$. In this column subgraph, we read from the bottom to the top and get a sequence of horizontal edges in the matching M. We then pair these edges into allowed pairs by the following steps.

1. If $S(i,j_1)$ and $N(i,j_2)$ where $j_1 \leq j_2$ are consecutive in the sequence, we pair the two.
2. Remove both $S(i,j_1)$ and $N(i,j_2)$ from the sequence, and repeat the first step until the sequence is empty.

We do this to all of the columns of G. The set P of all allowed pairs obtained by this process is called the *perfect pairing* of M. Proposition 3.12 will guarantee that the process works and the perfect pairing always exists. Now the pairing-weight is defined in the following definition.

Definition 3.10. Let P be the perfect pairing of a perfect matching M of G. The *pairing-weight* on M is defined to be:

$$w_p(M) := \prod_{x \in P} w_p(x),$$

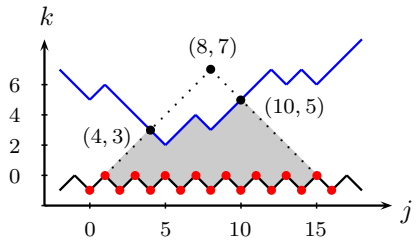

Figure 3.10: If $\mathbf{k}$ is the surface depicted in blue, then $w_p\binom{N(0,10)}{S(0,4)} = c_{0,0}c_{0,1}\dots c_{0,15} = J_{0,8,8}$ is shown in red. The picture is drawn in the section $i = 0$ of the 3-dimensional lattice.

where a contribution of an allowed pair in the product is defined as:

$$w_p\binom{N(i,j_2)}{S(i,j_1)} := J_{i,j',k'} = \prod_{a=j_1-\mathbf{k}(i,j_1)-1}^{j_2+\mathbf{k}(i,j_2)+1} c_{i,a},$$

and

$$\begin{aligned} j' &= j_1 - \mathbf{k}(i,j_1) + k' - 1 = j_2 + \mathbf{k}(i,j_2) - k' + 1, \\ k' &= \frac{\mathbf{k}(i,j_1) + \mathbf{k}(i,j_2) - j_1 + j_2}{2} + 1. \end{aligned}$$

A contribution of an allowed pair in the perfect pairing to the pairing-weight can be illustrated by Figure 3.10.

Example 3.11. Consider the following perfect matching M of the graph G from Example 3.8.

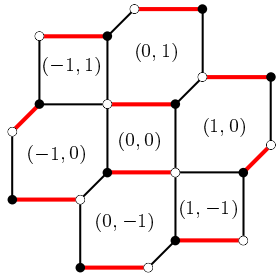

The perfect pairing is

$$P = \left\{ \binom{N(-1,1)}{S(-1,0)}, \binom{N(0,0)}{S(0,0)}, \binom{N(0,1)}{S(0,-1)}, \binom{N(1,0)}{S(1,-1)} \right\}.$$

We then have

$$w_p(M) = (c_{-1,-1}c_{-1,0}c_{-1,1})(c_{0,0})(c_{0,-2}c_{0,-1}\dots c_{0,2})(c_{1,-1}c_{1,0}c_{1,1}).$$

Also, the face-weight of M is $w_f(M) = t_{-2,0}t_{0,0}^{-1}t_{2,0}$.

Proposition 3.12. *Let M be a perfect matching of G. Then the following holds.*

1. *If all four adjacent faces of a face $(i,j) \in \mathring{F}$ have the same height, then the face (i,j) is a square. Also, the coloring around the face depends on the height of (i,j) and its neighbors as shown in Figure 3.11.*

2. *For each $i \in \mathbb{Z}$, we get $|\{S(i,j) \in M \mid j \in \mathbb{Z}\}| = |\{N(i,j) \in M \mid j \in \mathbb{Z}\}|$. That means the number of black-white horizontal edges in M and the number of white-black horizontal edges in M in the same column are equal.*

3. *For each $i, j \in \mathbb{Z}$, $|\{S(i,b) \in M \mid b \leq j\}| \geq |\{N(i,b) \in M \mid b \leq j\}|$. That means in any column of G the number of black-white horizontal edges in M dominates the number of the white-black edges in M when counting from bottom to top.*

Proof. (1) follows directly from Table 3.1. For (2) and (3), we first notice that if the point $p = (i_0, j_0, k_0)$ lies on the stepped surface $\mathbf{k}$ then the graph with open face associated to p and $\mathbf{k}$ is $(G, \partial F)$ where G is empty and $\partial F = \{(i_0, j_0)\}$. So (2) and (3) automatically hold.

If $k_0 > \mathbf{k}(i_0, j_0)$, then $G := G_{p,\mathbf{k}} = G_{p,\mathbf{k}_p}$, see (3.1). Without loss of generality, we can then assume that $\mathbf{k} = \mathbf{k}_p$. Then $\mathbf{k}$ is obtainable from the stepped surface $\mathbf{proj}_p$ by a finite number of downward mutations. We will show (2) and (3) using induction on the number of downward mutations from $\mathbf{proj}_p$.

When $\mathbf{k}$ is away from $\mathbf{proj}_p$ by only one downward mutation, G is a square of type (S1) in Figure 3.11. There are only two perfect matchings of the graph, which both satisfy (2) and (3).

Next, we assume that the claims hold for any surfaces which are away from $\mathbf{proj}_p$ by less than n mutations. Let $\mathbf{k}$ be a surface away from $\mathbf{proj}_p$ by n downward mutations. There must be an intermediate surface $\mathbf{k}'$ such that $\mathbf{k}'$ is obtained from $\mathbf{proj}_p$ by $n-1$ downward mutations and $\mathbf{k}$ is obtained from $\mathbf{k}'$ by one downward mutation, says at (i,j). We have two cases:

Figure 3.11: The only two possibilities of square faces. The values on the faces indicate their height.

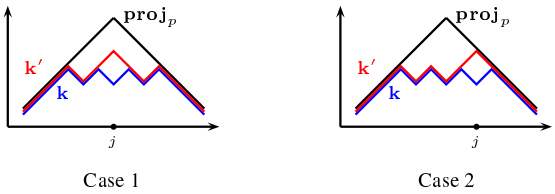

Case 1. If (i, j) is a closed face of $G_{p,\mathbf{k}'}$, then (i, j) is also a closed face of $G_{p,\mathbf{k}}$. $G_{p,\mathbf{k}}$ is obtained from $G_{p,\mathbf{k}'}$ by applying the urban renewal action at the face (i, j) then collapsing all degree-2 vertices created by the urban renewal. For any perfect matching M of $G_{p,\mathbf{k}}$, there exists a perfect matching M' of $G_{p,\mathbf{k}'}$ differing from M only at the face (i, j), see Figure 3.2. Since M' satisfies (2) and (3) by the induction hypothesis, we see from Figure 3.2 that M also satisfy (2) and (3). So they hold for any matchings of $G_{p,\mathbf{k}}$.

Case 2. If (i, j) is an open face of $G_{p,\mathbf{k}'}$, then (i, j) becomes a closed face of $G_{p,\mathbf{k}}$. We first consider the case when $i > i_0$ and $j > j_0$. $G_{p,\mathbf{k}}$ is obtained from $G_{p,\mathbf{k}'}$ by applying the urban renewal action at the face (i, j) and collapsing all degree-2 vertices created by the urban renewal. This yields the correspondence of the matchings of $G_{p,\mathbf{k}'}$ and $G_{p,\mathbf{k}}$ via Figure 3.3. With the same argument as for a closed face, (2) and (3) hold for any perfect matchings of $G_{p,\mathbf{k}}$. Similarly, if $i > i_0$ and $j = j_0$, the correspondence is shown in Figure 3.4, which implies (2) and (3) for any perfect matchings of $G_{p,\mathbf{k}}$. The other cases can be treated similarly.

From both cases, the statements (2) and (3) hold for every perfect matching of $G_{p,\mathbf{k}}$. By induction, we proved (2) and (3). □

We have defined face-weight and pairing-weight for perfect matchings of G. The previous proposition ensures that the pairing-weight is well-defined. We are now ready to state the main theorem.

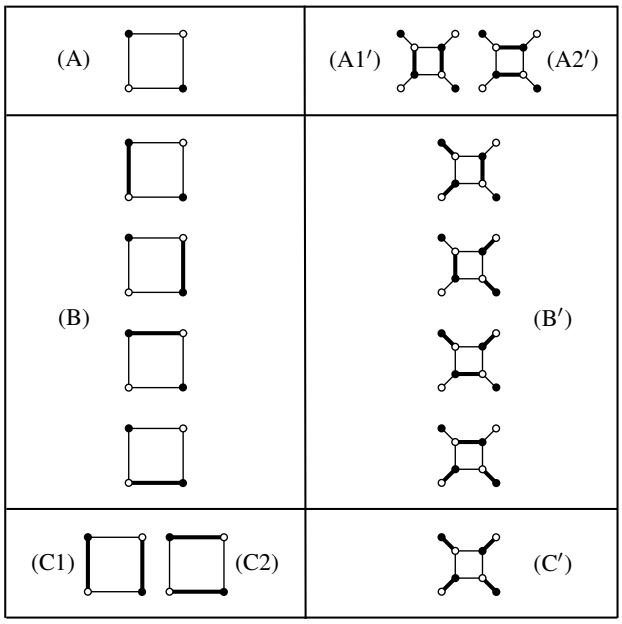

Table 3.2: The list of all correspondences between matchings before and after a single downward mutation at a closed face.

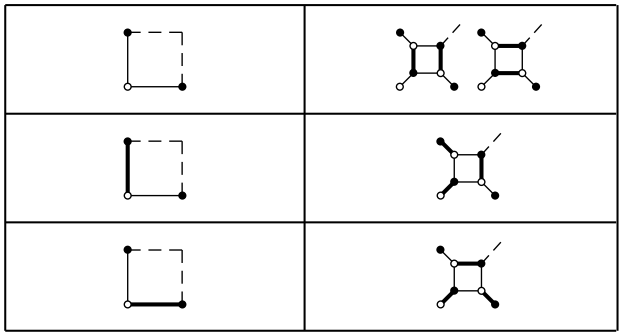

Table 3.3: The list of all correspondences between matchings before and after a single downward mutation at an open face (i, j) where $i > i_0$ and $j > j_0$.

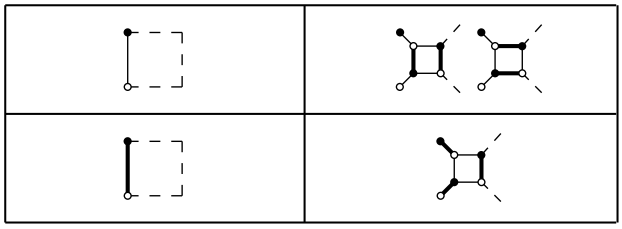

Table 3.4: The list of all correspondences between matchings before and after a single downward mutation at an open face (i, j) where $i > i_0$ and $j = j_0$.

3.3.3 Perfect-matching solution

Theorem 3.13 (Perfect-matching solution)**.** *Let $p = (i_0, j_0, k_0)$ and $\mathbf{k}$ be an admissible initial data stepped surface with respect to p where $k_0 \geq \mathbf{k}(i_0, j_0)$ and $\mathbf{k} \geq \mathbf{fund}$. Then*

$$T_{i_0,j_0,k_0} = \sum_{M \in \mathcal{M}} w_p(M) w_f(M) \tag{3.7}$$

where $\mathcal{M}$ is the set of all the perfect matchings of $G = G_{p,\mathbf{k}}$.

This solution specializes to the solution in [Spe07] for the coefficient-free T-system [Spe07, The Aztec Diamonds theorem] when $c_{i,j} = 1$ for all $(i, j) \in \mathbb{Z}^2$.

The proof of the theorem follows from the proof in [Spe07] using the "infinite completion" of $G = G_{p,\mathbf{k}}$, which is the same thing as $G_\infty = G_{\mathbf{k}_p}$ in our setup. To do so, we need to make sense of perfect matchings of G_∞ and weight on them.

Definition 3.14 (Acceptable perfect matching of G_∞)**.** We call a perfect matching M_∞ of G_∞ *acceptable* if $M_\infty \setminus E(G)$ is exactly the set of all the diagonal edges in $E(G_\infty) \setminus E(G)$.

We then extend the definition of the face-weight and the pairing-weight to acceptable perfect matchings of G_∞. Notice that G_∞ has no open faces. Also the weight of M and M_∞ are equal, i.e.

$$w_p(M_\infty) w_f(M_\infty) = w_p(M) w_f(M). \tag{3.8}$$

The following proposition gives a bijection between the perfect matchings of G and the acceptable perfect matching of G_∞.

Proposition 3.15 ([Spe07, Proposition 6])**.** *There exists a bijection between the set of all perfect matchings of G and the set of all acceptable perfect matchings of G_∞, which maps a perfect matching M of G to an acceptable perfect matching M_∞ of G_∞ where*

$$M_\infty = M \cup \{\textit{diagonal edges in } E(G_\infty) \setminus E(G)\}.$$

Example 3.16. Figure 3.12 shows an example of a perfect matching M of G and its corresponding acceptable perfect matching M_∞ of G_∞ from the bijection in Proposition 3.15. An edge in M_∞ is

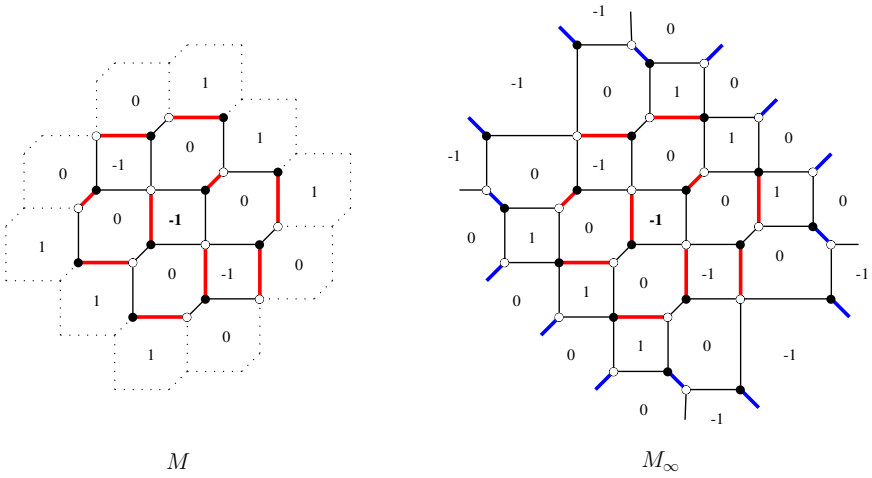

M M_∞

Figure 3.12: A perfect matching M of G and its corresponding acceptable perfect matching M_∞ of G_∞.

either an edge in M (described in red) or a diagonal edge in $E(G_\infty) \setminus E(G)$ (described in blue).

From (3.8) and Proposition 3.15, we can see that Theorem 3.13 is equivalent to the following theorem.

Theorem 3.17 (Perfect matching solution for G_∞)**.** *Let p and $\mathbf{k}$ be as in the assumption of Theorem 3.13 and $\mathbf{k}_p$ be defined as in (3.1). We have*

$$T_{i_0,j_0,k_0} = \sum_M w_p(M) w_f(M)$$

where the sum runs over all the acceptable perfect matchings of $G_\infty = G_{\mathbf{k}_p}$.

Proof. Since T_{i_0,j_0,k_0} depends only on $G_{p,\mathbf{k}} = G_{p,\mathbf{k}_p}$, we can assume without loss of generality that $\mathbf{k} = \mathbf{k}_p$. We will prove the theorem by using induction on the number of downward mutations from the top-most stepped surface $\mathbf{proj}_p$ to $\mathbf{k}$.

The base case is when $\mathbf{k} = \mathbf{proj}_p$. The graph $G_{\mathbf{proj}_p}$ is shown in Figure 3.13. There is only one acceptale perfect matching and its weight is $t_{i_0,j_0} = T_{i_0,j_0,k_0}$. So the theorem holds for the base case.

Assuming that the theorem holds for any stepped surfaces away from $\mathbf{proj}_p$ by less than n downward mutations, we let $\mathbf{k}$ be a surface obtained from $\mathbf{proj}_p$ by n downward mutations. Then

we can find an intermediate surface $\mathbf{k}'$ such that it is obtained from $\mathbf{proj}_p$ by $n-1$ downward mutations and $\mathbf{k}$ is obtained from $\mathbf{k}'$ by one downward mutation at (i,j). We also assume that $\mathbf{k}(i,j) = k-1$ and $\mathbf{k}'(i,j) = k+1$ for some $k \in \mathbb{Z}$. By the induction hypothesis we have

$$T_{i_0,j_0,k_0} = \sum_{\text{acceptable } M \text{ of } G_{\mathbf{k}'}} w_p(M) w_f(M).$$

Let M be any acceptable perfect matching of $G_{\mathbf{k}'}$. By Proposition 3.12, the face (i,j) of $G_{\mathbf{k}'}$ is a square of type (S2) in Figure 3.11. Then the matching M at the face (i,j) must be one of the 7 cases in the first column of Figure 3.2.

If M is of type (A) at (i,j), there are two matchings $M_{A1'}$ and $M_{A2'}$ of $G_{\mathbf{k}}$ of type $(A1')$ and $(A2')$, respectively, such that the matchings are the same except locally at the face (i,j). We then have

$$\begin{aligned} w_p(M_{A1'}) w_f(M_{A1'}) &= \frac{T_{i,j-1,k} T_{i,j+1,k}}{T_{i,j,k-1} T_{i,j,k+1}} w_p(M) w_f(M), \\ w_p(M_{A2'}) w_f(M_{A2'}) &= \frac{J_{i,j,k} T_{i-1,j,k} T_{i+1,j,k}}{T_{i,j,k-1} T_{i,j,k+1}} w_p(M) w_f(M). \end{aligned}$$

The term $J_{i,j,k}$ in the second equation came from an extra pair $\binom{N(i,j)}{S(i,j)}$ in $M_{A2'}$ which gives an extra term $J_{i,j,k}$ to the pairing-weight. By (3.2), we have

$$w_p(M_{A1'}) w_f(M_{A1'}) + w_p(M_{A2'}) w_f(M_{A2'}) = w_p(M_A) w_f(M_A). \tag{3.9}$$

If M is of type (B), there exists a unique corresponding matching $M_{B'}$ of $G_{\mathbf{k}}$ of type (B'). We see that the weight of M and $M_{B'}$ are equal. That is

$$w_p(M_{B'}) w_f(M_{B'}) = w_p(M) w_f(M). \tag{3.10}$$

If M is of type $(C1)$ (resp. $(C2)$), let M' be another matching of $G_{\mathbf{k}'}$ of type $(C2)$ (resp. $(C1)$) which is the same as M except for the two edges at the face (i,j). Without loss of generality, we assume that M is of type $(C1)$ and M' is of type $(C2)$. Then there exists a corresponding perfect

matching $M_{C'}$ of $G_{\mathbf{k}}$ of type (C'). We then have

$$w_p(M)w_f(M) = \frac{T_{i,j-1,k}T_{i,j+1,k}}{T_{i,j,k-1}T_{i,j,k+1}} w_p(M_{C'})w_f(M_{C'}).$$

To write $w_p(M')$ in terms of $w_p(M_{C'})$, we first notice that there must be two other edges $S(i,j_1), N(i,j_2) \in M'$ where $j_1 < j < j_2$ such that both pairs $\binom{N(i,j-1)}{S(i,j_1)}$ and $\binom{N(i,j_2)}{S(i,j+1)}$ are in the perfect pairing of M', while in its corresponding $M_{C'}$ there is only $\binom{N(i,j_2)}{S(i,j_1)}$. Thus we have

$$w_p(M') = \frac{\prod_{b=j_1-k_1-1}^{j-1+k+1} c_{i,b} \prod_{b=j+1-k-1}^{j_2+k_2+1} c_{i,b}}{\prod_{b=j_1-k_1-1}^{j_2+k_2+1} c_{i,b}} w_p(M_{C'}) = J_{i,j,k} w_p(M_{C'}),$$

and so

$$w_p(M')w_f(M') = \frac{J_{i,j,k}T_{i-1,j,k}T_{i+1,j,k}}{T_{i,j,k-1}T_{i,j,k+1}} w_p(M_{C'})w_f(M_{C'}).$$

Hence,

$$w_p(M)w_f(M) + w_p(M')w_f(M') = w_p(M_{C'})w_f(M_{C'}). \tag{3.11}$$

By (3.9), (3.10), (3.11) and the induction hypothesis, we can conclude that

$$\sum_{\text{acceptable } M \text{ of } G_{\mathbf{k}}} w_p(M)w_f(M) = \sum_{\text{acceptable } M \text{ of } G_{\mathbf{k}'}} w_p(M)w_f(M) = T_{i_0,j_0,k_0}.$$

So the statement holds for $\mathbf{k}$. By the induction, we proved the theorem. □

Now we have proved Theorem 3.13 and Theorem 3.17. In the proof of Theorem 3.17, we notice that for any acceptable perfect matching M_∞ of G_∞, any face outside $\mathring{F} \cup \partial F$ always gives 1 for its face-weight. Also edges in $M_\infty \setminus E(G)$ are all diagonal, so they will not contribute any weight to the partition function. We then have the following perfect-matching solution for the closure $\overline{G}$ of G.

Theorem 3.18 (Perfect matching solution for $\overline{G}$)**.** *Let p and $\mathbf{k}$ be as in the assumption of Theorem*

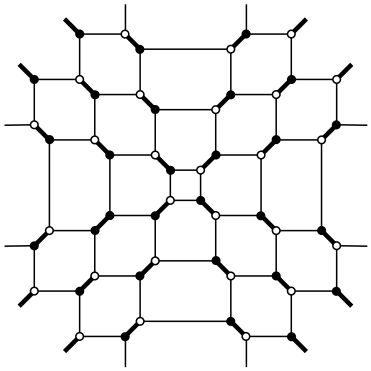

Figure 3.13: The only one acceptable perfect matching of $G_{\mathbf{proj}_p}$. The center face of the graph is (i_0, j_0).

3.13 and $\overline{G}$ *be the closure of* $G = G_{p,\mathbf{k}}$ *defined as in Definition 3.6. We have*

$$T_{i_0,j_0,k_0} = \sum_{\overline{M} \in \overline{\mathcal{M}}} w_p(\overline{M}) w_f(\overline{M})$$

where $\overline{\mathcal{M}} := \left\{ \overline{M} = M \cup \mathrm{Diag}(E(\overline{G}) \setminus E(G)) \mid M \in \mathcal{M} \right\}$, $\mathrm{Diag}(A)$ *is the set of all diagonal edges in* A*, and* $\mathcal{M}$ *is the set of all perfect matchings of* G*.*

We now have a combinatorial expression of T_{i_0,j_0,k_0} as a partition function of face-weight and pairing-weight over all perfect matchings of a graph. In the next section, we will combine the two weights together and construct an edge-weight. This will be the first step toward our next aim to construct a solution in terms of networks, analog to [DF14] for the coefficient-free T-system.

3.4 Perfect-matching solution via edge-weight

Now that we have multiple versions of the perfect matching solution to the T-system with principal coefficients in Theorem 3.13, Theorem 3.17 and Theorem 3.18, our next goal is to find a network solution analog to the network solution for coefficient-free T-systems studied in [DFK13, DF14]. One big advantage of the network solution is its explicit solution via the network matrices. In the perfect matching solution, we need to enumerate all the perfect matchings of the graph G in order to compute the solution. For the network solution, we associate an initial data stepped surface with a product of network matrices. Then the solution is just a certain minor of the product.

In order to get the network solution, we first transform the face-weight and the pairing-weight studied in the last section to the edge-weight w_e (Definition 3.19) on edges of the closure $\overline{G}$ of G, which also gives us a new perfect-matching solution but with the edge-weight w_e (Theorem 3.22). This solution will be used to construct a nonintersecting-path solution in the next section. We also note that our edge-weight coincide with the weight studied in [MS10] in the case when all $c_{i,j} = 1$. In [JMZ13], the edge-weight is exactly the same as our edge-weight except that the contribution of the coefficients is in the form of the height function, which is another interpretation of our pairing-weight.

Definition 3.19 (Edge-weight w_e)**.** Let $\mathbf{k}$ be an admissible initial stepped surface with respect to p, $\overline{G}$ be the closure of the graph $G = G_{p,\mathbf{k}}$. For each edge of $\overline{G}$ we assign the *edge-weight* w_e as follows:

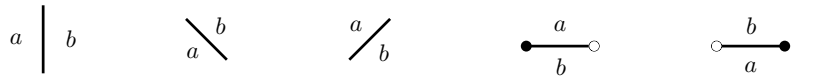

$(t_a t_b)^{-1}$ $\quad$ $(t_a t_b)^{-1}$ $\quad$ $(t_a t_b)^{-1}$ $\quad$ $p_a (t_a t_b)^{-1}$ $\quad$ $(\overline{p}_a)^{-1}(t_a t_b)^{-1}$

where p_a and $\overline{p}_a$ are the following formal products

$$p_a = \prod_{\alpha=j-k-1}^{\infty} c_{i,\alpha} \quad \text{and} \quad \overline{p}_a = \prod_{\alpha=i+k+2}^{\infty} c_{i,\alpha}$$

when $a = (i, j)$ and $k = \mathbf{k}(i, j)$. We also assume that $t_a = 1$ when $a \notin F(\overline{G})$ and $p_a = \overline{p}_a = 1$ when $a \notin F(G)$.

Definition 3.20. Let $\mathcal{M}$ be the set of all perfect matching of G. For a matching $M \in \mathcal{M}$, we let

$$\overline{M} := M \cup \mathrm{Diag}(E(\overline{G}) \setminus E(G))$$

be its corresponding (not necessary perfect) matching of $\overline{G}$ where $\mathrm{Diag}(A)$ is the set of all diagonal edges in A for $A \subseteq E(\overline{G})$. Also let

$$\overline{\mathcal{M}} := \left\{ \overline{M} \mid M \in \mathcal{M} \right\},$$
$$\overline{M}_0 := \left\{ \text{all white-black horizontal and diagonal edges of } \overline{G} \right\}.$$

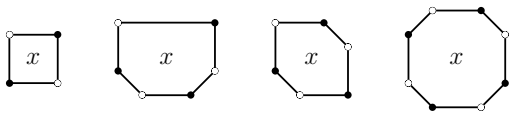

Figure 3.14: All possible faces of $\overline{G}$ up to $\frac{\pi}{2}$ rotation and i-axis reflexion.

Then the *edge-weight* of a matching $\overline{M} \in \overline{\mathcal{M}}$ is

$$w_e(\overline{M}) := \prod_{x \in \overline{M}} w_e(x). \tag{3.12}$$

We note that $\overline{M}$ and $\overline{M}_0$ are not necessary perfect matchings of $\overline{G}$. Also for $j_1 \leq j_2$,

$$p_{(i,j_1)}(\overline{p}_{(i,j_2)})^{-1} = \prod_{\alpha=j_1-\mathbf{k}(i,j_1)-1}^{j_2+\mathbf{k}(i,j_2)+1} = w_p\begin{pmatrix} N(i,j_2) \\ S(i,j_1) \end{pmatrix}.$$

By Proposition 3.12, the product in (3.12) is indeed a finite product of pairing-weights, hence a finite product of $c_{i,j}$'s.

The following lemma interprets the face-weight of a matching $\overline{M}$ as a function of $\overline{M}$ and our special matching $\overline{M}_0$.

Lemma 3.21. *For $x \in F(\overline{G})$ and $\overline{M} \in \overline{\mathcal{M}}$, we have*

$$w_f(x) = t_x^{N_x - D_x}$$

where $N_x = \big|\{e \in \overline{M}_0 \mid e \text{ is a side of } x\}\big|$ and $D_x = \big|\{e \in \overline{M} \mid e \text{ is a side of } x\}\big|$.

Proof. We can easily check that for all $x \in F(\overline{G}) = \mathring{F} \cup \partial F$, we get $w_f(x) = t_x^{\lceil \frac{N-D}{2} \rceil - 1}$ where N and $D = D_x$ are the numbers of sides of x which are not in $\overline{M}$ and are in $\overline{M}$, respectively. Let $S \in \{4, 6, 8\}$ be the number of sides of x. Then $N = S - D$. So

$$w_f(x) = t_x^{\lceil \frac{S-2D}{2} \rceil - 1} = t_x^{S/2-D-1}.$$

Since x must be one of the cases in Figure 3.14, we have $S/2 - 1 = N_x$. Hence $w_f(x) = t_x^{N_x - D_x}$. □

Theorem 3.22 (Perfect-matching solution for $\overline{G}$ with the edge-weight w_e)**.** *Let* $\mathbf{k}$ *be an admissible initial data stepped surface with respect to* $p = (i_0, j_0, k_0)$*,* $\overline{M}$ *and* $\overline{M}_0$ *be defined as in Definition 3.20. Then*

$$T_{i_0,j_0,k_0} = \sum_{\overline{M} \in \overline{\mathcal{M}}} w_e(\overline{M}) \Big/ w_e(\overline{M}_0)\big|_{c_{i,j}=1}$$

where $w_e(\overline{M}_0)\big|_{c_{i,j}=1}$ *denotes the substitution* $c_{i,j} = 1$ *for any* $(i,j) \in \mathbb{Z}^2$*.*

Proof. Let $\overline{M} \in \overline{\mathcal{M}}$. By Lemma 3.21, we get

$$w_f(\overline{M}) = \prod_{x \in F(\overline{G})} t_x^{N_x - D_x} = \prod_{x \in F(\overline{G})} t_x^{N_x} \prod_{x \in F(\overline{G})} t_x^{-D_x}.$$

By Definition 3.19, it equals to

$$w_f(\overline{M}) = \left(w_e(\overline{M}_0)\big|_{c=1} \right)^{-1} \prod_{x \in F(\overline{G})} t_x^{-D_x}.$$

Thus we have

$$\prod_{x \in F(\overline{G})} t_x^{-D_x} = w_f(\overline{M}) w_e(\overline{M}_0)\big|_{c=1}. \tag{3.13}$$

By the definition of w_e, we consider

$$w_e(\overline{M}) = \prod_{y \in \overline{M}} w_e(y) = \prod_{\bullet \overset{a}{-} \circ \in \overline{M}} p_a \prod_{\circ \overset{b}{-} \bullet \in \overline{M}} \overline{p}_b \prod_{x \in F(\overline{G})} t_x^{-D_x}.$$

From (3.13) and the fact that $\overline{M} \setminus M$ contains only diagonal edges, we then get

$$w_e(\overline{M}) = \prod_{\bullet \overset{a}{-} \circ \in M} p_a \prod_{\circ \overset{b}{-} \bullet \in M} \overline{p}_b \; w_f(\overline{M}) w_e(\overline{M}_0)\big|_{c=1}.$$

Since

$$\prod_{\bullet \overset{a}{-} \circ \in M} p_a \prod_{\circ \overset{b}{-} \bullet \in M} \overline{p}_b = w_p(\overline{M}),$$

we conclude that $w_f(\overline{M}) w_p(\overline{M}) = w_e(\overline{M}) / w_e(\overline{M}_0)\big|_{c=1}$ for any $\overline{M} \in \overline{\mathcal{M}}$. By Theorem 3.18, we have

$T_{i_0,j_0,k_0} = \sum_{\overline{M}\in\overline{\mathcal{M}}} w_e(\overline{M})/w_e(\overline{M}_0)|_{c=1}$. □

Now we have a combinatorial expression of T_{i_0,j_0,k_0} in terms of a partition function of edge-weight over all matchings $\overline{G}$. In the next section, we give an explicit bijection between perfect matchings and non-intersecting paths (with certain sources and sinks) in both G and $\overline{G}$. Using this bijection, we are able to transform the perfect-matching solutions to a solution in terms of non-intersecting paths.

3.5 Non-intersecting path solution

In this section, we provide an explicit bijection (Proposition 3.35) between the perfect matchings of G and the non-intersecting paths in the oriented graph G with certain sources and sinks. It can be extended to a bijection between the matchings in $\overline{\mathcal{M}}$ of $\overline{G}$ and the non-intersecting paths in the oriented graph $\overline{G}$ with certain sources and sinks (Proposition 3.37). Using this bijection and a new weight w'_e modified from the edge-weight w_e, we can write the solution to the T-system in terms of non-intersecting paths in $\overline{G}$ (Theorem 3.40).

3.5.1 Some setup

We first show some properties of the graph G and $\overline{G}$.

Proposition 3.23. *G and $\overline{G}$ are bipartite and connected.*

Proof. It was proved in [Spe07, Section 3.5] that G is bipartite and connected. The extended result to $\overline{G}$ follows from Proposition 3.7. □

Definition 3.24. For two vertices v, v' of a graph, we say that v (resp. v') is on the *left* (resp. *right*) of v' (resp. v) if there is a sequence of vertices of the graph $v = v_0, v_1, v_2, \ldots, v_n = v'$ such that any two consecutive vertices are connected by one of the following edges.

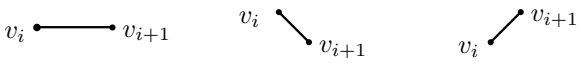

We center the graph at the face (i_0, j_0). Then the notions of the North-West, North-East, South-West and South-East of the center are well-defined.

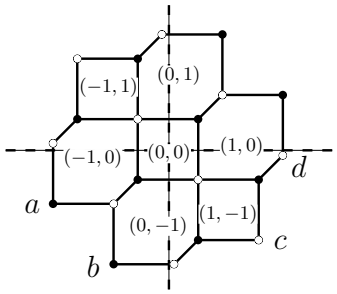

Figure 3.15: With $(0,0)$ as the center face, we have $|V_{SW}(G)| = 4$, $|V_{SE}(G)| = 6$, $V_{\text{leftSW}}(G) = \{a, b\}$ and $V_{\text{rightSE}}(G) = \{c, d\}$.

Definition 3.25. We denote by $V_{\text{NW}}(G)$, $V_{\text{NE}}(G)$, $V_{\text{SW}}(G)$ and $V_{\text{SE}}(G)$ the set of all the vertices of a graph G in the North-West, North-East, South-West and South-East of the center face (i_0, j_0), respectively. Also let $V_{\text{leftNW}}(G)$, $V_{\text{rightNE}}(G)$, $V_{\text{leftSW}}(G)$, $V_{\text{rightSE}}(G)$ be the set of all left-most NW vertices, right-most NE, left-most SW and right-most SE vertices of G, respectively. See Figure 3.15 for an example.

Proposition 3.26. *G has the following properties.*

1. *Vertices in $V_{\text{leftSW}}(G) \cup V_{\text{rightNE}}(G)$ are black.*
2. *Vertices in $V_{\text{rightSE}}(G) \cup V_{\text{leftNW}}(G)$ are white.*
3. $|V_{\text{leftSW}}(G)| = |V_{\text{rightSE}}(G)|$.
4. $|V_{\text{leftNW}}(G)| = |V_{\text{rightNE}}(G)|$.

Proof. To show (1), we use the same analysis as in the proof of Proposition 5 in [Spe07]. It is clear that a left-most vertex must be on the boundary of G. We then consider an open face $(i, j) \in \partial F$ on the South-West of (i_0, j_0) with height $k \in \mathbb{Z}$. All the eight possibilities are shown in Figure 3.16, where the face of height k in the circle is (i, j). We see that all the left-most South-West vertices must be black. A similar argument can be used to show the other case of (1) and (2). In order to show (3), we consider a maximal sequence $v_0, v_1, \ldots, v_n$ of vertices of G such that v_i is on the left of v_{i+1} for all i. We have $v_0 \in V_{\text{leftSW}}(G)$ if and only if $v_n \in V_{\text{rightSE}}(G)$. This gives a bijection between $V_{\text{leftSW}}(G)$ and $V_{\text{rightSE}}(G)$. So we proved (3). The similar argument also shows (4). □

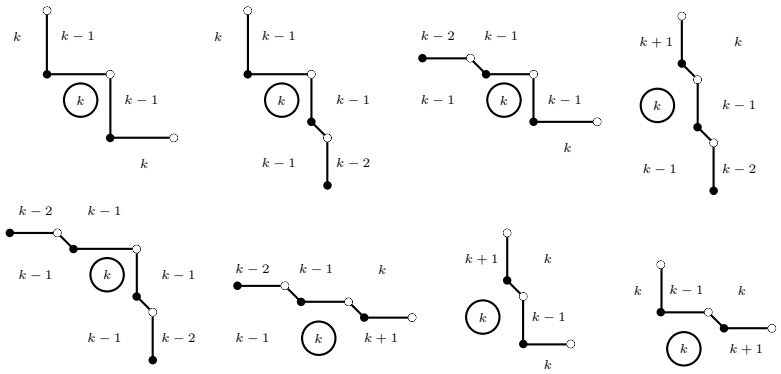

Figure 3.16: All the eight possibilities of the boundary near an open face in the South-West of the center. The face is of height k and is marked by a circle.

3.5.2 Non-intersecting paths and perfect matchings

We will give an explicit bijection between the perfect matchings of G and the non-intersecting paths from $V_{\text{leftSW}}(G)$ to $V_{\text{rightSE}}(G)$ in G (Proposition 3.35). This bijection can be extended to $\overline{G}$ in Proposition 3.37.

In order to define a path in G and $\overline{G}$, we need an orientation of the graphs.

Definition 3.27 (Edge orientation of G and $\overline{G}$)**.** Let the orientation of the edges of G and $\overline{G}$ be such that it goes from left to right for diagonal and horizontal edges and from a black vertex to a white vertex for the vertical as follows.

Definition 3.28. Let $G = G_{p,\mathbf{k}}$ and $\overline{G}$ be as in Definition 3.6. With the notations from Definition

3.25, we define

$$
\begin{aligned}
M_0 &:= \{\text{white-black horizontal and diagonal edges of } G\},\\
\overline{M}_0 &:= \{\text{white-black horizontal and diagonal edges of } \overline{G}\},\\
\mathcal{M} &:= \{\text{perfect matchings of } G\},\\
\overline{\mathcal{M}} &:= \{\overline{M} = M \cup \mathrm{Diag}(E(\overline{G}) \setminus E(G)) \mid M \in \mathcal{M}\},\\
\mathcal{P} &:= \{\text{non-intersecting paths from } V_{\mathrm{leftSW}}(G) \text{ to } V_{\mathrm{rightSE}}(G) \text{ on } G\},\\
\overline{\mathcal{P}} &:= \{\text{non-intersecting paths from } V_{\mathrm{leftSW}}(\overline{G}) \text{ to } V_{\mathrm{rightSE}}(\overline{G}) \text{ on } \overline{G}\}.
\end{aligned}
$$

The map Φ (resp. $\overline{\Phi}$) in the following definition is indeed the bijection between $\mathcal{M}$ and $\mathcal{P}$ (resp. between $\overline{\mathcal{M}}$ and $\overline{\mathcal{P}}$). They will be key ingredients to construct our nonintersecting-path solution.

Definition 3.29. We define a map $\Phi : \mathcal{M} \to \mathcal{P}$ by

$$\Phi(M) := M \triangle M_0, \quad \text{for } M \in \mathcal{M}.$$

This map can be extended to a map $\overline{\Phi} : \overline{\mathcal{M}} \to \overline{\mathcal{P}}$ defined by

$$\overline{\Phi}(\overline{M}) := \overline{M} \triangle \overline{M}_0, \quad \text{for } \overline{M} \in \overline{\mathcal{M}},$$

where $A \triangle B := A \cup B \setminus A \cap B = (A \setminus B) \sqcup (B \setminus A)$ is the symmetric difference of A and B. The notation $\sqcup$ represents the disjoint union.

Remark 3.30. It is worth mentioning that if we consider $M \in \mathcal{M}$ and $P \in \mathcal{P}$ as sets of dimers on edges of G, then the action of Φ can be interpreted as superposing with M_0 and counted the number of dimers on each edge modulo 2. Similarly, $\overline{\Phi}$ is the superposition with $\overline{M}_0$ with number of dimers being counted modulo 2.

Example 3.31. This example shows an interpretation of the map Φ on $\mathcal{M}$ as the superposition with M_0 modulo 2.

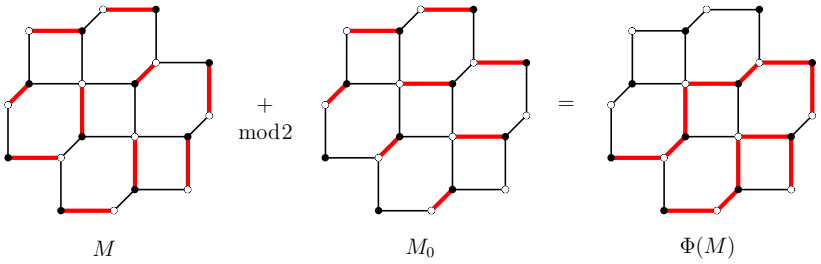

We notice that the image of the map is indeed an element in $\mathcal{P}$.

Using the following lemmas, Proposition 3.35 shows that Φ is a well-defined bijection from $\mathcal{M}$ to $\mathcal{P}$.

Lemma 3.32. *Let $M \in \mathcal{M}$. Then $\Phi(M)$ has the following properties.*

1. *For any vertex in $V_{\text{leftSW}}(G) \cup V_{\text{rightSE}}(G)$, exactly one of its incident edges is in $\Phi(M)$.*

2. *For the other vertices, either none or two of their incident edges are in $\Phi(M)$.*

Proof. To show (1), we first consider a vertex in $V_{\text{leftSW}}(G)$. By the fact that M is a perfect matching, exactly one of its incident edges is in M. By Proposition 3.26, the vertex is black. Since it is the left-most, none of its incident edges is in M_0. This is because there cannot be a white vertex on its left. So, exactly one of its incident edges is in $\Phi(M)$. Similarly, exactly one incident edge of a vertex in $V_{\text{rightSE}}(G)$ is in M. There is none of its edges is in M_0 because the vertex is white and the right-most. Hence (1) holds.

For (2), if a vertex is not in $V_{\text{leftSW}}(G) \cup V_{\text{rightSE}}(G)$, it must be either in $V_{\text{leftNW}}(G) \cup V_{\text{rightNE}}(G)$ or it has both left and right adjacent vertices. For a vertex in $V_{\text{leftNW}}(G) \cup V_{\text{rightNE}}(G)$, there is one of its incident edges in M, and also one in M_0. They can be the same or different. So, either none or two of its incident edges are in $\Phi(M)$. For a vertex having left and right adjacent vertices, one of its incident edges must be in M_0. This is because the vertex is either black and is on the right of a white vertex, or white and on the left of a black vertex. Also its one of the incident edges must be in M because M is a perfect matching. So either none or two of its incident edges are in $\Phi(M)$. Hence (2) holds. □

Lemma 3.33. *For a black vertex of G having two incident edges in $\Phi(M)$, the two edges must be of the form A, B or C in Figure 3.17 where the horizontal edges in the figure represent horizontal or diagonal edges of G.*

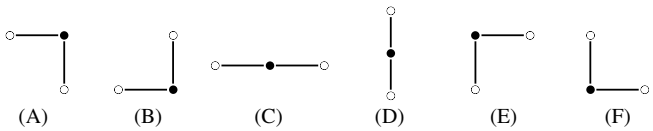

Figure 3.17: All configurations of two incident edges of a black vertex of G. The horizontal edges in the picture represent horizontal/diagonal edges of G.

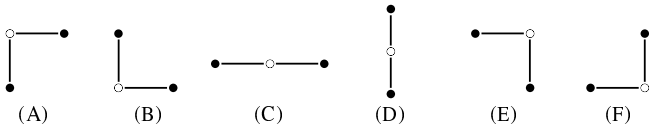

Figure 3.18: All configurations of two incident edges of a white vertex of G. The horizontal edges in the picture represent horizontal/diagonal edges of G.

Proof. It is easy to see that the six cases in Figure 3.17 are all configurations of two incident edges of a vertex of G. Since M is a perfect matching, one of the two edges must come from M_0. Since the cases (D), (E) and (F) contain no edge from M_0, they cannot happen. □

Lemma 3.34. *For a white vertex of G having two incident edges in $\Phi(M)$, the two edges must be of the form A, B or C in Figure 3.18 where the horizontal edges in the figure represent horizontal or diagonal edges of G.*

Proof. Similar to Lemma 3.33. □

Proposition 3.35. *$\Phi : \mathcal{M} \to \mathcal{P}$ is a bijection.*

Proof. To show that $\Phi(M)$ is well-defined, we need to show that $\Phi(M)$ is a collection of non-intersecting paths from $V_{\text{leftSW}}(G)$ to $V_{\text{rightSE}}(G)$ in G, where G is oriented as in Definition 3.27. From Lemma 3.33 and Lemma 3.34, only the case (A), (B) or (C) can happen at any vertex. From this, all the vertices incident to two edges in $\Phi(M)$ are neither source nor sink. So $\Phi(M)$ is a set of non-intersecting paths in the oriented graph G, where a source or a sink is incident to exactly one edge in $\Phi(M)$. From Lemma 3.32, the sources and the sinks must in $V_{\text{leftSW}}(G) \cup V_{\text{rightSE}}(G)$. But (1) and (2) of Proposition 3.26 guarantees that $V_{\text{leftSW}}(G)$ must be the source and $V_{\text{rightSE}}(G)$ must be the sink. It remains to show that there is no loop in $\Phi(M)$. Since every vertex in a loop

are neither source nor sink, there must be an horizontal/diagonal edge oriented from right to left. This contradicts the orientation of G. So $\Phi(M)$ contains no loop.

To show that Φ is a bijection, we construct another map $\Psi : \mathcal{P} \to \mathcal{M}$ by letting $\Psi(P)$ be the superposition of the path P with M_0 and counting dimers on each edge modulo 2. In other words $\Psi(P) = (P \cup M_0) \setminus (P \cap M_0)$. It is obvious that $\Psi \circ \Phi = \mathrm{id}_{\mathcal{M}}$ and $\Phi \circ \Psi = \mathrm{id}_{\mathcal{P}}$. So, $\Psi = \Phi^{-1}$ provided that Ψ is well-defined. To show that $\Psi(P)$ is a perfect matching of G, it suffices to show that any vertex has exactly one incident edge in $\Psi(P)$.

We first consider a black vertex.

- If it is in $V_{\mathrm{leftSW}}(G)$, it has one incident edge in P because it is a source. Also, it has no edge in M_0 since it is the left-most. So, it still has one incident edge in $\Psi(P)$ after the superposition.
- If it is not in $V_{\mathrm{leftSW}}(G)$, it has either none or two edges in P. In both cases, since the vertex is not the left-most, there must be a white vertex on its left. So it has an incident edge in M_0.
  - If it has no edge in P, it will receive an edge from M_0 after mapping by Ψ.
  - If it has two edges in P, it is either of the case A, B or C in Figure 3.17. So exactly one of the edges gets removed after superposing with M_0.

  From both cases, the vertex is incident to exactly one edge in $\Psi(P)$.

A similar argument holds for a white vertex. So we conclude that $\Psi(P) \in \mathcal{M}$. □

Proposition 3.36. *Let $e \in M_0$. Then $e \in M$ if and only $e \notin \Phi(M)$*

Proof. Let $e \in M_0$. If $e \in M$, then $e \in M \cap M_0$. Hence $e \notin (M \cup M_0) \setminus (M \cap M_0) = \Phi(M)$. On the other hand, if $e \notin M$, then $e \notin M \cap M_0$. Hence $e \in (M \cup M_0) \setminus (M \cap M_0) = \Phi(M)$. □

Now we have analogs to Proposition 3.35 and Proposition 3.36 for $\overline{G}$.

Proposition 3.37. *Let $\overline{\Phi}$ be defined as in Definition 3.29. Then we have the following:*

1. *$\overline{\Phi} : \overline{\mathcal{M}} \to \overline{\mathcal{P}}$ is a bijection,*

2. For $e \in \overline{M}_0$, $e \in \overline{M}$ if and only $e \notin \overline{\Phi}(\overline{M})$.

Proof. We recall that the symmetric difference $\triangle$ is commutative and associative. Let $\overline{D} = \text{Diag}(E(\overline{G}) \setminus E(G))$. Since $M \cap \overline{D} = \emptyset$ for $M \in \mathcal{M}$, $\mathcal{M}$ and $\overline{\mathcal{M}}$ are in bijection via the map:

$$f : M \mapsto M \cup \overline{D} = M \triangle \overline{D},$$

with the inverse map:

$$f^{-1} : \overline{M} \mapsto \overline{M} \triangle \overline{D}.$$

Consider $\overline{P} \in \overline{\mathcal{P}}$, we can see from Proposition 3.7 that the paths from $V_{\text{leftSW}}(\overline{G})$ must go to the right via horizontal or diagonal edges in $E(\overline{G}) \setminus E(G)$. Similarly, the paths will arrive $V_{\text{rightSE}}(\overline{G})$ via horizontal or diagonal edges in $E(\overline{G}) \setminus E(G)$. Since there is a unique choice of these edges, we have $\overline{P} = P \cup \overline{P}_0$ where $\overline{P}_0 \subset E(\overline{G}) \setminus E(G)$ is the set of all horizontal and diagonal edges in the South-West, South or South-East. Note that $\overline{P}_0$ is also equal to the set of white-black horizontal and black-white diagonal edges in $E(\overline{G}) \setminus E(G)$. Since $P \cap \overline{P}_0 = \emptyset$ for $P \in \mathcal{P}$, $\mathcal{P}$ and $\overline{\mathcal{P}}$ are in bijection via the map:

$$g : P \mapsto P \cup \overline{P}_0 = P \triangle \overline{P}_0$$

with the inverse map:

$$g^{-1} : \overline{P} \mapsto \overline{P} \triangle \overline{P}_0.$$

If we can show that $\overline{\Phi} = g \circ \Phi \circ f^{-1}$, (1) will automatically follows. To show this, we first show that that $\overline{M}_0 = \overline{D} \triangle M_0 \triangle \overline{P}_0$. Consider

$$\overline{D} \triangle M_0 \triangle \overline{P}_0 = \left(\overline{D} \triangle \overline{P}_0\right) \triangle M_0 = (\overline{M}_0 \setminus M_0) \triangle M_0 = (\overline{M}_0 \setminus M_0) \cup M_0 = \overline{M}_0.$$

From $\overline{M}_0 = \overline{D} \triangle M_0 \triangle \overline{P}_0$, we then have

$$\overline{\Phi}(\overline{M}) = \overline{M} \triangle \overline{M}_0 = \overline{M} \triangle (\overline{D} \triangle M_0 \triangle \overline{P}_0) = ((\overline{M} \triangle \overline{D}) \triangle M_0) \triangle \overline{P}_0 = (g \circ \Phi \circ f^{-1})(\overline{M})$$

for all $\overline{M} \in \overline{\mathcal{M}}$. So, $\overline{\Phi} = g \circ \Phi \circ f^{-1} : \overline{\mathcal{M}} \to \overline{\mathcal{P}}$ is a bijection.

For (2), since $\overline{\Phi} : \overline{M} \mapsto \overline{M} \triangle \overline{M}_0$, we have that for any $e \in \overline{M}_0$,

$$e \in \overline{M} \iff e \in \overline{M} \cap \overline{M}_0 \iff e \notin (\overline{M} \cup \overline{M}_0) \setminus (\overline{M} \cap \overline{M}_0) = \overline{\Phi}(\overline{M}).$$

Hence we proved (2). □

3.5.3 Modified edge-weight and nonintersecting-path solution

We recall the edge-weight w_e in Definition 3.19. It is compatible with the perfect-matching solution (Theorem 3.22). In order to construct a nonintersecting-path solution from the bijection $\overline{\Phi}$, the edge-weight w_e requires some modification. Due to Proposition 3.37, we only need to inverse the weight of all edges in $\overline{M}_0$.

Definition 3.38 (Modified edge-weight w'_e)**.** For $x \in E(\overline{G})$ we define the *modified edge-weight* as follows:

$$w'_e(x) := \begin{cases} w_e(x)^{-1}, & x \in \overline{M}_0, \\ w_e(x), & \text{otherwise}, \end{cases}$$

where w_e is the edge-weight defined in Definition 3.19.

Definition 3.39 (Modified edge-weight for paths in $\overline{G}$)**.** For a path $p = x_1 x_2 \dots x_n$ in $\overline{G}$, its *modified edge-weight* is defined to be the following product

$$w'_e(p) := \prod_{i=1}^{n} w'_e(x_i).$$

Then the weight for a non-intersecting path is defined by

$$w'_e(\overline{P}) := \prod_{p \in \overline{P}} w'_e(p) \quad \text{for } \overline{P} \in \overline{\mathcal{P}}.$$

Now we are ready for a nonintersecting-path solution for $\overline{G}$. Note that we can also consider the solution for G, but it turns out to be more complicated due to the present of open faces of G, which needs to be treated separately.

Theorem 3.40 (Nonintersecting-path solution for $\overline{G}$)**.** *Let* $\mathbf{k}$ *be an admissible initial data stepped surface with respect to* $p = (i_0, j_0, k_0)$*,* $\overline{M}_0$ *be defined as in Definition 3.28. Then*

$$T_{i_0,j_0,k_0} = \sum_{\overline{P} \in \overline{\mathcal{P}}} w'_e(\overline{P}) \Big/ \prod_{\circ \overset{b}{—} \bullet \in \overline{M}_0} \overline{p}_b,$$

where $\overline{\mathcal{P}}$ *is the set of all non-intersecting paths in* $\overline{G}$ *from* $V_{\text{leftSW}}(\overline{G})$ *to* $V_{\text{rightSE}}(\overline{G})$*.*

Proof. Let $\overline{M} \in \overline{\mathcal{M}}$. From Definition 3.38, we have

$$w'_e(\overline{M} \setminus \overline{M}_0) = w_e(\overline{M} \setminus \overline{M}_0) \text{ and } w'_e(\overline{M}_0 \setminus \overline{M}) = w_e(\overline{M}_0 \setminus \overline{M})^{-1}.$$

Since we can write the symmetric difference as the disjoint union $A \triangle B = (A \setminus B) \sqcup (B \setminus A)$, we have

$$\begin{aligned}
w_e(\overline{M}) &= w_e(\overline{M} \setminus \overline{M}_0) w_e(\overline{M} \cap \overline{M}_0) \\
&= w_e(\overline{M} \setminus \overline{M}_0) w_e(\overline{M}_0 \setminus \overline{M})^{-1} w_e(\overline{M}_0 \setminus \overline{M}) w_e(\overline{M} \cap \overline{M}_0) \\
&= w'_e(\overline{M} \setminus \overline{M}_0) w'_e(\overline{M}_0 \setminus \overline{M}) w_e(\overline{M}_0) \\
&= w'_e(\overline{M} \triangle \overline{M}_0) w_e(\overline{M}_0) \\
&= w'_e(\overline{\Phi}(\overline{M})) w_e(\overline{M}_0).
\end{aligned}$$

From Theorem 3.22 and the previous equality, we have

$$\begin{aligned}
T_{i_0,j_0,k_0} &= \sum_{\overline{M} \in \overline{\mathcal{M}}} w_e(\overline{M}) \Big/ w_e(\overline{M}_0)\big|_{c_{i,j}=1} \\
&= \sum_{\overline{M} \in \overline{\mathcal{M}}} w'_e\left(\overline{\Phi}(\overline{M})\right) \frac{w_e(\overline{M}_0)}{w_e(\overline{M}_0)\big|_{c_{i,j}=1}} \\
&= \sum_{\overline{P} \in \overline{\mathcal{P}}} w'_e(\overline{P}) \Big/ \prod_{\circ \overset{b}{—} \bullet \in \overline{M}_0} \overline{p}_b.
\end{aligned}$$

Hence we proved the theorem. □

The nonintersecting-path solution obtained in this section gives us a hint that it is possible

to have a network solution analog to [DFK13, DF14]. In the next section, we will transform the oriented graph $\overline{G}$ to a network. The modified edge-weight will be used on the network as well. This leads to a network solution and a network-matrix solution.

3.6 Network solution

In this section, we will construct a weighted directed network N associated with the oriented graph $\overline{G}$ and the modified edge-weight w'_e. We then decompose N into network chips and their associated elementary network matrices (adjacency matrices). The product of all the elementary matrices associated with the network chips, according to an order of the chips, is then called the network matrix associated to N. The nonintersecting-path solution for $\overline{G}$ (Theorem 3.40) can then be interpreted as a path solution on this network, and can also be computed from a certain minor of the network matrix. We also show that our network and elementary network matrices coincide with the objects studied in [DFK13] in the case of coefficient-free T-systems ($c_{i,j} = 1$ for all $(i, j) \in \mathbb{Z}^2$).

3.6.1 Network associated with a graph

We construct the *directed network* N associated with the oriented graph $\overline{G}$ by tilting all the diagonal edges so that they become horizontal, and tilting all the vertical edges so that the vertex on the left is black as shown in Figure 3.19. Also, the network is directed from left to right. So a path in the oriented graph $\overline{G}$ (Definition 3.27) corresponds to a path in N.

We then introduce the notion of "row" for vertices of N. Two vertices are said to be in the same row if they are joined by a connected path of horizontal or diagonal edges. In other words, they are on the left and right of each other in $\overline{G}$, see Definition 3.24. We number the rows so that they increase by one from bottom to top and the center face (i_0, j_0) of N lies between the row -1 and 0. See Figure 3.19. The precise definition is as the following.

Definition 3.41. The vertex $v \in V(\overline{G})$ is in *row* r if two of its incident faces are $(i, j_0 + r)$ and $(i, j_0 + r + 1)$ for some $i \in \mathbb{Z}$.

Let N be the directed network associated with $\overline{G}$, where $r_{\min}$ and $r_{\max}$ are the smallest and the largest row numbers of N. We then put weight on the network locally around each black vertex as

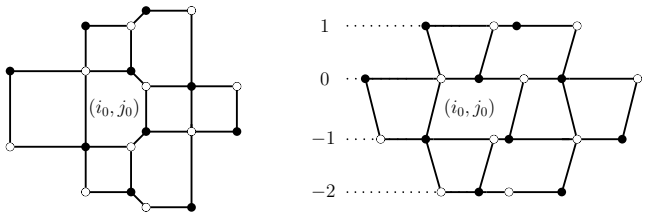

Figure 3.19: An example of $\overline{G}$ and its associated network N.

shown in Figure 3.5. The weight comes directly from the modified edge-weight w'_e on $\overline{G}$ (Definition 3.38), so we will carry the notation w'_e for the weight on N.

Remark 3.42. When a black vertex in Figure 3.5 is on the boundary, we will assume the following.

$$t_a = 1, \text{ when } a \notin F(\overline{G}),$$
$$p_b = \overline{p}_b = 1, \text{ when } b \notin F(G).$$

This assumption comes directly from Definition 3.19.

3.6.2 Nonintersecting-path solution for the network

We have already defined the weighted directed network N associated with $\overline{G}$, where the weight on N comes directly from the weight on $\overline{G}$. The nonintersecting-path solution for $\overline{G}$ (Theorem 3.40) can then be interpreted in terms of nonintersecting paths in N. The left-most SW vertices of $\overline{G}$ correspond to the left-most vertices in the rows $[r_{\min}, -1] := \{r_{\min}, \ldots, -2, -1\}$ of N while the right-most SE vertices of $\overline{G}$ corresponds to the right-most vertices in rows $[r_{\min}, -1]$ of N. We then get the following theorem.

Theorem 3.43 (Nonintersecting-path solution for N)**.** *Let N be the weighted directed network associated with $\overline{G}$. Then*

$$T_{i_0,j_0,k_0} = Q^{-1} \sum_P w'_e(P),$$

where the sum runs over all the non-intersecting paths on N starting from the rows $[r_{\min}, -1]$ on the left to $[r_{\min}, -1]$ on the right and $Q := \prod_{\circ \overline{b} \bullet \in \overline{M}_0} \overline{p}_b$.

Part of $\overline{G}$	Network chip	Network matrix
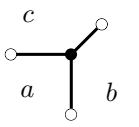	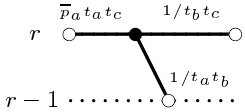	$U_r(t_a, t_b, t_c)$
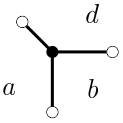	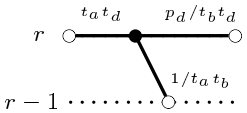	$U'_r(t_a, t_b, t_d)$
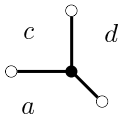	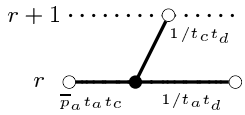	$V_r(t_a, t_c, t_d)$
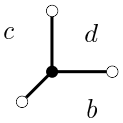	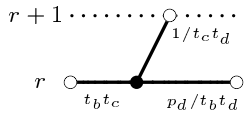	$V'_r(t_b, t_c, t_d)$
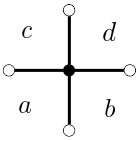	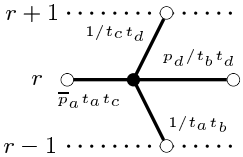	$W_r(t_a, t_b, t_c, t_d)$

Table 3.5: A table comparing a part of $\overline{G}$ around a black vertex, its corresponding elementary network chip in N and its corresponding elementary network matrix defined in Definition 3.45

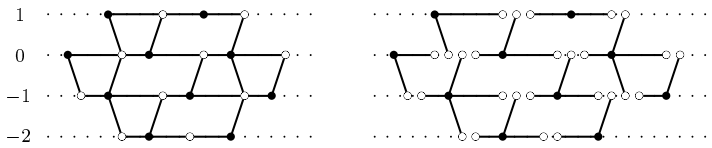

Figure 3.20: A network is decomposed into elementary network chips

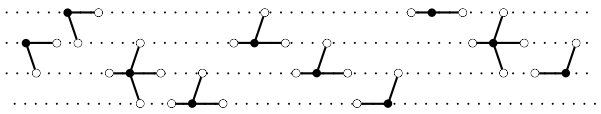

Figure 3.21: A totally-order from a decomposition in Figure 3.20

3.6.3 Network matrix

We will now decompose N into *elementary network chips*, which are small pieces of N around black vertices illustrated in Figure 3.5. This can be done by breaking the network at all of its white vertices. See Figure 3.20 for an example. We notice that we will have the following choice when there are two incident vertical edges at a white vertex.

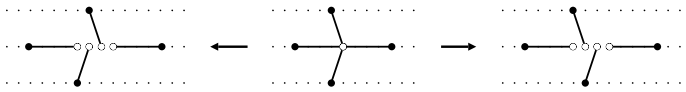

Since the weight of a path on N is independent of this choice, the nonintersecting-path solution is independent of this ambiguity.

A decomposition gives a partially-order on the network chips, we then pick a "finer" totally-order which does not contradict the partially-order. This totally-order can be thought as the order in which to pull chips out of the network from the left.

Example 3.44. From the example in Figure 3.19, we can pick a network decomposition as in Figure 3.20, and then pick a totally-orders as in Figure 3.21.

The next step is to associate each chip with an elementary network matrix shown in Figure 3.5. The matrices W_r, V_r, V'_r, U_r and U'_r are defined in the following definition.

Definition 3.45. We define an *elementary network matrix* associated with a network N, depending on its configuration around a black vertex in Figure 3.5, to be an square matrix of size $r_{\max} - r_{\min} + 1$

with entries:

$$(U_r(x,y,z))_{\alpha,\beta} := \begin{cases} (U(x,y,z))_{\alpha-r+2,\beta-r+2}, & \text{if } \alpha,\beta \in \{r-1,r\}, \\ \delta_{\alpha,\beta}, & \text{otherwise,} \end{cases}$$

$$(V_r(x,y,z))_{\alpha,\beta} := \begin{cases} (V(x,y,z))_{\alpha-r+1,\beta-r+1}, & \text{if } \alpha,\beta \in \{r,r+1\}, \\ \delta_{\alpha,\beta}, & \text{otherwise,} \end{cases}$$

$$(W_r(w,x,y,z))_{\alpha,\beta} := \begin{cases} (W(w,x,y,z))_{\alpha-r+2,\beta-r+2}, & \text{if } \alpha,\beta \in \{r-1,r,r+1\}, \\ \delta_{\alpha,\beta}, & \text{otherwise,} \end{cases}$$

and U'_r (resp. V'_r) is defined in the same way as U_r (resp. V_r) where

$$U(t_a,t_b,t_c) := \begin{pmatrix} 1 & 0 \\ \overline{p}_a \frac{t_c}{t_b} & \overline{p}_a \frac{t_a}{t_b} \end{pmatrix}, \qquad U'(t_a,t_b,t_d) := \begin{pmatrix} 1 & 0 \\ \frac{t_d}{t_b} & p_d \frac{t_a}{t_b} \end{pmatrix},$$

$$V(t_a,t_c,t_d) := \begin{pmatrix} \overline{p}_a \frac{t_c}{t_d} & \overline{p}_a \frac{t_a}{t_d} \\ 0 & 1 \end{pmatrix}, \qquad V'(t_b,t_c,t_d) := \begin{pmatrix} p_d \frac{t_c}{t_d} & \frac{t_b}{t_d} \\ 0 & 1 \end{pmatrix},$$

$$W(t_a,t_b,t_c,t_d) := \begin{pmatrix} 1 & 0 & 0 \\ \overline{p}_a \frac{t_c}{t_b} & \overline{p}_a p_d \frac{t_a t_c}{t_b t_d} & \overline{p}_a \frac{t_a}{t_d} \\ 0 & 0 & 1 \end{pmatrix}.$$

The (i,j) entry of a network matrix is just the weight of the edge from row i to row j in the network chip, see Figure 3.5.

If two network chips do not have an order from the decomposition, then their corresponding elementary network matrices commute. For a totally-order of the network chips, we define the product of all the elementary network matrices with the same order of the chips. This product is independent of a choice of totally-order and decomposition. We call it the *network matrix* associated with N.

Remark 3.46. The network matrix W_r defined in Definition 3.45 can be factored as follows:

$$V_r(t_a,t_c,t_d)U'_r(t_a,t_b,t_d) = W_r(t_a,t_b,t_c,t_d) = U_r(t_a,t_b,t_c)V'_r(t_b,t_c,t_d).$$

This corresponds to the following picture when collapsing a degree-2 vertex.

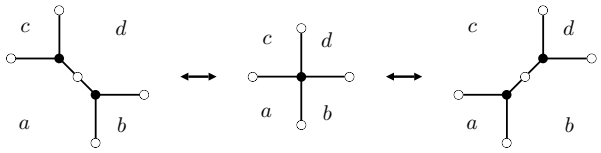

Remark 3.47. U_r, U'_r, V_r and V'_r defined in Definition 3.45 can also be factored. This factorization separates the coefficients $\overline{p}_a$'s and p_d's from the variables t_α's.

$$U(t_a,t_b,t_c)=\begin{pmatrix}1&0\\0&\overline{p}_a\end{pmatrix}\begin{pmatrix}1&0\\\frac{t_c}{t_b}&\frac{t_a}{t_b}\end{pmatrix},\quad U'(t_a,t_b,t_d)=\begin{pmatrix}1&0\\\frac{t_d}{t_b}&\frac{t_a}{t_b}\end{pmatrix}\begin{pmatrix}1&0\\0&p_d\end{pmatrix},$$
$$V(t_a,t_c,t_d)=\begin{pmatrix}\overline{p}_a&0\\0&1\end{pmatrix}\begin{pmatrix}\frac{t_c}{t_d}&\frac{t_a}{t_d}\\0&1\end{pmatrix},\quad V'(t_b,t_c,t_d)=\begin{pmatrix}\frac{t_c}{t_d}&\frac{t_b}{t_d}\\0&1\end{pmatrix}\begin{pmatrix}p_d&0\\0&1\end{pmatrix}.$$

Since the entry (i,j) of the network matrix is the partition function of weighted paths from row i to row j, by the Lindström-Gessel-Viennot theorem [Lin73, GV85], the partition function of weighted non-intersecting paths from the rows $[r_{\min},-1]$ on the left to the rows $[r_{\min},-1]$ to the right is the principal minor of the network matrix corresponding to the rows/columns $[r_{\min},-1]$. Theorem 3.43 then gives the following.

Theorem 3.48 (Network-matrix solution)**.** *Let M be the network matrix associated with the network N of the graph $\overline{G}$. Then*

$$T_{i_0,j_0,k_0}=Q^{-1}|M|^{r_{\min},\dots,-2,-1}_{r_{\min},\dots,-2,-1},$$

where $|M|^{r_{\min},\dots,-2,-1}_{r_{\min},\dots,-2,-1}$ denotes the principal minor of M corresponding to the rows $[r_{\min},-1]$ and columns $[r_{\min},-1]$, and $Q:=\prod_{\circ\!-\!\bullet\in\overline{M}_0}\overline{p}_b$.

We may absorb the factor Q^{-1} into the elementary network matrices, by defining the *modified*

elementary network matrices to be as follows.

$$\begin{aligned}
\overline{U}_r(t_a,t_b,t_c) &:= (\overline{p}_a)^{-1}U_r(t_a,t_b,t_c), \qquad & \overline{U}'_r(t_a,t_b,t_d) &:= U'_r(t_a,t_b,t_d),\\
\overline{V}_r(t_a,t_c,t_d) &:= (\overline{p}_a)^{-1}V_r(t_a,t_c,t_d), \qquad & \overline{V}'_r(t_b,t_c,t_d) &:= V'_r(t_b,t_c,t_d),\\
\overline{W}_r(t_a,t_b,t_c,t_d) &:= (\overline{p}_a)^{-1}W_r(t_a,t_b,t_c,t_d).
\end{aligned} \tag{3.14}$$

Then the *modified network matrix* associated with N is defined as the product of all modified elementary network matrices according to a totally-order of the network chips as before. Theorem 3.48 becomes the following.

Theorem 3.49 (Modified-network-matrix solution)**.** *Let $\overline{M}$ be the modified network matrix associated with the network N of the graph $\overline{G}$. Then*

$$T_{i_0,j_0,k_0} = |\overline{M}|^{r_{\min},\dots,-2,-1}_{r_{\min},\dots,-2,-1},$$

where $|\overline{M}|^{r_{\min},\dots,-2,-1}_{r_{\min},\dots,-2,-1}$ is the minor of $\overline{M}$ corresponding to the rows $[r_{\min},-1]$ and columns $[r_{\min},-1]$.

Remark 3.50 (Flatness condition)**.** It is worth pointing out that the condition

$$\overline{U}'_{k+1}(t_\ell,t_c,t_u)\overline{V}_k(t_d,t_c,t_r) = \overline{V}'_k(t_d,t_\ell,t'_c)\overline{U}_{k+1}(t'_c,t_r,t_u) \tag{3.15}$$

is equivalent to

$$t'_c t_c = J_{i,j,k}t_\ell t_r + t_u t_d$$

where $c=(i,j)$, $\ell=(i-1,j)$, $r=(i+1,j)$, $u=(i,j+1)$, $d=(i,j-1)$ and $k=\mathbf{k}(c)-1=\mathbf{k}(\ell)=\mathbf{k}(r)=\mathbf{k}(u)=\mathbf{k}(d)$. It corresponds to the following action on networks.

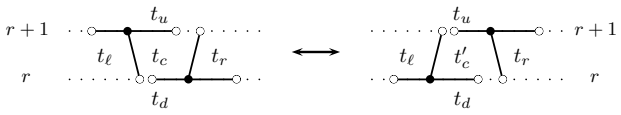

In the graph $\overline{G}$, this is the urban renewal (Figure 3.6) at the face c on the graph $\overline{G}$.

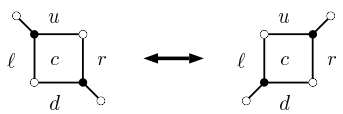

On the stepped surface $\mathbf{k}$, this is a downward-mutation at c. Elementary network matrices therefore encode the octahedron recurrence (3.2) as the flatness condition of (3.15).

3.6.4 Lozenge covering

In [DFK13] the authors construct a lozenge covering from a stepped surface and use it to construct a weighted network. Then the solution to the coefficient-free T-system is a partition function of non-intersecting paths in the network.

We recall the procedure in [DFK13] with some modification so that it fits in our setting. Starting from a stepped surface $\mathbf{k}$, a lozenge covering is constructed depending on the height of the four corners of a square: (i,j), $(i+1,j)$, $(i,j+1)$ and $(i+1,j+1)$. The rule can be summarized in the following table.

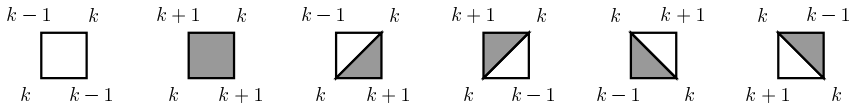

We note that a choice of triangulating the squares in the first two cases makes a lozenge covering not unique.

Next, we restrict the covering to the points (i,j)'s in $\mathring{F} \cup \partial F$. This gives a triangulation of a finite region. The next step is to group two triangles sharing a horizontal side together. As a result, we obtain "elementary chips" as follows.

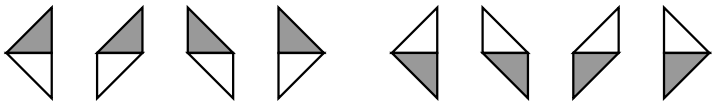

They are classified into two types depending on whether the shaded triangle is on the top or the bottom of the lozenge. An "elementary matrix" is then associated with each type depending on the corners of the shaded triangle of a lozenge as follows.

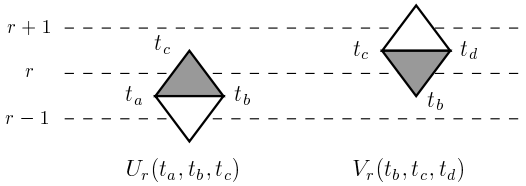

We recall the notion of row defined in Definition 3.41. The matrix $U_r(x,y,z)$ and $V_r(x,y,z)$ are square matrices of size $(r_{\max} - r_{\min} + 1) \times (r_{\max} - r_{\min} + 1)$ with entries

$$(U_r(x,y,z))_{\alpha,\beta} = \begin{cases} (U(x,y,z))_{\alpha-r+2,\beta-r+2}, & \text{if } \alpha,\beta \in \{r-1, r\}, \\ \delta_{\alpha,\beta}, & \text{otherwise,} \end{cases}$$

$$(V_r(x,y,z))_{\alpha,\beta} = \begin{cases} (V(x,y,z))_{\alpha-r+1,\beta-r+1}, & \text{if } \alpha,\beta \in \{r, r+1\}, \\ \delta_{\alpha,\beta}, & \text{otherwise,} \end{cases}$$

and similarly for $V_r(x,y,z)$. The 2×2 matrices $U(x,y,z)$ and $V(x,y,z)$ are defined as

$$U(x,y,z) = \begin{pmatrix} 1 & 0 \\ \frac{z}{y} & \frac{x}{y} \end{pmatrix}, \quad V(x,y,z) = \begin{pmatrix} \frac{y}{z} & \frac{x}{z} \\ 0 & 1 \end{pmatrix}.$$

We can immediately see that this is a specialization of the elementary network matrices in Definition 3.45 to the case when $c_{i,j} = 1$ for all $(i,j) \in \mathbb{Z}^2$. With the same idea as the network-chip decomposition in Section 3.6.3, the lozenge covering is decomposed. This gives an ordering of elementary network matrices. We then construct a "network matrix", which is a product of all elementary network matrices according to the order. The cluster variable T_{i_0,j_0,k_0} is then expressed as a certain minor of the network matrix, similar to Theorem 3.48 and Theorem 3.49.

Remark 3.51. In the original definition of U_r and V_r in [DFK13], the index of U is shifted by 1, i.e. $\mathcal{U}_r = U_{r+1}$ where $\mathcal{U}_r$ is the network matrix defined in [DFK13].

In our construction, the existence of coefficients forces us to make a finer classification of the elementary network matrices as follows:

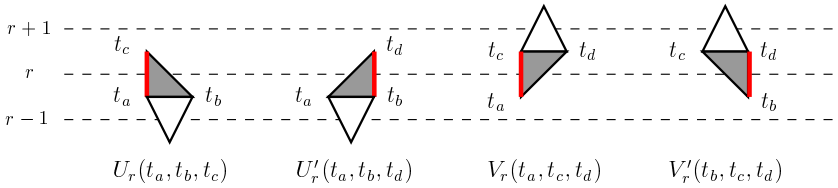

From Remark 3.47, we can think that the coefficients live on the vertical sides of shaded triangles. From Remark 3.46, the matrix W_r can be realized as a combination of two lozenges with the following choice of decomposition.

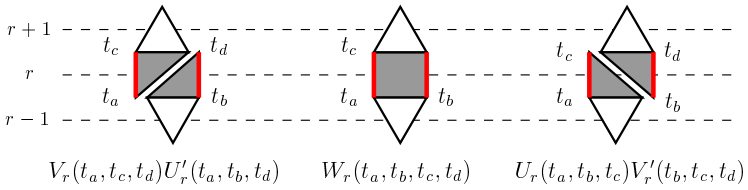

The main reason that the lozenge covering has a rich connection to our story is because it is indeed a dual of our bipartite graph. This can be locally described as follows:

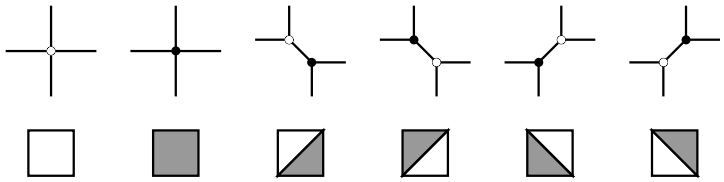

A choice to triangulate a white square corresponds to a choice of decomposing a white vertex, and a choice to triangulate a black square corresponds to a choice of collapsing a degree-2 white vertex in Remark 3.46. These can be illustrated by the following pictures:

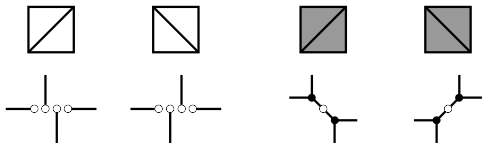

We have provided various solutions to the T-system with principal coefficients. These solutions give combinatorial expressions of T_{i_0,j_0,k_0} in terms of coefficients $c_{i,j}$'s and initial data $t_{i,j}$'s on $\mathbf{k}$ under the conditions:

$$k_0 \geq \mathbf{k}(i_0, j_0), \quad \mathbf{k}(i,j) \geq \mathbf{fund}(i,j) \text{ for } (i,j) \in \mathbb{Z}^2.$$

We will discuss some other cases in Section 3.8.

3.7 Other coefficients

In this section, we discuss a few examples of other choices of coefficients on T-systems: Speyer's octahedron recurrence [Spe07], generalized lambda-determinants [DF13] and (higher) pentagram maps [Gli11, GSTV12, GSTV16]. Almost all of them have their own explicit combinatorial solu-

tions and are treated with different techniques. Applying Theorem 1.15 and Theorem 1.18 to our solutions, we get a partial solution to each of them when the initial data stepped surface is **fund**.

In [Spe07], the author provides a perfect matching solution to the Speyer's octahedron recurrence, which is a partition function of perfect matchings of G. In fact, our perfect matching solution is developed from the method used in the paper. The author uses face-weight (same as Definition 3.9) which gives cluster variables and edge-weight (instead of our pairing-weight) which gives cluster coefficients. So the main difference is that the edge-weight is specific to a choice of coefficients.

For the generalized lambda-determinant in [DF13], the author provides a network solution which is a partition function of non-intersecting paths in a weighted directed network. This network is the same as the network discussed in Section 3.6. However, the weight used in [DF13] is different to our weight due to the choice of coefficients.

The (higher) pentagram maps [Sch92, OST10, Gli11, GSTV12, GSTV16] can be realized as a Y-pattern, i.e. a dynamic on cluster coefficients, not cluster variables. So it is not directly a T-system, but is instead a Y-pattern on the octahedron quiver. In [Gli11], the author gives a combinatorial solution to the pentagram map using alternating sign matrices.

3.7.1 Speyer's octahedron recurrence

The *Speyer's octahedron recurrence*, defined with coefficients, is a recurrence relation [Spe07] on the set of formal variables $\mathcal{T}^{(s)} = \{T^{(s)}_{i,j,k} \mid (i,j,k) \in \mathbb{Z}^3_{\text{odd}}\}$ together with a set of extra variables, called coefficients, $\{A_{i,j}, B_{i,j}, C_{i,j}, D_{i,j} \mid (i,j) \in \mathbb{Z}^2_{\text{even}}\}$ satisfying

$$T^{(s)}_{i,j,k-1}T^{(s)}_{i,j,k+1} = B_{i,j+k}D_{i,j-k}T^{(s)}_{i-1,j,k}T^{(s)}_{i+1,j,k} + A_{i+k,j}C_{i-k,j}T^{(s)}_{i,j-1,k}T^{(s)}_{i,j+1,k} \tag{3.16}$$

We note that in [Spe07], the condition on the index (i,j,k) of $T^{(s)}_{i,j,k}$ is $i+j+k \equiv 0 \bmod 2$, and the coefficients are defined on $\mathbb{Z}^2_{\text{odd}}$. With a shift in the indices, we make it coherent with our construction.

Speyer's octahedron recurrence can also be interpreted [Spe07] as a cluster algebra with coefficients. Its initial quiver is the octahedron quiver with initial cluster variables $T^{(s)}_{i,j,\mathbf{fund}(i,j)}$ similar

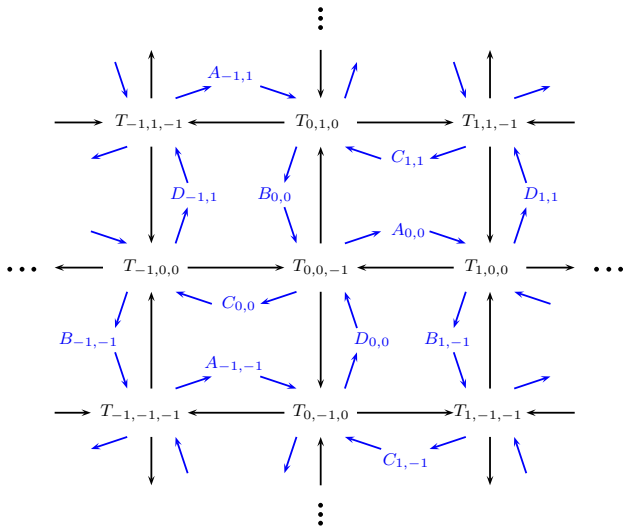

Figure 3.22: A portion of the infinite quiver of Speyer's octahedron recurrence. The frozen variables and their incident arrows are in blue.

to what we discussed in Section 3.2.1. The only difference is the initial coefficients:

$$y_{i,j} = \begin{cases} B_{i,j}D_{i,j}/A_{i,j}C_{i,j}, & i+j \equiv 0 \bmod 2, \\ A_{i-1,j}C_{i+1,j}/B_{i,j-1}D_{i,j+1}, & i+j \equiv 1 \bmod 2, \end{cases}$$

in the semifield $\mathbb{P} = \mathrm{Trop}(A_{i,j}, B_{i,j}, C_{i,j}, D_{i,j} : (i,j) \in \mathbb{Z}^2_{\mathrm{even}})$. By Remark 1.10, it can be interpreted as a coefficient-free cluster algebra with frozen variables $\{A_{i,j}, B_{i,j}, C_{i,j}, D_{i,j} \mid (i,j) \in \mathbb{Z}^2_{\mathrm{even}}\}$ with the quiver illustrated in Figure 3.22.

Since we will only consider the initial stepped surface **fund**, we let $T^{(s)}_{i_0,j_0,k_0}$ denote its expression in terms of the initial data $t_{i,j} := T^{(s)}_{i,j,\mathbf{fund}(i,j)}$ and the coefficients $A_{i,j}, B_{i,j}, C_{i,j}, D_{i,j}$ for $(i,j) \in \mathbb{Z}^2$. For the T-system with principal coefficients, T_{i_0,j_0,k_0} denotes its expression in terms of $t_{i,j} := T_{i,j,\mathbf{fund}(i,j)}$ and $c_{i,j}$ for $(i,j) \in \mathbb{Z}^2$. In order to get $T^{(s)}_{i_0,j_0,k_0}$, we will have to specialize values of $t_{i,j}$ and $c_{i,j}$ in T_{i_0,j_0,k_0} according to Theorem 1.15. Let $T_{i_0,j_0,k_0}(c_{i,j} = y_{i,j})$ denote the expression of T_{i_0,j_0,k_0} where $t_{i,j}$ stayed untouched but $c_{i,j}$ is substituted by $y_{i,j}$. $T_{i_0,j_0,k_0}|_{\mathbb{P}}(t_{i,j} = 1; c_{i,j} = y_{i,j})$ denotes the expression of T_{i_0,j_0,k_0} where $t_{i,j}$ is set to 1, $c_{i,j}$ is set to $y_{i,j}$, and then the whole expression is finally computed in $\mathbb{P}$.

By the separation formula (Theorem 1.15), we get a solution to the Speyer's octahedron recur-

rence from the solution to the T-system with principal coefficients:

$$T^{(s)}_{i_0,j_0,k_0} = \frac{T_{i_0,j_0,k_0}(c_{i,j} = y_{i,j})}{T_{i_0,j_0,k_0}|_{\mathbb{P}}(t_{i,j} = 1; c_{i,j} = y_{i,j})} \tag{3.17}$$

where $\mathbb{P} = \mathrm{Trop}(A_{i,j}, B_{i,j}, C_{i,j}, D_{i,j} : (i,j) \in \mathbb{Z}^2_{\mathrm{even}})$ and

$$y_{i,j} = \begin{cases} B_{i,j}D_{i,j}/A_{i,j}C_{i,j}, & i+j \equiv 0 \bmod 2, \\ A_{i-1,j}C_{i+1,j}/B_{i,j-1}D_{i,j+1}, & i+j \equiv 1 \bmod 2. \end{cases} \tag{3.18}$$

We now compare our result to the solution in [Spe07]. From our perfect matching solution (Theorem 3.13), we then have

$$T^{(s)}_{i_0,j_0,k_0} = \frac{\sum_{M\in\mathcal{M}} w_p(M) w_f(M)}{\bigoplus_{M\in\mathcal{M}} w_p(M)} \tag{3.19}$$

where $\mathcal{M}$ is the set of perfect matchings of the graph $G_{p,\mathbf{fund}}$. The denominator is a sum in $\mathbb{P} = \mathrm{Trop}(A_{i,j}, B_{i,j}, C_{i,j}, D_{i,j} : (i,j) \in \mathbb{Z}^2_{\mathrm{even}})$, hence a monomial in $\{A_{i,j}, B_{i,j}, C_{i,j}, D_{i,j} \mid (i,j) \in \mathbb{Z}^2_{\mathrm{even}}\}$.

Theorem 3.52 ([Spe07])**.** *For a point $p = (i_0, j_0, k_0)$ and an admissible initial stepped surface $\mathbf{k}$, we have*

$$T^{(s)}_{i_0,j_0,k_0} = \sum_{M\in\mathcal{M}} w_s(M) w_f(M)$$

where the sum runs over all the perfect matchings of $G = G_{p,\mathbf{k}}$. The weight w_s is defined by $w_s(M) := \prod_{x\in M} w_s(x)$ and the weight $w_s(x)$ is defined for $x \in E(G)$ as follows:

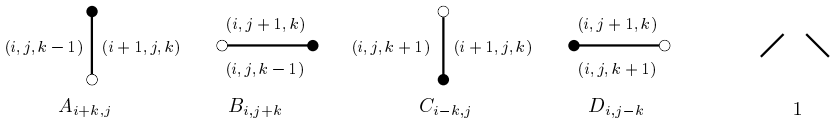

Comparing (3.19) to Theorem 3.52, we can write w_s on a perfect matching on $G_{p,\mathbf{fund}}$ in terms of the pairing weight as follows:

$$w_s(M) = \frac{w_p(M)}{\bigoplus_{M\in\mathcal{M}_{\mathbf{fund}}} w_p(M)}. \tag{3.20}$$

The sum in the denominator is computed in the semifield $\mathbb{P} = \mathrm{Trop}(A_{i,j}, B_{i,j}, C_{i,j}, D_{i,j})$.

Example 3.53. Let $p = (0, 0, 1)$, then we get the graph G and its two matchings as follows:

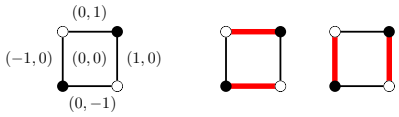

Let $T_{i,j,\mathbf{fund}(i,j)} = t_{i,j}$ be the initial data. From Theorem 3.52, we have

$$T^{(s)}_{0,0,1} = B_{0,0}D_{0,0}\, t_{-1,0}t^{-1}_{0,0}t_{1,0} + A_{0,0}C_{0,0}\, t_{0,-1}t^{-1}_{0,0}t_{0,1}.$$

On the other hand, to apply the separation formula, we set $c_{0,0} = \frac{B_{0,0}D_{0,0}}{A_{0,0}C_{0,0}}$ as in (3.18). Equation (3.17) then gives

$$\begin{aligned} T^{(s)}_{0,0,1} &= \frac{c_{0,0}\, t_{-1,0}t^{-1}_{0,0}t_{1,0} + t_{0,-1}t^{-1}_{0,0}t_{0,1}}{c_{0,0} \oplus 1} \\ &= B_{0,0}D_{0,0}\, t_{-1,0}t^{-1}_{0,0}t_{1,0} + A_{0,0}C_{0,0}\, t_{0,-1}t^{-1}_{0,0}t_{0,1}. \end{aligned}$$

3.7.2 Lambda determinants

The generalized lambda-determinant [DF13] can be considered as a recurrence relation on $\mathcal{T}^{(\lambda)} = \{T^{(\lambda)}_{i,j,k} \mid (i, j, k) \in \mathbb{Z}^3_{\text{odd}}\}$ together with a set of coefficients $\{\lambda_i, \mu_i \mid i \in \mathbb{Z}\}$ satisfying

$$T^{(\lambda)}_{i,j,k-1}T^{(\lambda)}_{i,j,k+1} = \lambda_i T^{(\lambda)}_{i-1,j,k}T^{(\lambda)}_{i+1,j,k} + \mu_j T^{(\lambda)}_{i,j-1,k}T^{(\lambda)}_{i,j+1,k} \tag{3.21}$$

for all $(i, j, k) \in \mathbb{Z}^3_{\text{odd}}$.

It can also be realized [DF13] as a cluster algebra with coefficients. The quiver is the octahedron quiver, the initial cluster variables are $T_{i,j,\mathbf{fund}(i,j)}$ and the initial coefficients are

$$y_{i,j} = \begin{cases} \lambda_i/\mu_j, & i + j \equiv 0 \bmod 2, \\ \mu_j/\lambda_i, & i + j \equiv 1 \bmod 2, \end{cases} \tag{3.22}$$

in $\mathbb{P} = \text{Trop}(\lambda_i, \mu_i : i \in \mathbb{Z})$. By Remark 1.10, we can also interpret it as a coefficient-free cluster algebra with frozen variables $\{\lambda_i, \mu_i \mid i \in \mathbb{Z}\}$ with the quiver illustrated in Figure 3.23.

With the initial data stepped surface **fund**, we let $T^{(\lambda)}_{i_0,j_0,k_0}$ be the expression in terms of the

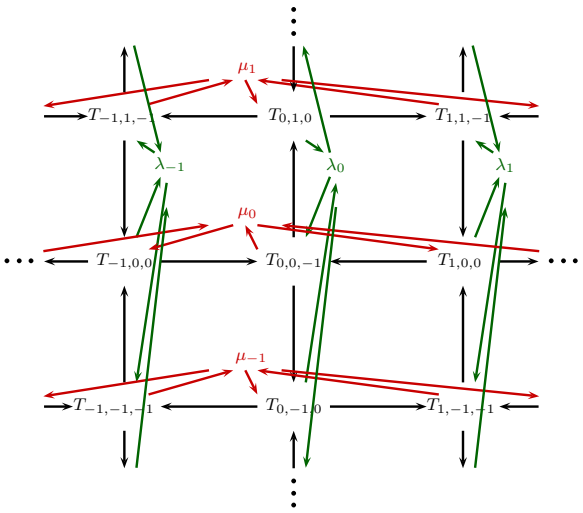

Figure 3.23: A portion of the infinite quiver of the lambda-determinant.

initial data $t_{i,j} := T_{i,j,\mathbf{fund}(i,j)}$ and λ_i, μ_j. By the separation formula (Theorem 1.15), we have

$$T^{(\lambda)}_{i_0,j_0,k_0} = \frac{T_{i_0,j_0,k_0}(c_{i,j} = y_{i,j})}{T_{i_0,j_0,k_0}|_{\mathbb{P}}(t_{i,j} = 1; c_{i,j} = y_{i,j})} \tag{3.23}$$

where $\mathbb{P} = \mathrm{Trop}(\lambda_i, \mu_i : i \in \mathbb{Z})$ and

$$y_{i,j} = \begin{cases} \lambda_i/\mu_j, & i + j \equiv 0 \bmod 2, \\ \mu_j/\lambda_i, & i + j \equiv 1 \bmod 2. \end{cases} \tag{3.24}$$

3.7.3 Pentagram maps

Recall definition of the higher pentagram map in Section 2.3. The quiver for the higher pentagram map is shown in Figure 2.9. Wrapping this finite quiver around a torus, we can then interpret it as the octahedron quiver with certain identification of vertices, along the two periods of the torus: $(i, j) \equiv (i + \kappa, j + 2 - \kappa)$ and $(i, j) \equiv (i + n, j - n)$ [DFK13]. Hence we can realize the higher pentagram map as a Y-pattern on the octahedron quiver with periodic initial data $p_1, \ldots, p_n, q_1, \ldots, q_n$ in $\mathbb{Q}_{sf}(p_1, \ldots, p_n, q_1, \ldots, q_n)$, where only mutations at the vertex with exactly two incoming and two outgoing arrows are allowed.

Let $\pi : \mathbb{Z}^2 \to \{p_1, \ldots, p_n, q_1, \ldots, q_n\}$ be the map identifying the vertex of the octahedron quiver

with the vertex of the generalized Glick's quiver. We pick π by starting with $\pi(0,0) = p_n$ and then continuing by the following patterns:

$$\begin{array}{ccc} & q_{i-r'-1} & \\ q_{i+r} & p_i & q_{i-r'} \\ & q_{i+r+1} & \end{array} \quad \text{and} \quad \begin{array}{ccc} & p_{i-r-1} & \\ p_{i+r'} & q_i & p_{i-r} \\ & p_{i+r'+1} & \end{array}$$

where the indices are read modulo n. This choice of π agrees with the map ϕ used for unfolding periodic two dimensional quivers in [GP15, Section 12] in the case when $S = \{(0,0), (\kappa - 1, 0), (r, 1), (r+1, 1)\}$ is a Y-pin for the higher pentagram map. The following is an example of the assignment by the map π where the indices are read modulo n and the center is $(0,0)$.

$$\begin{array}{ccccccc} & & & \vdots & & & \\ & & p_{n-2} & q_{n-r'-2} & p_{n-\kappa} & q_{n-\kappa-r'} & p_{n-2\kappa+2} \\ & & q_{r-1} & p_{n-1} & q_{n-r'-1} & p_{n-\kappa+1} & q_{n-\kappa-r'+1} \\ \cdots & & p_{\kappa-2} & q_r & p_n & q_{n-r'} & p_{n-\kappa+2} & \cdots \\ & & q_{\kappa+r-1} & p_{\kappa-1} & q_{r+1} & p_1 & q_{n-r'+1} \\ & & p_{2\kappa-2} & q_{\kappa+r} & p_\kappa & q_{r+2} & p_2 \\ & & & \vdots & & & \end{array}$$

Let $p_\ell^{(k)}$ and $q_\ell^{(k)}$ ($\ell \in [1,n]$) be the pentagram variables after the k-th iterate of the higher pentagram map. Then

$$p_\ell^{(k)} = 1/q_\ell^{(k+1)} \text{ for all } \ell \in [1,n],$$

and $q_\ell^{(k)}$ is the coefficient at a vertex (i,j,k) on $\mathbf{k}$ such that

$$\pi(i,j) = q_\ell \quad \text{and} \quad \mathbf{k}(i,j) = k = \mathbf{k}(i \pm 1, j \pm 1) + 1.$$

At the vertex (i,j,k), the quiver associated with $\mathbf{k}$ will be as the following.

$$\begin{array}{ccccc} & & (i,j+1,k-1) & & \\ & & \downarrow & & \\ (i-1,j,k-1) & \longleftarrow & (i,j,k) & \longrightarrow & (i+1,j,k-1) \\ & & \uparrow & & \\ & & (i,j-1,k-1) & & \end{array}$$

By Theorem 1.18 and Proposition 3.3, we then have

$$\begin{aligned} q_\ell^{(k)} &= y_{(i,j),\mathbf{k}} \frac{T_{i,j-1,k-1}T_{i,j+1,k-1}}{T_{i-1,j,k-1}T_{i+1,j,k-1}}\Bigg|_{\substack{T_{i,j,\mathbf{fund}(i,j)}=1 \\ c_{i,j}=\pi(i,j)}} \\ &= \frac{I_{i,j,k-1}}{J_{i,j,k-1}} \frac{T_{i,j-1,k-1}T_{i,j+1,k-1}}{T_{i-1,j,k-1}T_{i+1,j,k-1}}\Bigg|_{\substack{T_{i,j,\mathbf{fund}(i,j)}=1 \\ c_{i,j}=\pi(i,j)}} \end{aligned} \tag{3.25}$$

where $y_{(i,j),\mathbf{k}}$ is defined as in Proposition 3.3. This gives an expression of all the pentagram variables in terms of the solution to the T-system with principal coefficients.

3.8 Conclusion and discussion

In this chapter, we have defined the T-system with principal coefficients from cluster algebra aspect. We obtain the octahedron recurrence with principal coefficients, which is a recurrence relation governing the T-system with principal coefficients. Various explicit combinatorial solutions and their connection have been established. This is for a special case when the point p and the initial data stepped surface $\mathbf{k}$ satisfy the following conditions

$$k_0 \geq \mathbf{k}(i_0, j_0), \tag{3.26}$$

$$\mathbf{k}(i,j) \geq \mathbf{fund}(i,j) \quad \text{for } (i,j) \in \mathbb{Z}^2. \tag{3.27}$$

These solutions to the T-system with principal coefficients allow us to solve any other systems having other choices of coefficients on the T-system as we seen in the previous section. In particular, we are able to give a solution to the higher pentagram maps as a product of T-system variables and coefficients, see (3.25).

We notice a symmetry $\{i \leftrightarrow j, k \leftrightarrow -k-1\}$ of the T-system with principal coefficients (3.2). This

symmetry basically switches the roles between i and j and reflects the system upside down. So if we have a point p and an initial data stepped surface $\mathbf{k}$ such that $k_0 \leq \mathbf{k}(i_0, j_0)$ and $\mathbf{k}(i, j) \leq \mathbf{fund}(i, j)$ for $(i, j) \in \mathbb{Z}^2$, after applying the symmetry the system will satisfy the conditions (3.26) and (3.27). Furthermore, the condition (3.27) can be relaxed a little more. Since the expression of T_{i_0,j_0,k_0} depends only on the values of $\mathbf{k}(i, j)$ when $(i, j) \in \mathring{F} \cup \partial F$ (see (3.6)), Condition (3.27) can be relaxed to

$$\mathbf{k}(i, j) \geq \mathbf{fund}(i, j) \quad \text{for } (i, j) \in \mathring{F} \cup \partial F.$$

Nevertheless, an explicit combinatorial solution for arbitrary p and $\mathbf{k}$ is still unknown.

Our general solution for the T-systems with principal coefficients may be applied to various problems related to the octahedron recurrence. For instance, there are known connections between the T-systems and Bessenrodt-Stanley polynomials discussed in [DF15]. We expect the solutions to the T-systems with principal coefficients to provide generalizations of this family of polynomials. It would also be interesting to apply our solutions to study the arctic curves of the octahedron equation with principal coefficients in the same spirit as [DFSG14]. We expect the coefficients to act as additional probability for dimer configurations, which may give other shapes to the arctic curves. Lastly, it would be interesting to investigate the quantum version of the T-systems with principal coefficients analog to [DF11, DFK12].

Chapter 4

Conserved quantities of Q-systems from dimer integrable systems

4.1 Introduction

The material in this chapter is a work in progress and is expected to be published in the near future.

The dimer model is an important model and has a long history in statistical mechanics [Kas63]. It is a study of perfect matchings, a collection of edges in which each vertex of the graph is incident to exactly one edge, on a bipartite graph. Cluster algebras introduced in [FZ02] are commutative algebras equipped with a distinguished set of generators called cluster variables. There is a transformation called mutation which creates a new set of generators from an old one. This transformation allows us to consider a dynamical system inside the cluster algebra. One important feature of cluster dynamics is the Laurent property, namely any cluster variables can be expanded as a Laurent polynomial on initial cluster variables. In many cases, this expansion can be written as a partition function of dimer configurations over a certain graph, see for examples [Spe07, MP07, MS10, JMZ13]. As a discrete dynamical system, many cluster dynamics have been shown to be Liouville-Arnold integrable [FM11, GK13, FH14, HI14, GSTV12, GSTV16, Wil15, FM16]. In [GK13], dimer models are used to construct a class of integrable systems enumerated by integral polygons.

The dimer integrable system introduced in [GK13] is a continuous Liouville-Arnold integrable system whose phase space is the space of line bundles with connections on a bipartite torus graph G obtained from an integral convex polygon. Let n be the number of faces of G. The phase space can be combinatorially viewed as the space of weights on oriented loops of G compatible with loop multiplication. The space of oriented loops is generated by all counterclockwise loops around each face W_i ($i \in \{1, \ldots, n\}$) and two extra loops Z_1, Z_2 whose homology classes on the torus $\mathbb{T}$ generate

$H_1(\mathbb{T}, \mathbb{Z}) \cong \mathbb{Z} \times \mathbb{Z}$. The condition $\prod_i W_i = 1$ is the only nontrivial relation among these generators. So the phase space is generated by the weight assignment w_i ($i \in \{1, \ldots, n\}$) together with z_1, z_2 on all the loops W_i and Z_1, Z_2. The only condition among these weights is $\prod_i w_i = 1$.

The phase space is equipped with a Poisson bracket defined from the intersection pairing on the twisted ribbon graph obtained from G. A Y-seed [FZ07] of rank $n + 2$ indexed by the loop generators is assigned to the weighted graph G where an entry of the exchange matrix is the intersection pairing of the generators and y-variables are their weights.

Hamiltonians are defined on the phase space as Laurent polynomials on $w_1, \ldots, w_n, z_1, z_2$. For $(a, b) \in \mathbb{Z} \times \mathbb{Z}$, a Hamiltonian is written as the partition function over weighted perfect matchings on G where the exponent of z_1 and z_2 in their weights is a and b, respectively. The Hamiltonians vanish for all but finitely many (a, b). There is a move called urban renewal on the weighted graph G, which acts on its corresponding Y-seed as a Y-seed mutation. This transformation is a change of coordinates on the phase space, and the Hamiltonians are invariant under the transformation. By thinking of this change of coordinates as a map on the phase space, it becomes an evolution of a discrete dynamical system. The evolution can also be written as a Y-seed mutation. Various discrete dynamical systems has been studied in this framwork [EFS12].

The first goal of this paper is to rethink the discrete dimer integrable system of [GK13] in cluster variable setting and extend it to bipartite torus graphs not necessary obtained from integral polygons. We study, in Sections 4.2 and 4.3, a system associated with a general bipartite torus graph not necessary be obtained from an integral polygon. Recall that the loop weights in [GK13] are the y-variables in the associated Y-seed. In our study, we instead associate weights that act as cluster variables in the associated cluster seed. We show that the Hamiltonians are invariant under the evolution, see Theorem 4.16.

Q-systems first appeared in an analysis of Bethe ansatz of generalized Heisenberg spin chains. They were first introduced as sets of recurrence relations on commuting variables for the classical algebras [KR87] and later generalized for exceptional algebras [HKO$^+$99], twisted quantum affine algebras [HKO$^+$02] and double affine algebras [Her10]. See [KNS11] for a review on the subject.

They can also be normalized and then realized as mutations on cluster variables [Ked08, DFK09, Wil15]. Explicit conserved quantities for Q-systems of types A have been studied in [DFK10] as

partition functions of hard particles on a graph. For simply-laced finite type and twisted affine type, conserved quantities arise by identifying the systems with the dynamics of factorization mappings on quotients of double Bruhat cells [Wil15].

The second goal of the chapter is to use perfect matchings on graphs to compute conserved quantities of Q-systems associated with a finite Dynkin diagram of type A and B in Section 4.4 and 4.5, respectively. The conserved quantities of type A coincide with the partition functions obtained in [DFK10].

The chapter is organized as follows. In Section 4.2, we introduce weighted bipartite torus graphs, weight of perfect matchings and weight of loops on the graph. A move on weighted graphs is defined. In Section 4.3, we define Hamiltonians and show that they are invariant under the move. In Section 4.4 (resp. Section 4.5), a graph for A_r (resp. B_r) Q-system is constructed. The Hamiltonians are shown to be conserved quantities of the system. They can also be written as partition functions of hard particles on a certain graph. A nondegenerate Poisson bracket is constructed. The conserved quantities Poisson-commute in type A and is conjectured to Poisson-commute in type B.

4.2 Weighted bipartite torus graphs

We think of a torus $\mathbb{T} = \mathbb{R}^2/\mathbb{Z}^2$ as a rectangle with opposite edges identified. A *torus graph* is a graph embedded on the torus with no crossing edges. We do not require that every face is contractible. A *weighted graph* $(G, \mathbf{A})$ is a pair of a graph G with n faces and a collection $\mathbf{A} = (A_i)_{i=1}^n$ of variables or nonzero complex numbers called *weights*. A *bipartite graph* is a graph whose vertices can be colored into two colors (black and white) such that every edge connects two vertices of different colors.

Throughout the chapter, we let G be a bipartite torus graph with n faces. We label the faces by the numbers 1 to n, so $F(G) = [1, n]$.

4.2.1 Quivers associated with graphs and mutations

For a bipartite torus graph G, we let $\mathcal{Q}_G$ be the *quiver associated with* G defined as follows. The nodes of $\mathcal{Q}_G$ are indexed by the faces of G. There will be an arrow between node i and node j for

each edge adjacent to face i and face j. The arrow is oriented in the way that the black vertex of G is on the right of the arrow, see the following figure.

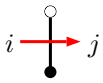

Lastly, any 2-cycles are removed one by one until the directed graph has no 2-cycles. We also let B_G denote the signed adjacency matrix of $\mathcal{Q}_G$. Note that from the construction the resulting directed graph can possibly contain 1-cycles.

To a weighted bipartite torus graph $(G, \mathbf{A})$ whose $\mathcal{Q}_G$ has no 1-cycles, we can associate a cluster seed $(\mathbf{A}, \mathcal{Q}_G)$ of rank n.

We then define two moves on weighted bipartite graphs.

Definition 4.1. An *urban renewal* [Ciu98] (a.k.a. spider move [GK13], square move [Pos06]) at a quadrilateral face k whose four sides are distinct sends $(G, \mathbf{A})$ to $(G', \mathbf{A}')$ as follows.

- The graph G' is obtained from G by replacing the subgraph of G containing four edges around the face k with a graph described in the following picture. The labels are face indices. The four outer vertices connect to the rest of the graph.

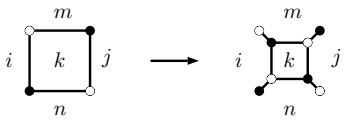

- The weight $\mathbf{A}' = (A'_i) = \mu_k(\mathbf{A})$ are transformed according to the cluster transformation in direction k (Definition 1.3). That is,

$$A'_\ell = \begin{cases} (A_i A_j + A_m A_n)/A_k, & \ell = k, \\ A_\ell, & \ell \neq k. \end{cases} \tag{4.1}$$

Definition 4.2. A *shrinking of a 2-valent vertex* sends $(G, \mathbf{A})$ to $(G', \mathbf{A})$ where G' is obtained from G by removing a 2-valent vertex and identifies its two adjacent vertices, while the weights of the graph stay unchanged. It can be visualized in the following picture. (We also have another version of the move when the colors of the vertices are switched.)

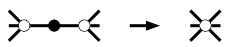

Definition 4.3 (Mutations of weighted bipartite graphs)**.** Let k be a quadrilateral face of a weighted bipartite graph $(G, \mathbf{A})$. A *mutation* at face k, μ_k, is a combination of an urban renewal at face k and shrinking of all 2-valent vertices. Two weighted graphs are *mutation equivalent* if one is obtained from another by a sequence of mutations.

Theorem 4.4. *Let $(G, \mathbf{A})$ be a weighted bipartite graph whose $\mathcal{Q}_G$ has no 1-cycles, k be a quadrilateral face of G.*

If every pair of adjacent faces of k are distinct except possibly pairs of opposite faces, then the mutation μ_k on $(G, \mathbf{A})$ is equivalent to a cluster mutation μ_k on a seed $(\mathbf{A}, \mathcal{Q}_G)$. In particular, $\mathcal{Q}_{\mu_k(G)} = \mu_k(\mathcal{Q}_G)$ and the weight on G are transformed according to the cluster transformation with respect to the quiver $\mathcal{Q}_G$.

Proof. Consider the following picture where k_i are adjacent faces of k.

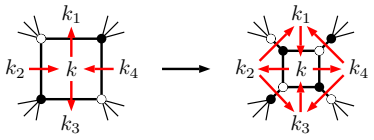

Since $k_i \neq k_{i+1}$ for all i (reading modulo 4), the vertex k of $\mathcal{Q}_G$ has exactly two incoming and two outgoing arrows. (There is no cancellation of arrows incident to k.) The arrows of $\mathcal{Q}_G$ are then transformed according to the rule of quiver mutations. Also, the mutation does not introduce any 1-cycles because k_i and k_{i+1} are distinct. This also shows that the weights on the graph are transformed according the cluster mutation:

$$A'_k = (A_{k_1} A_{k_3} + A_{k_2} A_{k_4})/A_k.$$

Shrinking of a 2-valent vertex corresponds to removing a pair of arrows with opposite orientations that may appear between k_i and k_{i+1}. This also follows the rule of quiver mutations.

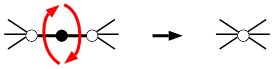

So we can conclude that $\mathcal{Q}_{\mu_k(G)} = \mu_k(\mathcal{Q}_G)$. □

Example 4.5. The following is an example of graph mutations.

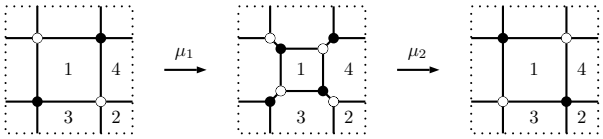

We consider the first mutation μ_1. Using the notations in the proof of Theorem 4.4, when $k = 1$, we have $(k_1, k_2, k_3, k_4) = (3, 4, 3, 4)$. We see that $k_i \neq k_{i+1}$ for all $i \in [1, 4]$. So the mutation μ_1 on the weighted graph is equivalent to the mutation μ_1 on the corresponding cluster seed. Similarly, we can see that μ_2 satisfies the requirement in Theorem 4.4.

The corresponding mutations of quivers are shown as follows.

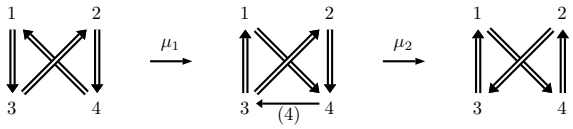

The weight changes as follows.

$$(A_1, A_2, A_3, A_4) \xrightarrow{\mu_1} (A_1', A_2, A_3, A_4) \xrightarrow{\mu_2} (A_1', A_2', A_3, A_4)$$

where $A_1' = (A_4^2 + A_3^2)/A_1$ and $A_2' = (A_3^2 + A_4^2)/A_2$.

4.2.2 Perfect matchings and oriented loops

A *perfect matching* of a graph G is a subset $M \subseteq E(G)$ of the set of all edges in which every vertex of G is incident to exactly one edge in M.

Definition 4.6 (Weight of perfect matchings)**.** Let M be a perfect matching of a weighted graph $(G, \mathbf{A})$. The *weight* of M is defined by

$$w(M) := \prod_{e \in M} w(e).$$

The contribution $w(e)$ is defined by $w(e) := (A_i A_j)^{-1}$ when edge e is adjacent to the faces i and j.

Definition 4.7. Let M, M' be perfect matchings of G. Let $[M]$ denote the collection of all edges in M oriented from black to white. Similarly, $-[M]$ is the collection of edges in M oriented from white to black.

We then define $[M]-[M']$ to be the superimposition of $[M]$ and $-[M']$ with all double edges having opposite orientations removed. In other word, $[M]-[M']$ is the set of edges $(M \setminus M') \cup (M' \setminus M)$ where an edge is oriented from black to white (resp. white to black) if it is in M (resp. M').

It will be proved in Proposition 4.8 that $[M]-[M']$ is a loop on G (possibly contains more than one connected component).

Let $L_1, \ldots, L_m$ be loops on G. The *product of loops* $\prod_{i=1}^{m} L_i$ is the superimposition of $L_1, \ldots, L_m$ with edges having opposite orientation removed one by one. It is clear that the homology class of the product of loops is the sum of their homology classes.

Proposition 4.8. *Let M and M' be perfect matchings of a bipartite torus graph G. Then $[M]-[M']$ is a product of non-intersecting simple loops on G.*

Proof. Since M and M' are both perfect matchings of G, any vertex v in G is incident to exactly one edge in M and exactly one edge in M' (possibly distinct edges). If the two edges are the same, v has no incident edge in $[M]-[M']$. If the two edges are different, v has exactly two incident edges in $[M]-[M']$ with different orientation. (One is oriented from black to white, while the other is from white to black.) Hence $[M]-[M']$ is a product of non-intersecting oriented simple loops on G. □

Since G is a torus graph, a loop on G can be embedded on the torus. Using the identification $H_1(\mathbb{T}, \mathbb{Z}) \cong \mathbb{Z} \times \mathbb{Z}$, we let a horizontal loop going from left to right have homology class $(1, 0)$, and let a vertical loop going from bottom to top have homology class $(0, 1)$.

Definition 4.9 (Homology class of M with respect to M')**.** Let M, M' be perfect matchings of G. Let $[M]_{M'} \in H_1(\mathbb{T}, \mathbb{Z})$ denote the homology class of $[M]-[M']$ on the torus.

Definition 4.10 (Weight of paths)**.** For an oriented path ρ on a weighted graph $(G, \mathbf{A})$, we define the *weight* of ρ to be

$$w(\rho) := \prod_{e} w(e)$$

where the product runs over all directed edges in ρ. Let the edge e be adjacent to faces i and j. The contribution from e is $w(e) := (A_i A_j)^{-1}$ when e is oriented from black to white, while

$w(e) := A_i A_j$ when e is oriented from white to black. See the following figures.

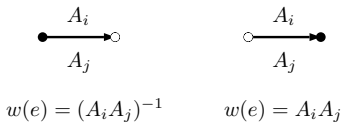

Comparing to the weight of perfect matchings, we notice that

$$w([M] - [M']) = w(M)/w(M')$$

for any perfect matchings M, M' of G.

Example 4.11. Let G be a weighted bipartite torus graph whose weight is shown at each face in the following picture. The perfect matchings M and M' are depicted below.

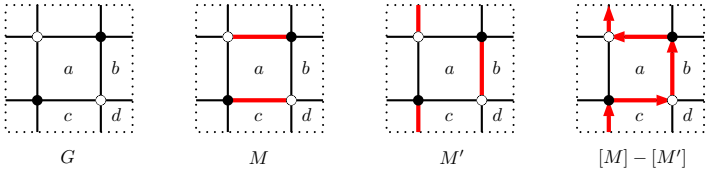

We have $w(M) = a^{-2}c^{-2}$ and $w(M') = (abcd)^{-1}$. The loop $[M] - [M]'$ has weight $w([M] - [M']) = bd/ac = w(M)/w(M')$. Lastly, $[M]_{M'} = (0, 1)$.

4.3 Hamiltonians

In this section, we define Hamiltonians on a weighted graph $(G, \mathbf{A})$ with respect to a perfect matching M_0, and show that they are invariant under certain conditions. They will be used to compute conserved quantities of Q-systems of type A in Section 4.4 and type B in Section 4.5.

4.3.1 Hamiltonians

We modify the Hamiltonians defined in [GK13] and use the weight of perfect matchings induced from the weight of G in Definition 4.6.

Definition 4.12. Let $(G, \mathbf{A})$ be a weighted torus graph, M_0 be a perfect matching of G, $(i, j) \in H_1(\mathbb{T}, \mathbb{Z}) \cong \mathbb{Z} \times \mathbb{Z}$. The *Hamiltonian* of $(G, \mathbf{A})$ with respect to (i, j) and M_0 is a Laurent polynomial

Figure 4.1: The induced reference perfect matching from an urban renewal (left) and from shrinking of a 2-valent vertex (right).

in $\{A_i\}_{i=1}^n$ defined by

$$H_{(i,j),G,M_0}(A_1,\dots,A_n) := \sum_{M:[M]_{M_0}=(i,j)} w(M)/w(M_0), \tag{4.2}$$

where the sum runs over all perfect matchings M of G such that the homology of $[M]-[M_0]$ is (i,j). The weight w is defined as in Definition 4.6. We say that M_0 is a *reference perfect matching*.

Definition 4.13 (Induced perfect matching by an urban renewal)**.** Let k be a quadrilateral face of G. Let G' be a graph obtained from G by an urban renewal at k. Let M be a perfect matching of G containing exactly one side of k. We say that a perfect matching M' of G' is *induced from M by an urban renewal* if M' coincides with M on all edges of G not related to the urban renewal, and on the subgraph replaced by the urban renewal M and M' are related as in Figure 4.1.

Definition 4.14 (Induced perfect matching by shrinking of a 2-valent vertex)**.** Let G' be a graph obtained from G by shrinking of a 2-valent vertex. We say that a perfect matching M' of G' is *induced from M by shrinking of a 2-valent vertex* if M' coincides with M on all edges of G not removed by the move. The perfect matching M' can be described in Figure 4.1.

Definition 4.15 (Induced perfect matching by a mutation)**.** Let $\mu_k(G)$ is a graph obtained from G by a mutation at k. The *induced perfect matching from M by a mutation at k* is the perfect matching $\mu_k(M)$ induced from M by an urban renewal at k and then by shrinking of all 2-valent vertices.

Theorem 4.16. *Let $(G,\mathbf{A})$ be a weighted bipartite torus graph with n faces, $(\mu_k(G),\mathbf{A}')$ be obtained from $(G,\mathbf{A})$ by a mutation at a contractible quadrilateral face k of G. Let M_0 be a perfect matching of G containing exactly one side of k, $\mu_k(M_0)$ be induced from M_0 by the mutation. Then the Hamiltonians are invariant under the mutation:*

$$H_{(i,j),G,M_0}(A_1,\dots,A_n) = H_{(i,j),\mu_k(G),\mu_k(M_0)}(A'_1,\dots,A'_n).$$

Proof. It suffices to show that the Hamiltonians are invariant under an urban renewal and shrinking of a 2-valent vertex.

Consider shrinking of a 2-valent vertex. Let G' be obtained from G by shrinking a 2-valent vertex v. Let assume first that the 2-valent vertex is white. The other case can be treated in a similar manner. Let v be adjacent to faces i, j and edges e_1, e_2. Consider a perfect matching M of G. Since M is a perfect matching, exactly one of e_1, e_2 must be in M. Assume without loss of generality that $e_1 \in M$. From the following picture, there is a unique perfect matching M' of G' which is identical to M except on e_1 and e_2. Similarly, any perfect matching M' of G' has a unique perfect matching of G such that they agree on $E(G')$. Hence this map is a bijection between the perfect matchings of G and of G'.

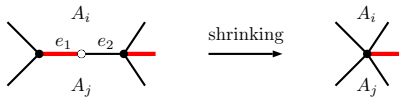

We also have

$$w(M) = w(e_i)w(M') = (A_iA_j)^{-1}w(M').$$

Similarly, for the reference perfect matching M_0 of G, we have

$$w(M_0) = (A_iA_j)^{-1}w(M_0')$$

regardless of whether M_0 contains e_1 or e_2. Hence we have

$$w(M)/w(M_0) = w(M')/w(M_0').$$

Since the move does not change the homology class of a perfect matching i.e. $[M]_{M_0} = [M']_{M_0'}$, from (4.2) we have that the Hamiltonians are invariant under the move:

$$H_{(i,j),G,M_0}(A_1, \ldots, A_n) = H_{(i,j),G',M_0'}(A_1, \ldots, A_n).$$

For an urban renewal, let $(G', \mathbf{A}')$ be obtained from $(G, \mathbf{A})$ by an urban renewal at the face k.

Let M_0 (resp. M_0') be the reference perfect matching of G (resp. G'). There are 4 involved edges before the move and 8 involved edges after the move. Let $x \in \{A_i\}_{i=1}^n$ be the weight at the face k of G, $a, b, c, d \in \{A_i\}_{i=1}^n$ be weights at the four adjacent faces, and $x' \in \{A_i'\}_{i=1}^n$ be a weight at the face k of G'. We then have

$$xx' = ac + bd.$$

Without loss of generality, we assume that the edge adjacent to the faces whose weights are x and c is in M_0. The following picture show M_0 and M_0' on subgraph involved in the urban renewal.

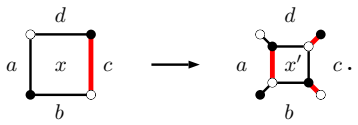

(4.3)

Now we write $H_{(i,j),G,M_0} = H_0 + H_1 + H_2$ where H_0 consists of all the contributions from perfect matchings containing no edges from the four sides of the face k, H_1 consists of the contributions from matchings containing one such edge, and H_2 consists of the contributions from matchings containing two such edges. Similarly, we write $H_{(i,j),G',M_0'} = H_0' + H_1' + H_2'$. We claim that $H_0 = H_2'$, $H_1 = H_1'$ and $H_2 = H_0'$.

In order to show $H_1 = H_1'$, we define a bijection between the matchings contributing terms to H_1 and the matchings contributing terms to H_1'. The bijection maps a matching M in H_1 to another matching M' in H_1' which differs from M only on the edges involving in the urban renewal. The bijection can be described as follows.

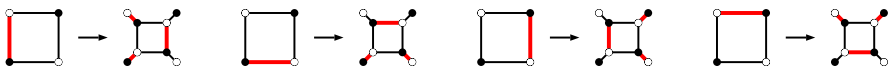

Since M and M' differ only on edges involved in the urban renewal, their contribution of the edges other than such edges near the face k to $w(M)/w(M_0)$ and $w(M')/w(M_0')$ are the same. Now we consider the contributions from the edges involved in the urban renewal. Recalling the weights in (4.3), in the first case, the contribution of such edges to $w(M)/w(M_0)$ is $xc/xa = c/a$, and the contribution to $w(M')/w(M_0')$ is $(x'abc^2d)/(x'a^2bcd) = c/a$. Similarly, the contributions in the second case (resp. the third and the fourth case) from before and after the move are the same and equal to c/b (resp. 1 and c/d). Hence $H_1 = H_1'$.

In order to show $H_0 = H'_2$, we define a one-to-two map from the matchings contributing terms to H_0 to the matchings contributing terms to H'_2. The map can be described as the following.

Let M be a matching of G contributing to a term in H_0, M' and M'' be the corresponding matchings of G' from the one-to-two map. The contribution from the four edges around the face k of G to $w(M)/w(M_0)$ is xc. The contribution to $w(M')/w(M_0)$ (resp. $w(M'')/w(M_0)$) from the eight edges of G' resulting from the move is $x'abc^2d/(x')^2bd = ac^2/x'$ (resp. $x'abc^2d/(x')^2ac = bcd/x'$). From (4.3), $xc = ac^2/x' + bcd/x'$. Hence $H_0 = H'_2$.

In order to show $H_2 = H'_0$, we define a two-to-one map from the matchings contributing terms to H_2 to the matchings contributing terms to H'_0 as the following.

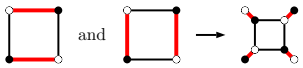

The contribution from the four edges around the face k of G is

$$\frac{xc}{x^2bd} + \frac{xc}{x^2ac} = \frac{c}{abcd}\frac{ac+bd}{x},$$

and the contribution from the eight edges of G' is

$$\frac{x'abc^2d}{a^2b^2c^2d^2} = \frac{c}{abcd}x'.$$

From (4.3), they are equal. Hence $H_2 = H'_0$. This conclude that $H_{(i,j),G,M_0} = H_{(i,j),G',M'_0}$. □

4.4 A_r Q-systems

In this section, we apply Theorem 4.16 to construct conserved quantities for A_r Q-systems, and show that they coincide with the quantities shown in [DFK10]. We also give a Poisson structure to the phase space and show that the conserved quantities mutually Poisson-commute.

4.4.1 A_r Q-systems and weighted graph mutations

Consider the following quiver of an A_r Q-system. See Theorem 1.22 for the detail.

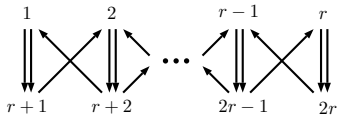

We recall that Theorem 4.16 requires every mutation to happen at a quadrilateral face. This means every quiver mutation in the sequence μ in (1.10) has to be at a vertex with exactly two incoming and two outgoing arrows. In order to archive this, we add another vertex labeled by 0 which will not be mutated, called *frozen vertex*, and assign a value of 1 as its cluster variable. According to the formula of a cluster mutation in Definition 1.3, adding a frozen vertex with value 1 does not effect the system. The following is the resulting quiver $\mathcal{Q}$. The vertex labeled by 0 on the left and on the right are identified. So it has four incident arrows.

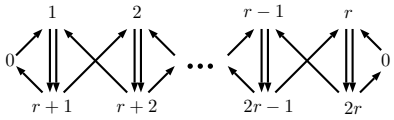

The bipartite torus graph G associated with $\mathcal{Q}$ is depicted below. Since every vertex of $\mathcal{Q}$ is of degree 4, every face of G has 4 sides. We note that the face 0 is not contractible. It is indeed homotopy equivalent to a cylinder.

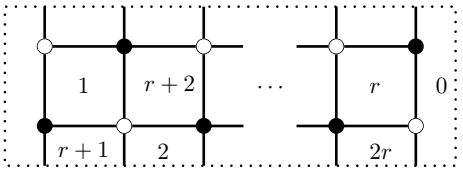

odd r

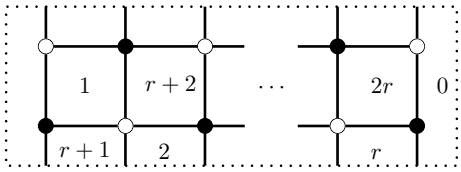

even r

Let M_0 be the perfect matching of G containing all vertical edges whose top vertex is black. It can be depicted as the following.

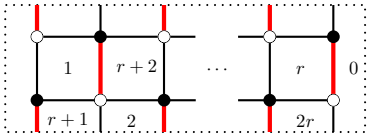

odd r

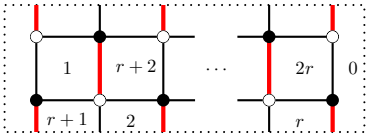

even r

We also let the weight at face i be A_i.

Theorem 4.17. *Let $(G, (A_i))$ be a weighted bipartite torus graph defined above. Then the Hamiltonians $H_{(i,j),G,M_0}(A_1, \ldots, A_{2r})$ are conserved quantities of the A_r Q-system dynamic $Q_{\alpha,k} \mapsto Q_{\alpha,k+1}$.*

Proof. We want to show

$$\begin{aligned} &H_{(i,j),G,M_0}(Q_{1,k},\dots,Q_{r,k},Q_{1,k+1},\dots,Q_{r,k+1}) \\ &\qquad = H_{(i,j),G,M_0}(Q_{1,k+1},\dots,Q_{r,k+1},Q_{1,k+2},\dots,Q_{r,k+2}) \end{aligned}$$

for $k \in \mathbb{Z}$.

Consider $(G,(A_{i,k}))$ where $A_{i,k}$ are defined in equation (1.10). By Theorem 1.22, there is a sequence of mutation $\mu = \mu_r \cdots \mu_1$ and a relabeling $\sigma : i \mapsto i + r \bmod 2r$ such that $\sigma\mu$ sends $\mathcal{Q}$ to $\mathcal{Q}$, and the Q-system variables are shifted by $n \to n+1$. We first claim that the conditions in Theorem 4.4 and Theorem 4.16 hold along the sequence of mutations μ:

- Each mutation happens at a contractible quadrilateral face.
- The mutating face contains exactly one edges in the induced reference perfect matching from M_0.
- Two adjacent faces of the mutating face are distinct, except possibly when they are opposite faces.

Consider the first mutation μ_1. It is clear that face 1 is a contractible quadrilateral face and contains exactly one edge of M_0. Although its adjacent faces are not distinct, the non-distinct faces are opposite. So the conditions hold. The following graph on the left is the resulting graph after an urban renewal at face 1. The graph on the right is the result after shrinking all 2-valent vertices, hence it is $\mu_1(G)$. The induced reference perfect matching from M_0 are shown on the graphs. The weight is now $(A_{1,k+2}, A_{2,k}, \dots, A_{2r,k})$.

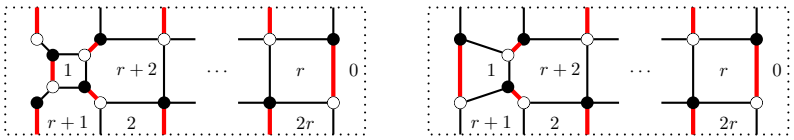

We continue to the mutation μ_2. Again, we see that all the conditions are satisfied. The following graphs are the result after an urban renewal at face 2 and shrinking all 2-valent vertices. The graph $\mu_2(\mu_1(G))$ is shown on the right with the weight

$$(A_{1,k+2}, A_{2,k+2}, A_{3,k}, \dots, A_{2r,k}).$$

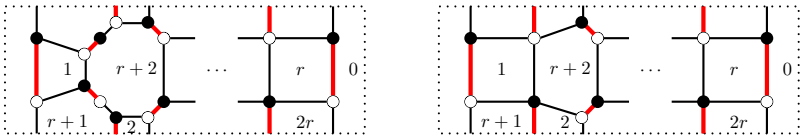

Now it is easy to see that all the conditions hold at every mutation. After applying every mutation along the sequence $\mu_1, \mu_2, \ldots, \mu_r$, we have the following graph $\mu(G)$ together with the induced reference perfect matching $\mu(M_0)$ with weight

$$(A_{1,k+2}, \ldots, A_{r,k+2}, A_{r+1,k}, \ldots, A_{2r,k}) = (Q_{1,k+2}, \ldots, Q_{r,k+2}, Q_{1,k+1}, \ldots, Q_{r,k+1}).$$

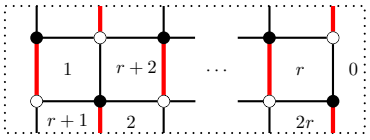

We then continue on to the relabeling $\sigma : i \mapsto i + r \bmod 2r$. This gives the following graph on the left. By vertical translation, we obtain the graph on the right. The weight after relabeling is $(Q_{1,k+1}, \ldots, Q_{r,k+1}, Q_{1,k+2}, \ldots, Q_{r,k+2})$.

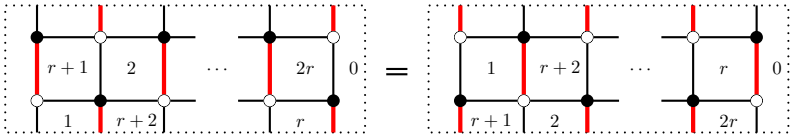

We obtain back the original graph G and reference perfect matching M_0, while the weight is shifted from k to $k+1$. Since , $\sigma\mu(G) = G$ and $\sigma\mu(M_0) = M_0$, we have

$$H_{(i,j),\sigma\mu(G),\sigma\mu(M_0)} = H_{(i,j),G,M_0}.$$

By Theorem 4.4 and Theorem 4.16, we get

$$\begin{aligned} &H_{(i,j),G,M_0}(Q_{1,k}, \ldots, Q_{r,k}, Q_{1,k+1}, \ldots, Q_{r,k+1}) \\ &\qquad = H_{(i,j),G,M_0}(Q_{1,k+1}, \ldots, Q_{r,k+1}, Q_{1,k+2}, \ldots, Q_{r,k+2}). \end{aligned}$$

Hence $H_{(i,j),G,M_0}$ are conserved quantities of the A_r Q-system. □

4.4.2 Partition function of hard particles

In [DFK10], conserved quantities for A_r Q-system are shown to be partition functions of hard particles on a certain weighted graph. We will show that they coincide with the Hamiltonians $H_{(i,j),G,M_0}$ computed in the previous section.

From Proposition 4.8, $[M] - [M_0]$ is always a product of non-intersecting simple loops of G. Given the reference perfect matching M_0 defined in the previous section, we then try to find such simple loops Γ_i on G. We modify the construction in [EFS12] and define Γ_i as the following.

Definition 4.18. For $i = 1, 2, \ldots, 2r+1$, we define Γ_i to be the following loops.

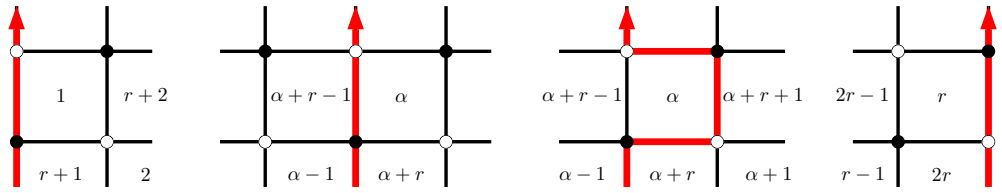

Γ_1 $\Gamma_{2\alpha-1}$ $\Gamma_{2\alpha}$ Γ_{2r+1}

Let $\gamma_i := w(\Gamma_i)$ be the weight of Γ_i on G, see Definition 4.10. We note that when $A_i = A_{i,k}$ defined in equation (1.10), we get the same expressions as in [DFK10]:

$$\gamma_{2\alpha-1} = \frac{Q_{\alpha-1,k}Q_{\alpha,k+1}}{Q_{\alpha,k}Q_{\alpha-1,k+1}}, \quad \gamma_{2\alpha} = \frac{Q_{\alpha-1,k}Q_{\alpha+1,k+1}}{Q_{\alpha,k}Q_{\alpha,k+1}},$$

where we assume that $Q_{0,k} := 1$ and $Q_{r+1,k} := 1$ for all $k \in \mathbb{Z}$.

Theorem 4.19. *Let M be a perfect matching of G. Then $[M]-[M_0]$ is a nonintersecting collection of Γ_i's. Furthermore, every nonintersecting collection of Γ_i's is $[M] - [M_0]$ for a unique perfect matching M of G.*

Proof. Consider all possible local pictures at a white vertex v of G. Since M (resp. M_0) is a perfect matching of G, there is exactly one edge in M (resp. M_0) which touches the vertex v. If the two edges (one from M and one from M_0) are the same, no loop passes through v. If they are different, we have the following possibilities:

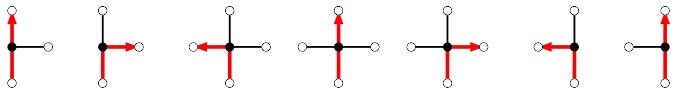

Similarly, we have the following possibilities for a white vertex.

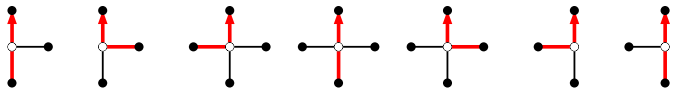

From all the possibilities at black and white vertices, $[M] - [M_0]$ consists of nonintersecting loops Γ_i's.

On the other hand, let E be the edge set of a nonintersecting collection of Γ_i's. Notice from the pictures in Definition 4.18 that if there is a loop passes through a vertex v, one of the two incident edges belongs to M_0. Then

$$M = (E \setminus M_0) \cup (M_0 \setminus E)$$

is the unique perfect matching such that $[M] - [M_0] = \prod_{i \in I} \Gamma_i$. □

Definition 4.20 ([DFK10, Section 3.3])**.** Let G_r be the following graph with $2r+1$ vertices indexed by the index set $[1, 2r+1]$.

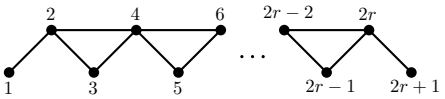

It is easy to see that Γ_i intersects Γ_j if and only if the vertices i and j are connected in G_r. So for any subset $I \subseteq [1, 2r+1]$, the loops in $\{\Gamma_i \mid i \in I\}$ are pairwise disjoint if and only if I is a subset of pairwise nonadjacent vertices of G_r, a.k.a. a *hard particle configuration* on G_r. Hence, nonintersecting collections of Γ_i's are parametrized by subsets of pairwise nonadjacent vertices of G_r. Also, nonintersecting collections of Γ_i's of size n are in bijection with n-subsets of pairwise nonadjacent vertices of G_r.

By Theorem 4.19, the possible homology classes of $[M] - [M_0]$ are $(0, k)$ for $k \in [0, r+1]$. Let

$$H_k := H_{(0,k),G,M_0}.$$

It is easy to see that $H_0 = H_{r+1} = 1$. By an interpretation of $[M] - [M_0]$ as a hard particle configuration on G_r, we get the following theorem and conclude that the Hamiltonians coincide with the conserved quantities computed in [DFK10].

Theorem 4.21. *Let $k \in [1, r]$. Then*

$$H_k(A_1, \ldots, A_{2r}) = \sum_{|I|=k} \prod_{i \in I} \gamma_i$$

where the sum runs over all k-subsets I of pairwise nonadjacent vertices of G_r.

4.4.3 Poisson-commutation

Let C be the Cartan matrix of type A_r. The signed adjacency matrix of the quiver of A_r Q-system is

$$B = \begin{bmatrix} C - C^T & C^T \\ -C & 0 \end{bmatrix} = \begin{bmatrix} 0 & C \\ -C & 0 \end{bmatrix}.$$

Recall that the phase space $\mathcal{X}$ has coordinates $(A_1, \ldots, A_{2r})$. We then define a Poisson bracket on the algebra $\mathcal{O}(\mathcal{X})$ of functions on $\mathcal{X}$ by

$$\{A_i, A_j\} = \Omega_{ij} A_i A_j \quad (i, j \in [1, 2r])$$

where the coefficient matrix Ω is defined by

$$\Omega = (B^T)^{-1} = -B^{-1} = \begin{bmatrix} 0 & -C \\ C & 0 \end{bmatrix}^{-1} = \begin{bmatrix} 0 & C^{-1} \\ -C^{-1} & 0 \end{bmatrix}.$$

Using this Poisson bracket, the bracket $\{\gamma_i, \gamma_j\}$ is in a nice form.

Proposition 4.22. *Let $i \sim j$ denote vertices i and j are connected in G_r. Then*

$$\{\gamma_i, \gamma_j\} = \epsilon(\Gamma_i, \Gamma_j) \gamma_i \gamma_j$$

where

$$\epsilon(\Gamma_i, \Gamma_j) = \begin{cases} 1, & \text{if } i < j \text{ and } i \sim j, \\ -1, & \text{if } i > j \text{ and } i \sim j. \\ 0, & \text{otherwise.} \end{cases}$$

In order to prove Proposition 4.22, we introduce an intersection pairing on a twisted ribbon graph from G. We refer to [GK13] for more details. The pairing is defined for oriented loops on G. It is skew-symmetric and can be described combinatorially as follows.

Definition 4.23. For a pair of oriented loops W and W' on G, the *intersection pairing* $\epsilon(W, W')$ is the sum of all the following contributions over the shared vertices of W and W'.

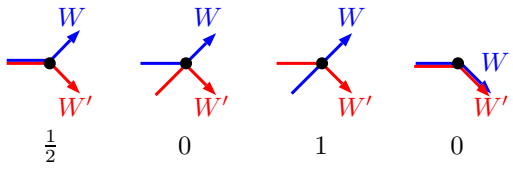

The sign of the contribution is switched (between plus and minus) each time the vertex coloring is switched or the orientation of a path is reversed.

Proposition 4.24. *For any loops W and W' on G with weight w and w', respectively. We have*

$$\{w, w'\} = \epsilon(W, W')ww'. \tag{4.4}$$

Proof. For $j \in [1, 2r]$ we let Y_j be the counterclockwise loop around the face j of G. Since $Y_1, \ldots, Y_{2r}$ together with the oriented loop Γ_1 (Definition 4.18) generate all the oriented loops on G, we only need to show (4.4) on such generators. It is easy to see that

$$\epsilon(Y_i, Y_j) = B_{ij}, \quad \epsilon(\Gamma_1, Y_j) = \delta_{j,1} - \delta_{j,r+1}.$$

Let y_j be the weight of Y_j. We need to show that

$$\{y_i, y_j\} = B_{ij} y_i y_j, \quad \{\gamma_1, y_j\} = (\delta_{j,1} - \delta_{j,r+1})\gamma_1 y_j.$$

This is equivalent to

$$\{\log(y_i), \log(y_j)\} = B_{ij}, \tag{4.5}$$

$$\{\log(\gamma_1), \log(y_j)\} = \delta_{j,1} - \delta_{j,r+1}. \tag{4.6}$$

From the graph G we have

$$y_j = \prod_{i=1}^{2r} A_i^{B_{ij}}, \quad \gamma_1 = \frac{A_{r+1}}{A_1}.$$

We also note that $\{\log(A_i), \log(A_j)\} = \Omega_{ij}$ and $\Omega = -B^{-1}$. To show (4.5), we consider

$$\begin{aligned}
\{\log(y_i), \log(y_j)\} &= \Big\{ \sum_k B_{ki} \log(A_k), \sum_\ell B_{\ell j} \log(A_\ell) \Big\} \\
&= \sum_{k,\ell} B_{ki} B_{\ell j} \{\log(A_k), \log(A_\ell)\} \\
&= \sum_{k,\ell} B_{ki} B_{\ell j} \Omega_{k\ell} = \sum_{k,\ell} (-B_{ik})(-(B^{-1})_{k\ell})(B_{\ell j}) \\
&= (BB^{-1}B)_{ij} = B_{ij}.
\end{aligned}$$

To show (4.6), we consider

$$\begin{aligned}
\{\log(\gamma_1), \log(y_j)\} &= \big\{ \log(A_{r+1}) - \log(A_1), \sum_i B_{ij} \log(A_i) \big\} \\
&= \sum_i \Big(\{\log(A_{r+1}), \log(A_i)\} - \{\log(A_1), \log(A_i)\} \Big) B_{ij} \\
&= \sum_i (\Omega_{r+1,i} - \Omega_{1,i}) B_{ij} = (\Omega B)_{r+1,j} - (\Omega B)_{1,j} \\
&= -I_{r+1,j} + I_{1,j} = -\delta_{r+1,j} + \delta_{1,j}.
\end{aligned}$$

This proved (4.5) and (4.6). Hence we proved the proposition. □

Proof of Proposition 4.22. It is easy to see that

$$\epsilon(\Gamma_i, \Gamma_j) = \begin{cases} 1, & \text{if } i < j \text{ and } i \sim j, \\ -1, & \text{if } i > j \text{ and } i \sim j. \\ 0, & \text{otherwise.} \end{cases}$$

From Proposition 4.24, we have $\{\gamma_i, \gamma_j\} = \epsilon(\Gamma_i, \Gamma_j)\gamma_i\gamma_j$. This finished the proof. □

Recall that a Hamiltonian can be written as

$$H_k = \sum_{|I|=k} \prod_{i \in I} \gamma_i$$

where the sum runs over all n-subsets $I \subseteq [1, 2r+1]$ of pairwise nonadjacent vertices of G_r. The following lemma gives an involution which will be use to cancel out terms in a computation of $\{H_i, H_j\}$.

Lemma 4.25. *Let $i_1 < j_1 < i_2 < j_2 < \cdots < i_k < j_k < i_{k+1}$ be a connected sequence of vertices of G_r of odd length. Then*

$$\{\gamma_{i_1}\gamma_{i_2}\ldots\gamma_{i_{k+1}}, \gamma_{j_1}\gamma_{j_2}\ldots\gamma_{j_k}\} = 0.$$

Proof. We consider

$$\{\log(\gamma_{i_1}\ldots\gamma_{i_{k+1}}), \log(\gamma_{j_1}\ldots\gamma_{j_k})\} = \sum_{a=1}^{k+1}\sum_{b=1}^{k}\{\log\gamma_{i_a}, \log\gamma_{j_b}\} = \sum_{a=1}^{k+1}\sum_{b=1}^{k}\epsilon(\Gamma_{i_a}, \Gamma_{j_b}).$$

From Proposition 4.22, we have

$$\sum_{a=1}^{k+1}\sum_{b=1}^{k}\epsilon(\Gamma_{i_a}, \Gamma_{j_b}) = \sum_{a=1}^{k}\epsilon(\Gamma_{i_a}, \Gamma_{j_a}) + \sum_{b=1}^{k}\epsilon(\Gamma_{i_{b+1}}, \Gamma_{j_b}) = k - k = 0.$$

The $2k$ contributions on the right hand side of the first equality can be view graphically as the following.

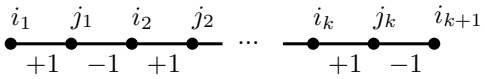

Hence $\{\gamma_{i_1}\gamma_{i_2}\dots\gamma_{i_{k+1}}, \gamma_{j_1}\gamma_{j_2}\dots\gamma_{j_k}\} = 0$. □

Theorem 4.26. *The Hamiltonians Poisson-commute.*

Proof. This proof is adapted from the proof of [GK13, Theorem 3.7]. Let $m, n \in [1, r]$. We would like to show that $\{H_m, H_n\} = 0$.

Consider an involution $\iota : (I, J) \mapsto (I', J')$ on the set of pairs of index subsets (I, J) where $I, J \subseteq [1, 2r+1]$ are subsets of pairwise nonadjacent vertices of G_r, $|I| = m$ and $|J| = n$. For a pair (I, J), we define (I', J') by the following steps.

First, we think of I and J as subsets of $V(G_r)$, and then plot all the elements of I and J on the graph G_r. For each even length maximal chain of vertices, we have an alternating sequence between elements of I and elements of J. Then I' (resp. J') is obtained from I (resp. J) by swapping all the elements in every even-length maximal chain. As a result, $|I'| = |I|$ and $|J'| = |J|$. So, both I and I' (resp. J and J') contribute terms to H_m (resp. H_n). It is also clear that ι is an involution.

From Lemma 4.25, the vertices in odd-length maximal chains contribute nothing to the bracket $\{\prod_{i\in I}\gamma_i, \prod_{j\in J}\gamma_j\}$. So

$$\{\log(\prod_{i\in I}\gamma_i), \log(\prod_{j\in J}\gamma_j)\} = \sum_C \{\log(\prod_{i\in C\cap I}\gamma_i), \log(\prod_{j\in C\cap J}\gamma_j)\}$$

where the sum runs over all even-length maximal chain $C \subseteq I \cup J$. By the construction, $C \cap I' = C \cap J$ and $C \cap J' = C \cap I$. Hence,

$$\{\prod_{i\in I}\gamma_i, \prod_{j\in J}\gamma_j\} = -\{\prod_{i\in I'}\gamma_i, \prod_{j\in J'}\gamma_j\}.$$

A fixed point of ι is a pair (I, J) where all maximal chains are odd. We have that

$$\{\prod_{i\in I}\gamma_i, \prod_{j\in J}\gamma_j\} = 0.$$

Hence, $\{H_m, H_n\} = 0$. □

Example 4.27. Let $r = 1$, $I = \{1, 4\}$ and $J = \{-1, 2, 5\}$. The following picture show three maximal chains of $I \cup J$: $\{-1\}$, $\{1, 2\}$ and $\{4, 5\}$.

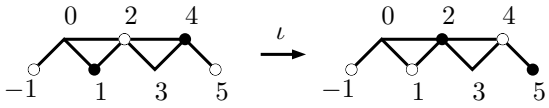

So $I' = \{2, 5\}$ and $J' = \{-1, 1, 4\}$. The black (resp. white) dots are elements of I and I' (resp. J and J').

4.4.4 Another proof of Theorem 4.26

The proof is based on the proof of [GK13, Theorem 3.7]. We denote by $\overline{G}$ the following bipartite torus graph. It differs from G by two extra edges.

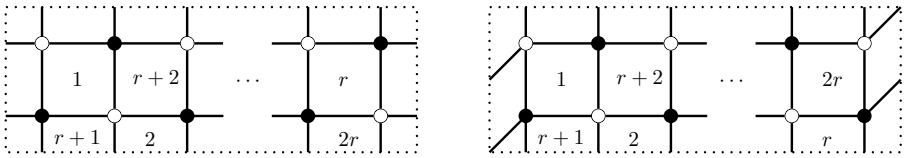

Using notations in Section 4.6.1, it can be obtained from an integral convex polygon with edge vectors:

- $e_1 = (1, \frac{r+1}{2})$, $e_2 = (-1, \frac{r+1}{2})$, $e_3 = (-1, -\frac{r+1}{2})$, $e_4 = (1, -\frac{r+1}{2})$ when r is odd
- $e_1 = (1, \frac{r+2}{2})$, $e_2 = (-1, \frac{r}{2})$, $e_3 = (-1, -\frac{r+2}{2})$, $e_4 = (1, -\frac{r}{2})$ when r is even.

The integral convex polygon can be depicted as the following.

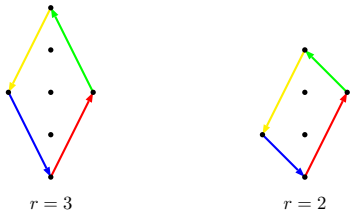

The following pictures are $\overline{G}$ with oriented loops.

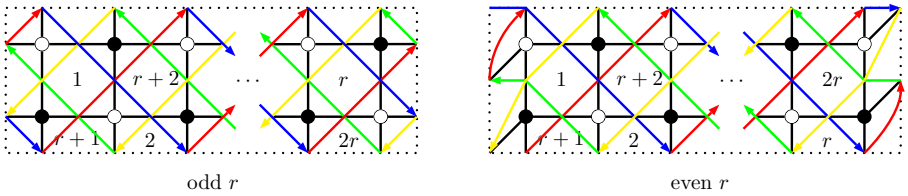

We define a reference perfect matching from a sequence e_1, e_2, e_3, e_4 according to the construction in 4.6.3. It coincides with the perfect matching M_0 defined at the beginning of Section 4.4. We denote by M_0 this perfect matching of $\overline{G}$.

Let $\overline{G}$ be a bipartite torus graph obtained from an integral polygon with edge vectors $\{e_i\}_{i=1}^n$ in Section 4.6.3. Let v be a vertex in a loop Γ. Let $\varphi_{M_0} : E(\overline{G}) \to \{0, 1\}$ defined by $\varphi_{M_0}(e) = 1$ if and only if $e \in M_0$. Define $b_v(\Gamma, M_0)$ by

$$b_v(\Gamma, M_0) := \sum_{e \in R_v} \varphi_{M_0}(e) - \sum_{e \in L_v} \varphi_{M_0}(e) \in \mathbb{Z}$$

where R_v (resp. L_v) be the set of all edges incident to v which are on the right (resp. left) of the loop Γ (not including edges in Γ).

The following lemma says that for any homologically nontrivial loop Γ on $\overline{G}$, the number of edges in M_0 incident to Γ on the left is equal to the number of edges in M_0 incident to Γ on the right.

Lemma 4.28 ([GK13, Lemma 3.9])**.** *Let M_0 be the reference perfect matching obtained from edge vectors. (See Section 4.6.3.) For any simple topologically nontrivial loop Γ on $\overline{G}$,*

$$\sum_{v \in \Gamma} b_v(\Gamma, \varphi_{M_0}) = 0.$$

Let $a, b \in H_1(\mathbb{T}, \mathbb{Z})$. We will show that $\{H_{a,\overline{G},M_0}, H_{b,\overline{G},M_0}\} = 0$. We simplify the notation by letting $H_a := H_{a,\overline{G},M_0}$. Let $\mathcal{M}_a$ be the set of all perfect matchings of $\overline{G}$ whose homology class with respect to M_0 is a, i.e. $[M]_{M_0} = a \in \mathbb{Z} \times \mathbb{Z}$. Then $H_a = \sum_{M \in \mathcal{M}_a} w(M)/w(M_0)$.

Let $M_1 \in \mathcal{M}_a$ and $M_2 \in \mathcal{M}_b$. By Proposition 4.8, $[M_1] - [M_2]$ is a collection of non-intersecting simple loops. There are two types of simple loops: homologically trivial loops and homologically nontrivial loops. Define an involution $\iota : \mathcal{M}_a \times \mathcal{M}_b \to \mathcal{M}_a \times \mathcal{M}_b$ by $(M_1, M_2) \mapsto (M_1', M_2')$ where M_1', M_2' are obtained from M_1, M_2 by exchanging all edges in each homologically trivial loop of $[M_1] - [M_2]$. See the following example.

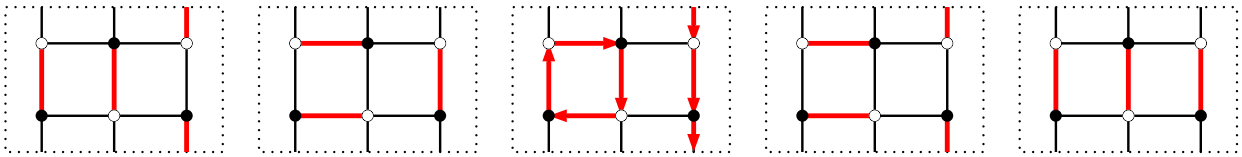

The involution ι define an equivalence relation on $\mathcal{M}_a \times \mathcal{M}_b$ by $(M_1, M_2) \sim (M_1', M_2')$ if $\iota((M_1, M_2)) = (M_1', M_2')$. So each equivalence class has either one or two elements. Each fixed point of ι is in its own singleton class.

Consider

$$\{H_a, H_b\} = \sum_{(M_1,M_2)\in\mathcal{M}_a\times\mathcal{M}_b} \left\{\frac{w(M_1)}{w(M_0)}, \frac{w(M_2)}{w(M_0)}\right\}$$

The sum is then divided into two sums:

- The first summation runs over all the fixed points of ι:

$$\sum_{\{(M_1,M_2)\}} \left\{\frac{w(M_1)}{w(M_0)}, \frac{w(M_2)}{w(M_0)}\right\} \tag{4.7}$$

- The second summation runs over all equivalence classes $\{(M_1, M_2), (M_1', M_2')\}$ of size 2:

$$\sum_{\{(M_1,M_2),(M_1',M_2')\}} \left\{\frac{w(M_1)}{w(M_0)}, \frac{w(M_2)}{w(M_0)}\right\} + \left\{\frac{w(M_1')}{w(M_0)}, \frac{w(M_2')}{w(M_0)}\right\} \tag{4.8}$$

To calculate the first sum (4.7), let (M_1, M_2) be a fixed point of ι. By Proposition 4.24 we have

$$\left\{\frac{w(M_1)}{w(M_0)}, \frac{w(M_2)}{w(M_0)}\right\} = \sum_v \epsilon_v\left([M_1]-[M_0], [M_2]-[M_0]\right) \frac{w(M_1)w(M_2)}{w(M_0)^2}$$

where ϵ_v is the contribution from vertex v to the intersection pairing. For each vertex v, there are edges e_0, e_1, e_2 incident to v and belong to M_0, M_1, M_2, respectively. If $e_1 = e_2$, then $\epsilon_v\left([M_1]-[M_0], [M_2]-[M_0]\right) = 0$. If $e_1 \neq e_2$, the vertex v must belong to the loop $[M_1]-[M_2]$, and vice versa. Since $[M_1]-[M_2]$ is a fixed point of ι, it has no homologically trivial loops. So every loop is homologically nontrivial.

Consider a homologically nontrivial simple loop Γ of the loop $[M_1] - [M_2]$ (a connected component of $[M_1] - [M_2]$). We have the following four configurations of e_0, e_1, e_2 depending whether e_0 is on the left/right of Γ or whether v is black/white. Note that e_1 (resp. e_2) goes from black to white (resp. white to black) in Γ.

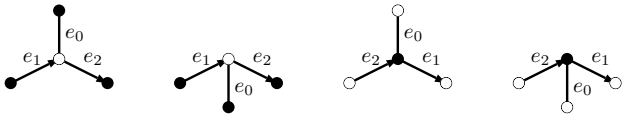

The local contribution to $\epsilon_v([M_1] - [M_0], [M_2] - [M_0])$ from each configuration is $1/2$, $-1/2$, $1/2$ and $-1/2$, respectively. We can conclude that the contribution is $1/2$ (resp. $-1/2$) when e_0 is on the left (resp. right) of Γ. By Lemma 4.28, we can conclude that

$$\epsilon_v([M_1] - [M_0], [M_2] - [M_0]) = 0.$$

Hence the first summation vanishes.

For the second sum, since $w(M_1)w(M_2) = w(M_1')w(M_2')$ the summand is equal to

$$\sum_v \left(\epsilon_v([M_1] - [M_0], [M_2] - [M_0]) + \epsilon_v\left([M_1'] - [M_0], [M_2'] - [M_0]\right)\right) \frac{w(M_1)w(M_2)}{w(M_0)^2}. \tag{4.9}$$

For each vertex v, there are edges incident to v and belong to M_1, M_2 and M_0. Similarly to the computation for the first sum, if such edges of M_1 and M_2 are the same, then the summand vanishes. If v belongs to a homologically nontrivial loop, by Lemma 4.28, the summand also vanishes. If v belongs to a homologically trivial loop, we see that $[M_1] - [M_0]$ (resp. $[M_2] - [M_0]$) is locally the same as $[M_2'] - [M_0]$ (resp. $[M_1'] - [M_0]$) at v. Hence

$$\begin{aligned}\epsilon_v\left([M_1'] - [M_0], [M_2'] - [M_0]\right) &= \epsilon_v([M_2] - [M_0], [M_1] - [M_0]) \\ &= -\epsilon_v([M_1] - [M_0], [M_2] - [M_0]).\end{aligned}$$

Hence the summand (4.9) vanishes. This concludes that the second summation vanishes.

Thus $\{H_a, H_b\} = 0$. This finishes the proof.

4.5 B_r Q-systems

We construct a "double cover" of B_r Q-system quiver and compute Hamiltonians on the weighted bipartite torus graph associated with the quiver.

4.5.1 B_r Q-systems and weighted graph mutations

Consider the following quiver of an B_r Q-system. See Theorem 1.22 for the detail.

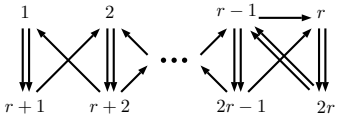

In the case of A_r Q-system, we added a frozen vertex to the quiver so that it has an associated bipartite torus graph. Unlike the previous case, the quiver of B_r Q-system does not have an associated bipartite torus graph. We resolve this issue by considering instead a double-cover of the quiver together with a frozen vertex as in the following picture. Let $\mathcal{Q}$ denote the resulting quiver.

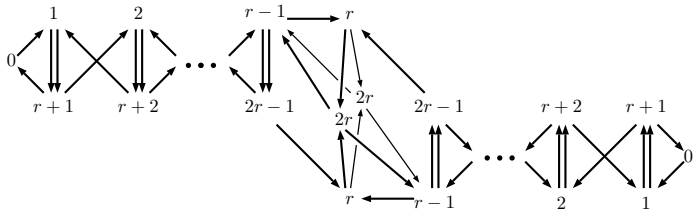

Notice that $\mathcal{Q}$ and the original quiver are locally the same. There are two copies for each vertex. So we can think of this quiver similar to a double-cover of the original quiver with an extra frozen vertex. The bipartite torus graph G associated with $\mathcal{Q}$ is depicted below.

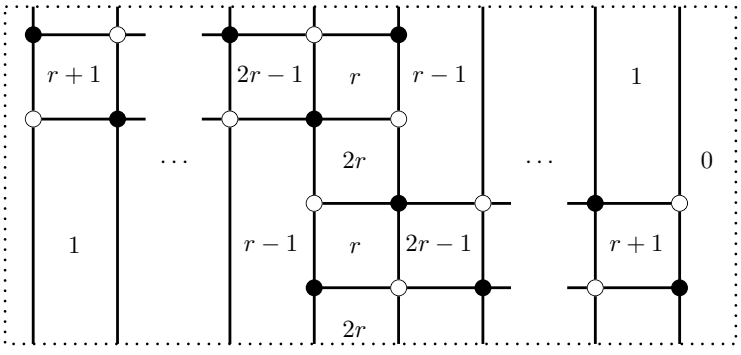

even r

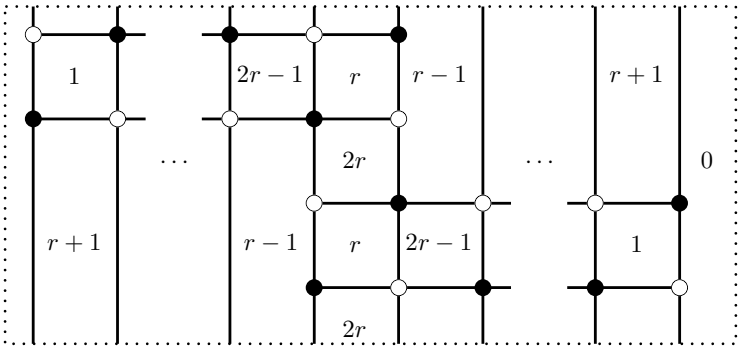

odd r

We then assign Q-system variables as weights of G according to face labels, see Theorem 1.22. We abuse the notation and use μ for a sequence of mutations where the mutation at i actually means the mutations at both faces labeled by i. Then $\sigma\mu$ sends $\mathcal{Q}$ to itself and the Q-variables are shifted by $k \to k+1$ as well. To be precise, $Q_{i,k} \mapsto Q_{i,k+1}$ for $i \in [1, r-1]$ while $Q_{r,2k} \mapsto Q_{r,2k+2}$ and $Q_{r,2k+1} \mapsto Q_{r,2k+3}$.

Let M_0 be the perfect matching of G containing all vertical edges whose top vertex is black. It can be depicted as the following when r is odd and similarly when r is even.

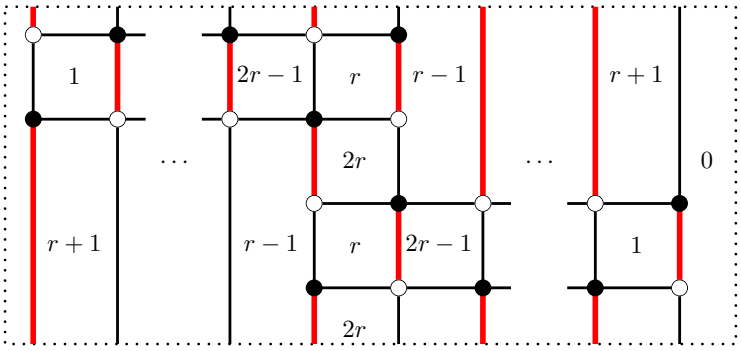

odd r

Similarly to the proof of Theorem 4.17, we can check that all the conditions in Theorem 4.4 and Theorem 4.16 hold. Hence we have

$$H_{(i,j),G,M_0}(A_{1,k}, \dots, A_{2r,k}) = H_{(i,j),G,M_0}(A_{1,k+1}, \dots, A_{2r,k+1})$$

where

$$A_{i,k} = \begin{cases} Q_{i,k}, & i \in [1, r-1], \\ Q_{r,2k}, & i = r, \\ Q_{i-r,k+1}, & i \in [r+1, 2r-1], \\ Q_{r,2k+1}, & i = 2r. \end{cases}$$

Hence the Hamiltonians $H_{(i,j),G,M_0}$ are conserved quantities of the B_r Q-system. This proved the following theorem.

Theorem 4.29. *Let $(G, (A_i))$ be a weighted bipartite torus graph defined above. Then the Hamiltonians $H_{(i,j),G,M_0}(A_1, \ldots, A_{2r})$ are conserved quantities of the B_r Q-system dynamic $Q_{\alpha,k} \mapsto Q_{\alpha,k+t_\alpha}$ where $t_\alpha = 1$ for $\alpha \in [1, r-1]$ and $t_r = 2$.*

4.5.2 Partition function of hard particles

In this section, we write the Hamiltonians as partition functions of hard particles on a weighted graph, analog to what has been done for Q-systems of type A.

From Proposition 4.8, $[M] - [M_0]$ is a product of non-intersecting simple loops of G. The following loops are all connected simple loops that can be appeared (given our choice of M_0). This will be proved in Theorem 4.30.

We first define $2r$ straight loops on G and denote them by Γ_{2a-1} for $a \in [1, 2r]$.

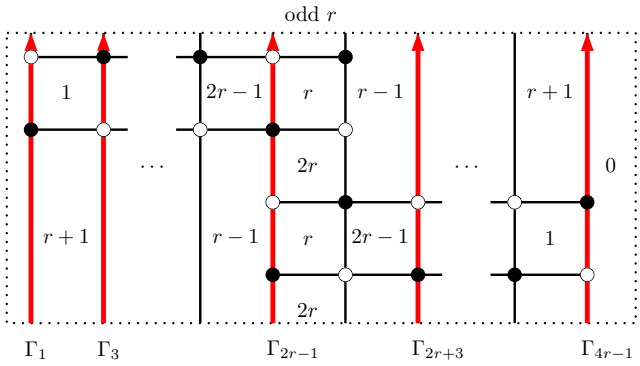

Next, we define zig-zag loops Γ_{2a} for $a \in [1, r-1] \cup [r+1, 2r-1]$ as follows.

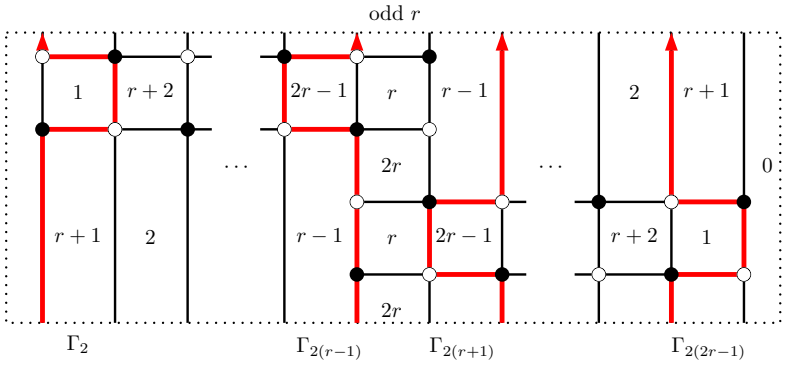

We notice that when $a \in [1, r-1]$, Γ_{2a} always goes counterclockwise around face a and clockwise around face $r+a$. When $a \in [r+1, 2r-1]$, Γ_{2a} goes counterclockwise around face $2r-a$ and clockwise around face $3r-a$.

Lastly, we define $\Gamma_{2r,j}$ for $j \in [1,6]$. They are depicted as follows.

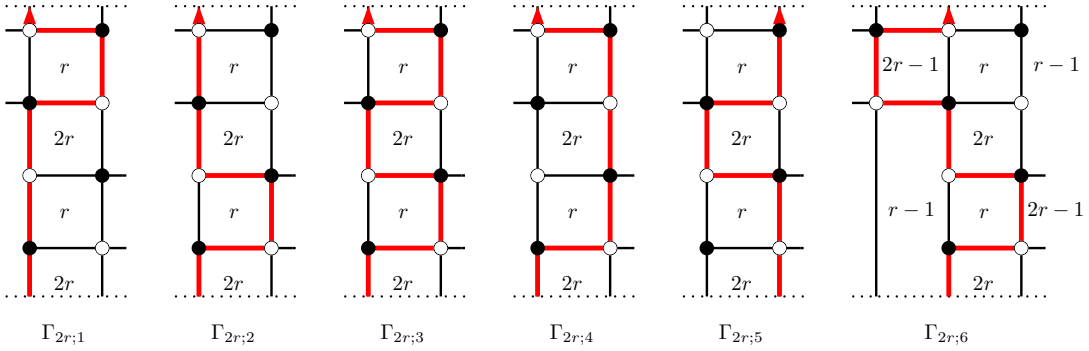

We then have the following theorem analog to Theorem 4.19.

Theorem 4.30. *Let M be a perfect matching of G. Then $[M]-[M_0]$ is a nonintersecting collection of Γ. Furthermore, every nonintersecting collection of Γ is $[M]-[M_0]$ for a unique perfect matching M of G.*

Proof. Using exactly the same proof as in Theorem 4.19, we can see that all the loops Γ listed above are all possible simple loops appeared in $[M]-[M_0]$. □

Let G_r be the following graph with $4r+4$ vertices indexed by the set $[1, 2r-1] \cup [2r+1, 4r-1] \cup \{(2r, i) \mid i \in [1,6]\}$ defined as the following

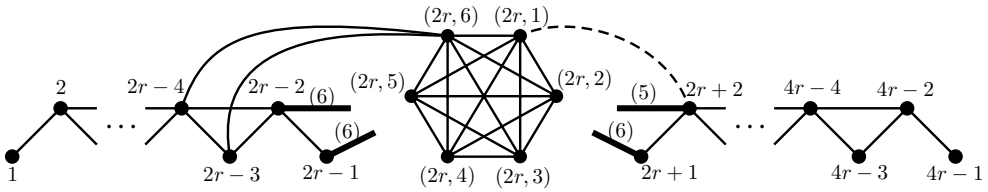

There is a complete graph K_6 as a subgraph of G_r in the middle. The label (6) on the three thick lines indicates that the vertex connects to all six vertices in K_6. There is a thick line with label (5); vertex $2r+2$ connects to all vertices in K_6 except to the vertex $(2r, 1)$. (This is indicated by a dotted line between $(2r, 1)$ and $(2r + 2)$.) The vertex $(2r, 6)$ has two extra edges connecting to vertex $2r - 4$ and $2r - 3$.

The loop Γ_i intersects Γ_j if and only if the vertices i and j are connected in G_r. For any subset $I \subseteq [1, 2r-1] \cup [2r+1, 4r-1] \cup \{(2r, i) \mid i \in [1, 6]\}$, the loops in $\{\Gamma_i \mid i \in I\}$ are pairwise disjoint if and only if I is a subset of pairwise nonadjacent vertices of G_r. Also, nonintersecting collections of Γ of size n are in bijection with n-subsets of pairwise nonadjacent vertices of G_r.

By Theorem 4.30, the possible homology classes of $[M] - [M_0]$ are $(0, k)$ for $k \in [0, 2r]$. Let γ_i be the weight of Γ_i. Theorem 4.30 implies the following theorem.

Theorem 4.31. *Let $k \in [0, 2r]$. Then*

$$H_{(0,k),G,M_0}(A_1, \ldots, A_{2r}) = \sum_{|I|=k} \prod_{i \in I} \gamma_i$$

where the sum runs over all k-subsets I of pairwise nonadjacent vertices of G_r.

Example 4.32. When $r = 2$, the graph G_2 for B_2 Q-system has 12 vertices and can be depicted as the following.

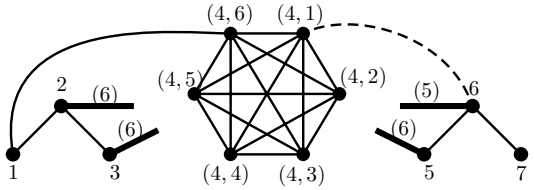

We have the following weights.

$$\gamma_1 = \frac{Q_{1,k+1}}{Q_{1,k}}, \qquad \gamma_2 = \frac{Q_{2,2k+1}^2}{Q_{1,k}Q_{1,k+1}Q_{2,2k}}, \qquad \gamma_3 = \frac{Q_{1,k}Q_{2,2k+1}^2}{Q_{1,k+1}Q_{2,2k}^2},$$
$$\gamma_{4;1} = \frac{Q_{1,k}^2}{Q_{2,2k}^2}, \qquad \gamma_{4;2} = \frac{Q_{1,k}^2}{Q_{2,2k}^2}, \qquad \gamma_{4;3} = \frac{Q_{1,k}^3 Q_{1,k+1}}{Q_{2,2k}^2 Q_{2,2k+1}^2},$$
$$\gamma_{4;4} = \frac{Q_{1,k}Q_{1,k+1}}{Q_{2,2k+1}^2}, \qquad \gamma_{4;5} = \frac{Q_{1,k}Q_{1,k+1}}{Q_{2,2k+1}^2}, \qquad \gamma_{4;6} = \frac{1}{Q_{2,2k}},$$
$$\gamma_5 = \frac{Q_{1,k+1}Q_{2,2k}^2}{Q_{1,k}Q_{2,2k+1}^2}, \qquad \gamma_6 = \frac{Q_{2,2k}}{Q_{1,k}Q_{1,k+1}}, \qquad \gamma_7 = \frac{Q_{1,k}}{Q_{1,k+1}}.$$

For $H_k := H_{(0,k),G,M_0}(A_{1,k}, \ldots, A_{2r,k})$, we have

$$\begin{aligned}
H_0 &= 1 \\
H_1 &= \frac{Q_{1,k+1}}{Q_{1,k}} + \frac{Q_{2,2k+1}^2}{Q_{1,k}Q_{1,k+1}Q_{2,2k}} + \frac{Q_{1,k}Q_{2,2k+1}^2}{Q_{1,k+1}Q_{2,2k}^2} + \frac{Q_{1,k}^2}{Q_{2,2k}^2} + \frac{Q_{1,k}^2}{Q_{2,2k}^2} + \frac{Q_{1,k}^3 Q_{1,k+1}}{Q_{2,2k}^2 Q_{2,2k+1}^2} + \\
&\quad + \frac{Q_{1,k}Q_{1,k+1}}{Q_{2,2k+1}^2} + \frac{Q_{1,k}Q_{1,k+1}}{Q_{2,2k+1}^2} + \frac{1}{Q_{2,2k}} + \frac{Q_{1,k+1}Q_{2,2k}^2}{Q_{1,k}Q_{2,2k+1}^2} + \frac{Q_{2,2k}}{Q_{1,k}Q_{1,k+1}} + \frac{Q_{1,k}}{Q_{1,k+1}}, \\
H_2 &= \frac{Q_{1,k}^4}{Q_{2,2k}^2 Q_{2,2k+1}^2} + \frac{2Q_{1,k}^3}{Q_{1,k+1}Q_{2,2k}^2} + \frac{Q_{2,2k+1}^2 Q_{1,k}^2}{Q_{1,k+1}^2 Q_{2,2k}^2} + \frac{2Q_{1,k}^2}{Q_{2,2k+1}^2} + \frac{Q_{1,k+1}^2 Q_{1,k}^2}{Q_{2,2k}^2 Q_{2,2k+1}^2} + \\
&\quad + \frac{2Q_{1,k}}{Q_{1,k+1}Q_{2,2k}} + \frac{2Q_{1,k+1}Q_{1,k}}{Q_{2,2k}^2} + \frac{Q_{2,2k+1}^2}{Q_{1,k}^2 Q_{1,k+1}^2} + \frac{2Q_{2,2k+1}^2}{Q_{1,k+1}^2 Q_{2,2k}} + \frac{Q_{2,2k+1}^2}{Q_{2,2k}^2} + \\
&\quad + \frac{2Q_{2,2k}}{Q_{1,k}^2} + \frac{2Q_{1,k+1}^2}{Q_{2,2k+1}^2} + \frac{Q_{2,2k}^2}{Q_{2,2k+1}^2} + \frac{Q_{1,k+1}^2 Q_{2,2k}^2}{Q_{1,k}^2 Q_{2,2k+1}^2} + 2, \\
H_3 &= H_1, \\
H_4 &= 1.
\end{aligned}$$

We notice that $H_0 = H_4$ and $H_1 = H_3$. In fact, we will show that $H_i = H_{2r-i}$ ($i \in [0, 2r]$) for the Hamiltonians of the B_r Q-system.

Proposition 4.33. *Let $H_k := H_{(0,k),G,M_0}(A_1, \ldots, A_{2r})$ be the Hamiltonians for the B_r Q-system. Then for $k \in [0, 2r]$,*

$$H_k = H_{2r-k}.$$

Proof. Fix $r \geq 2$. Let $\pi : [1, 2r-1] \cup \{(2r; j)\}_{j=1}^6 \cup [2r+1, 4r-1] \to [1, 2r]$ be a projection defined

by

$$\pi : \begin{cases} i \mapsto i, & i \in [1, 2r-1], \\ (2r; j) \mapsto 2r, & j \in [1, 6], \\ i \mapsto 4r - i, & i \in [2r+1, 4r-1]. \end{cases}$$

Let F_r be the following graph with $2r$ vertices.

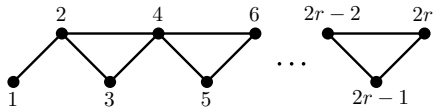

Conceptually F_r is obtained from G_r by collapsing all six vertices $(2r; 1), \ldots, (2r; 6)$ into one vertex $2r$ and folding the resulting graph by identifying vertices $i \leftrightarrow 4r - i$. The projection π sends a vertex of G_r to a vertex of F_r by the collapsing/folding procedure.

Let $\mathcal{C}$ be the set of all hard particle configurations on G_r, and let $\mathcal{C}_k$ be the set of all k hard particle configurations on G_r. We have $\mathcal{C}_k \neq \emptyset$ for $k \in [0, 2r]$. (The set $\mathcal{C}_0$ contains exactly one configuration, the empty configuration.) So

$$\mathcal{C} = \bigsqcup_{k=0}^{2r} \mathcal{C}_k.$$

We identify a hard particle configuration with a subset of $[1, 2r-1] \cup \{(2r; j)\}_{j=1}^{6} \cup [2r+1, 4r-1]$. Let $A \in \mathcal{C}$. We then associate each element $i \in A$ with a black or white dot on the vertex $\pi(i)$ F_r as follows.

- An element $i \in [1, 2r-1]$ is associated with a black dot on vertex $\pi(i)$.
- An element $i \in [2r+1, 4r-1]$ is associated with a white dot on vertex $\pi(i)$.
- An element $(2r; j)$, for $j \in [1, 5]$, is associated with a black dot together with a label j on vertex $2r$.
- The element $(2r, 6)$ is associated with a white dot together with a label 6 on vertex $2r$ and a black dot on vertex $2r - 2$.

See an example in Figure 4.2. Notice that we can recover the hard particle configuration on G_r

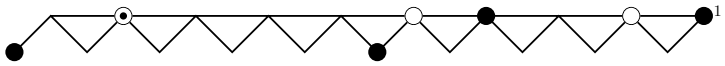

Figure 4.2: An example of dots on F_{10} associated with a configuration $\{1, 4, 11, 14, 20, 27, 33, 41\}$ in $\mathcal{C}$. The dot $\odot$ indicates two dots of different colors on the same vertex.

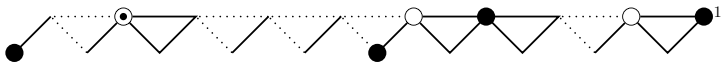

Figure 4.3: A running example from Figure. 4.2 showing F_{10} decomposed into blocks.

from a configuration of dots on F_r. It is obvious that not every dot configuration on F_r is associated with a configuration in $\mathcal{C}$.

We define an involution $\iota : \mathcal{C} \to \mathcal{C}$ by the following steps.

1. Let $A \in \mathcal{C}$. Consider the dot configuration on F_r associated with A. We have a collection of connected chains of dots. Since A is a hard particle configuration, each chain is a chain of dots of alternate colors or A pair of white and black dots on the same vertex.

   For each connected chain $i_1 < \cdots < i_k$ or a pair of black and white dots $i_1 = i_2$ $(k = 2)$, we let i be the largest odd integer such that $i \leq i_1$, j be the smallest even integer such that $i_k < j$. When $j > 2r$, we set $j = 2r$. We then delete edges $(i-1, i)$, $(i-1, i+1)$, $(j, j+1)$ and $(j, j+2)$ of F_r when possible. As a result, F_r is decomposed into disconnected blocks (isomorphic to F_n, $n \leq r$). Lastly any block of $2n$ vertices containing no dots is decomposed into n blocks of 2 vertices. See Figure 4.3 for an example.

2. For each block we define an involution on dot configurations as in Figure 4.4 and 4.5. The blocks in Figure 4.6 are fixed by the involution.

3. The hard particle configuration $\iota(A)$ is the configuration associated with the resulting dot configuration. See Figure 4.7 for an example.

For a block of $2n$ vertices the involution sends a dot configuration of size k to a configuration of size $2n - k$, where we do not count the black dot at $2r - 2$ when the white dot with label 6 on $2r$ is present. The sum of all the number of vertices of all blocks is $2r$. So the involution is a bijection between $\mathcal{C}_k$ and $\mathcal{C}_{2r-k}$.

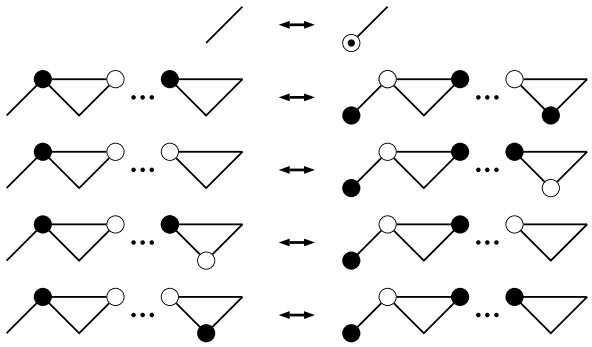

Figure 4.4: An involution on dot configurations when the vertex $2r$ is unoccupied. We have another version of each picture when all of the colors are switched.

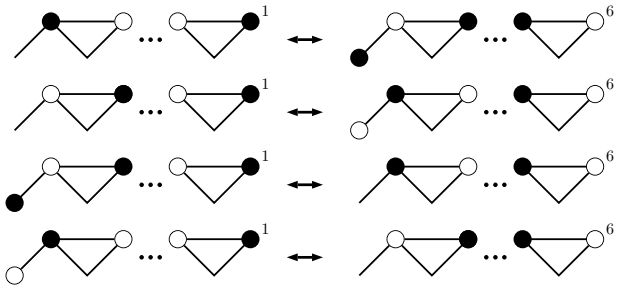

Figure 4.5: An involution on dot configurations when the vertex $2r$ is occupied.

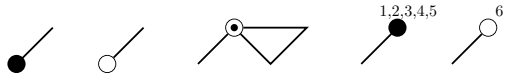

Figure 4.6: The blocks which are fixed by the involution.

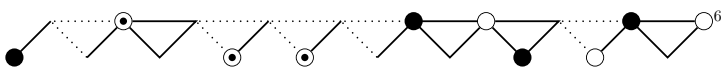

Figure 4.7: The resulting dot configuration after an involution of a configuration A in Figure 4.2. So we have $\iota(A) = \{1, 4, 7, 9, 12, 15, 25, 28, 31, 36, 38, 41\}$.

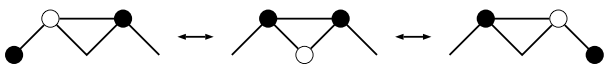

Figure 4.8: The involution on a block can be written as a sequence of moves in (4.11).

It is left to show that if $A \in \mathcal{C}_k$ and $B = \iota(A) \in \mathcal{C}_{2r-k}$ then

$$\prod_{i \in A} w(\gamma_i) = \prod_{j \in B} w(\gamma_j). \tag{4.10}$$

By a direct computation, we have

$$\gamma_{4r-(2a-1)}\gamma_{2a} = \gamma_{4r-2a}\gamma_{2a+1}, \qquad \gamma_{2a-1}\gamma_{4r-2a} = \gamma_{2a}\gamma_{4r-(2a+1)},$$
$$\gamma_{2b-1}\gamma_{4r-(2b-1)} = 1, \qquad \gamma_{(2r;1)}\gamma_{2r+2} = \gamma_{(2r+6)}\gamma_{2r+3},$$

for $a \in [1, r-1]$ and $b \in [1, r]$. These equations say that the following moves preserve the weight of the associated hard particle configuration.

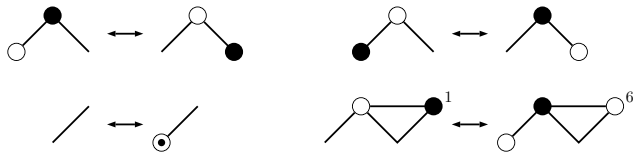

(4.11)

Since the involution on each block can be written as a sequence of the moves (4.11) (see Figure 4.8 for an example), the involution preserves the weight for each block. Hence the equation (4.10) holds. □

4.5.3 Poisson bracket

Similar to type A, we let let C be the Cartan matrix of type B_r. The signed adjacency matrix of the quiver of B_r Q-system is

$$B = \begin{bmatrix} C - C^T & C^T \\ -C & 0 \end{bmatrix}.$$

Let $\mathcal{X}$ be a phase space with coordinates $(A_1, \ldots, A_{2r})$. Define a Poisson bracket on the algebra $\mathcal{O}(\mathcal{X})$ of functions on $\mathcal{X}$ by

$$\{A_i, A_j\} = \Omega_{ij} A_i A_j \quad (i, j \in [1, 2r])$$

where the coefficient matrix Ω is defined by

$$\Omega = (B^T)^{-1} = -B^{-1}.$$

Comparing to Proposition 4.24, the Poisson bracket for B_r Q-system cannot be written as the intersection pairing. This is due to the existence of faces with the same weight, which makes the Poisson bracket not local. Nevertheless, experimental data still show that the Hamiltonians Poisson-commute.

Conjecture 4.34. *The Hamiltonians of the B_r Q-system Poisson-commute.*

4.6 Dimer integrable systems

In this section, we compare our constructions and results to [GK13]. First we summarize the result from [GK13].

4.6.1 Minimal bipartite torus graphs from convex polygons

Let N be a convex polygon in $\mathbb{R}^2$ with corners in $\mathbb{Z}^2$, called *integral polygon*, considered up to translation by vectors in $\mathbb{Z}^2$. We pick all the integral vertices on the boundary of N (i.e. every vertex in $\partial N \cap \mathbb{Z}^2$) counterclockwise, and get a sequence of vertices $v_1, v_2, \ldots, v_n$ where n is the number of integral vertices on ∂N and the indices are read modulo n. Let vectors e_i be vectors pointing from v_i to v_{i+1}. We get from the construction that each $e_i = (a_i, b_i)$ is a primitive vector, i.e. $a_i, b_i \in \mathbb{Z}$ and $\gcd(a_i, b_i) = 1$. We then get a collection $\{e_i\}$ of integral primitive vectors in $\mathbb{Z}^2$.

Consider the torus $\mathbb{T} = \mathbb{R}^2/\mathbb{Z}^2$. Each e_i determines a homology class $(a_i, b_i) \in H_1(\mathbb{T}, \mathbb{Z}) = \mathbb{Z} \times \mathbb{Z}$, and there is a unique up to translation geodesic representing this class. In other words, it is an oriented straight line on $\mathbb{T}$ with slope b_i/a_i, i.e. a projection of e_i on the torus $\mathbb{T}$. Note that the

geodesics are indeed oriented loops on $\mathbb{T}$ since their slopes are rational.

We then take a family of distinct oriented loops $\{\alpha_i\}$ on $\mathbb{T}$ such that the isotopy class of α_i matches the isotopy class of the geodesic representing e_i. By Theorem 4.37 we can choose $\{\alpha_i\}$ such that the loops are in generic position (no intersection of more than two loops) and satisfy the following conditions [GK13, Definition 2.2]:

1. (admissibility) Going along any loops α_i, the directions of the other loops intersecting it alternate (left-to-right or right-to-left).

2. (minimality) The total number of intersections is minimal.

The collection $\{\alpha_i\}$ provides a decomposition of $\mathbb{T}$ into a union of polygons whose oriented sides are parts of α_i and vertices are intersection points of the loops α_i. Then the first condition is equivalent to

(1′) (admissibility) The sides of any polygon P_i are either oriented clockwise, counterclockwise or alternate.

The family of oriented loops $\{\alpha_i\}$ gives rise to an oriented graph on the torus $\mathbb{T}$. We call an oriented graph on $\mathbb{T}$ satisfying the above conditions *minimal admissible graph on a torus*.

Example 4.35. Starting from an integral polygon on the left, we obtained four primitive vectors depicted in the middle picture.

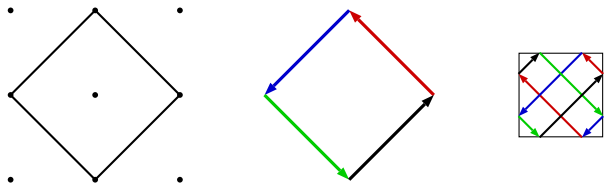

The vectors are then associated with oriented loops on a torus, which gives a minimal admissible graph shown in the picture on the right.

Given an admissible minimal torus graph, we construct a bipartite graph G on $\mathbb{T}$ by constructing vertices from the polygons P_i where the coloring is determined as follows:

- Polygons P_i with counterclockwise orientation are associated with black vertices.

- Polygons P_i with clockwise orientation are associated with white vertices.

From the construction, every intersection is a vertex shared by exactly two well-oriented polygons having opposite orientations. We then associate each shared vertex with an edge connecting the two vertices of G associated to the two polygons.

We see that G is indeed a bipartite graph, and we will call it a *minimal bipartite torus graph*. For the rest of the section, unless stated otherwise we assume that G is a minimal bipartite torus graph obtained from an integral polygon N.

Example 4.36. In our running example, there are eight polygons and eight intersection points.

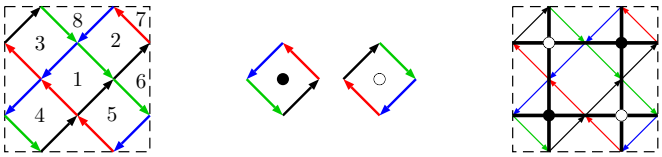

In the picture, the polygons labeled by $2, 3$ (resp. $4, 5$) are oriented counterclockwise (resp. clockwise), so they are associated with black (resp. white) vertices of G. The polygons labeled by $1, 6, 7, 8$ have alternate orientation. The eight intersection points are associated with eight edges of G.

From the bipartite graph G, we can uniquely (up to translation) recover the starting integral polygon by reversing the process. The convexity condition on the integral polygon will guarantee the uniqueness of the polygon. We also note that a 180-degree rotation of N corresponds to reversion of the orientation of all loops in the admissible minimal graph. This will switch the color of the vertices of G.

For an arbitrary integral polygon N, a minimal admissible graph on a torus associated with N and a minimal bipartite torus graph associated with N always exist. Furthermore, we can obtain one minimal bipartite torus graph from another by use of the two elementary moves (definitions 4.1 and 4.2), as stated in the following theorem.

Theorem 4.37 ([GK13, Theorem 2.5])**.** *For any integral polygon N there exists a minimal admissible graph on a torus associated with N. It produces a minimal bipartite torus graph G associated with N. Furthermore, any two minimal bipartite graphs on a torus associated with N are related by a sequence of urban renewals and shrinking of 2-valent vertices.*

Remark 4.38. Our bipartite torus graphs for the Q-systems of type A and B in sections 4.4 and 4.5 are not obtained from non-degenerate convex polygons.

For A_r Q-system, we reverse the process and construct oriented loops on the torus as in the following picture.

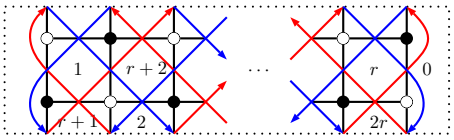

We get only two oriented loops depicted in blue and red whose homology classes are $(0, -r-1)$ and $(0, r+1)$, respectively. Notice that they are not primitive, and they form a vertical degenerate bigon with sides of length $r+1$.

For B_r Q-system, we have the following picture.

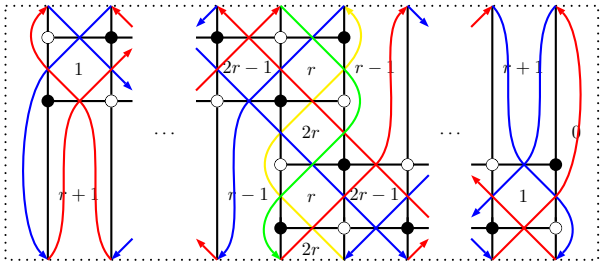

There are four oriented loops depicted in blue, green, yellow and red whose homology classes are $(0, -2r+1), (0, -1), (0, 1)$ and $(0, 2r-1)$, respectively. The blue and red loops are not primitive when $r > 1$. The loops form a vertical degenerate quadrilateral.

4.6.2 Phase space and Poisson structure

For a minimal bipartite torus graph G with n faces, let $\mathcal{L}_G$ be the moduli space of line bundles with connections on G. We have $\mathcal{L}_G \cong \mathrm{Hom}(H_1(G, \mathbb{Z}), \mathbb{C}^*)$, so combinatorially $\mathcal{L}_G$ is the set of all weight assignments to all the loops on G compatible with loop multiplication. (The weight of a product of loops coincides with the product of their weights.)

For $j \in [1, n]$, let y_j be the weight assigned to the counterclockwise loop Y_j around the face j of G. Since G is a graph embedded on a torus, there is a projection $H_1(G, \mathbb{Z}) \to H_1(\mathbb{T}, \mathbb{Z})$. We then pick two loops Z_1, Z_2 having homology classes $(1, 0), (0, 1) \in H_1(\mathbb{T}, \mathbb{Z})$ under the projection, and assign weight z_1, z_2 to them, respectively. Any loop on G can then be generated by y_j's together

with z_1 and z_2, where a product of the variables corresponds to a product of loops. Since the product of all the face loops is trivial, we must have $\prod_{j=1}^{n} w_j = 1$. This is the only condition among the generators. So $\dim \mathcal{L}_G = n+1$ and the algebra $\mathcal{O}(\mathcal{L}_G)$ of functions on $\mathcal{L}_G$ has $(y_1, \ldots, y_{n-1}, z_1, z_2)$ as coordinates.

Note that this weight is different from our weight in Definition 4.10. The connection between the two is discussed in Remark 4.39.

For any loops Γ_1, Γ_2 on G, the Poisson bracket of their weights is defined in terms of the intersection pairing of the twisted ribbon graph associated with G as in Definition 4.23.

Now we define a Y-seed $(B, (y_1, \ldots, y_n, z_1, z_2))$ of rank $n+2$ associated with $\mathcal{L}_G$, where the exchange matrix $B = (B_{ij})$ and

$$B_{ij} = \epsilon(Y_i, Y_j) \quad \text{for } i, j \in [1, n+2]$$

with $Y_{n+1} := Z_1$ and $Y_{n+2} := Z_2$.

Let G and G' be two minimal bipartite torus graphs associated with the same integral polygon N. By Theorem 4.37, they are related by a sequence of elementary moves. These moves induce an isomorphism $i_{G,G'} : \mathcal{L}_G \to \mathcal{L}_{G'}$ according to Y-seed mutations. Let $\mathcal{X}_N$ be the *phase space* defined by gluing the spaces $\mathcal{L}_G$ by the isomorphisms. The phase space depends only on N and each isomorphism $i_{G,G'}$ can be viewed as a change of coordinate.

Remark 4.39. Let G be a minimal bipartite torus graph with n faces. Each choice of face weight $(A_i) \in (\mathbb{C}^*)^n$ induces a weight assignment on oriented edges of G by Definition 4.10. This then induces a weight assignment on $Y_1, \ldots, Y_n, Z_1, Z_2$, hence a loop weight in $\mathcal{L}_G$. Since $\mathcal{L}_G$ has dimension $n+1$, not all loop weights of [GK13] can be obtained from our weight in Definition 4.10.

In addition, the weight y_j around face j of G is the j^{th} $\tau-$coordinates (Definition 1.20) of a cluster seed $(\mathbf{A}, B)$, i.e.

$$y_j = \prod_{i=1}^{n} A_i^{B_{ij}}$$

where $B = B_G$ is the signed adjacency matrix of the quiver associated to G (see Section 4.2.1).

Example 4.40. Let G be the following graph on the left. It is obtained from a integral polygon whose counterclockwise edge vectors e_i are $(1,1)$, $(-1,1)$, $(-1,-1)$ and $(1,-1)$. Let Y_i be the

counterclockwise loop around the face i, and Z_1 (resp. Z_2) be the loop in the middle (resp. right) picture.

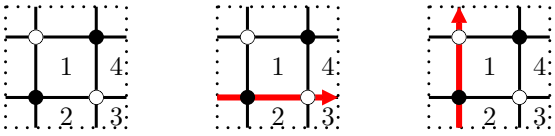

Let $(A_1, A_2, A_3, A_4) \in (\mathbb{C}^*)^4$ be an arbitrary face weight on G. It induces the following weights

$$y_1 = \frac{A_4^2}{A_2^2}, \quad y_2 = \frac{A_1^2}{A_3^2}, \quad y_3 = \frac{A_2^2}{A_4^2}, \quad y_4 = \frac{A_3^2}{A_1^2}, \quad z_1 = \frac{A_3 A_4}{A_1 A_2}, \quad z_2 = \frac{A_2 A_3}{A_1 A_4}.$$

They satisfy the following conditions

$$y_1 y_3 = 1, \quad y_2 y_4 = 1, \quad z_1^2 = y_1/y_2, \quad z_2^2 = 1/(y_1 y_2).$$

Since y_1 and y_2 are algebraically independent, the induced loop weight is a subspace of dimension 2 inside $\mathcal{L}_G$ of dimension 5. (L_G is of dimension 5 because every loop weight in $\mathcal{L}_G$ satisfies $y_1 y_2 y_3 y_4 = 1$.) The map from face weight to loop weight is not injective. We have the following 2-dimensional symmetries

$$(A_1, A_2, A_3, A_4) \mapsto (\lambda A_1, \mu A_2, \lambda A_3, \mu A_4)$$

for $\lambda, \mu \in \mathbb{C}^*$.

4.6.3 Casimirs and Hamiltonians

A *zig-zag path* on G is an oriented path on G which turns maximally left at white vertics and turns maximally right at black vertices [Ken02, Pos06]. They will always close up to form loops. Notice that the projection of the zig-zag loops on the torus are in the same isotopy classes with the oriented loops α_i obtained from the primitive edges e_i of N (See Section 4.6.1). So the oriented zig-zag loops are in bijection with $\{\alpha_i\}$.

The weight of these zig-zag loops, called *Casimirs*, generate the center of the Poisson algebra $\mathcal{O}(\mathcal{L}_G)$ as described in the following proposition.

Proposition 4.41 ([GK13, Lemma 1.1])**.** *We consider the oriented zig-zag loops on a bipartite*

oriented surface graph G. Then as Z runs over zig-zag loops, the functions w_Z generate the center of the Poisson algebra $\mathcal{O}(\mathcal{L}_G)$ of functions on $\mathcal{L}_G$. The product of all of them is 1. This is the only relation between them.

Recall the construction of G from a minimal admissible graph (an arrangement of $\{\alpha_i\}_{i=1}^n$) in Section 4.6.1. We see that each edge e of G has exactly two loops $\alpha_i, \alpha_j \in \{\alpha_1, \dots, \alpha_n\}$ crossing it. Let α_i and α_j be as the following.

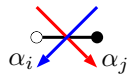

Then we define a *reference perfect matching* M_0 to be the matching containing all edges e such that $i > j$. It is shown in [GK13, Theorem 3.3] that M_0 is indeed a perfect matching of G.

We note that M_0 is not unique. Since the indices of α_i can be read modulo n, another cyclic ordering gives another reference perfect matching. There are also many other choices of M_0 including "fractional matchings", see [GK13, Section 3.2-3.4] for details.

Remark 4.42. We can show from [GK13, Lemma 3.4] that every quadrilateral face in G has exactly one side in M_0. So every reference perfect matching M_0 constructed above always satisfies the requirement in Theorem 4.16.

Given a reference perfect matching M_0, the *weight* $w_{M_0}(M)$ of a perfect matching M with respect to M_0 is defined to be the weight of the loop $[M]-[M_0]$, written in terms of $y_1, \dots, y_n, z_1, z_2$.

Recall the definition of $[M]_{M_0}$, the homology class of M with respect to M_0, in Definition 4.9. The polygon with vertices at all homology classes $[M]_{M_0} \in H_1(\mathbb{T}, \mathbb{Z}) = \mathbb{Z} \times \mathbb{Z}$ coincides with the convex polygon N up to translation [GK13, Theorem 3.12]. Given a homology class $a \in H_1(\mathbb{T}, \mathbb{Z})$, we let

$$H_{M_0;a} := \sum_M w_{M_0}(M)$$

where the sum runs over all perfect matchings M of G having homology class a. The *(modified) partition function* of perfect matchings of G is defined to be

$$P_{M_0} := \sum_a \operatorname{sgn}(a) H_{M_0;a}$$

where the sum runs over all possible homology classes of perfect matchings with respect to M_0. The sign $\mathrm{sgn}(a) \in \{-1, 1\}$ can be determined from a "Kasteleyn matix", and they show up in the formula from the use of the determinant of a "Kasterleyn operator", see [GK13, Section 3.2] for more details.

For $a \in H_1(\mathbb{T}, \mathbb{Z}) \cap \mathrm{int}(N)$, a homology class which is an interior point of N, the function $H_{M_0;a}$ is called a *Hamiltonian*. We note that a different choice of M_0 gives a different partition function and a different set of Hamiltonians. However, they differ from each other by a common factor which lies in $\mathcal{O}(\mathcal{L}_G)$.

These Hamiltonians are independent and commute under the Poisson bracket.

Theorem 4.43 ([GK13, Theorem 3.7])**.** *Let G be a minimal bipartite torus graph. Then*

1. *The Hamiltonians $H_{M_0;a}$ commute under the Poisson bracket on $\mathcal{L}_G$.*
2. *The Hamiltonians are independent and their number is the half of the dimension of the generic symplectic leaf.*

We also have that the partition function is invariant under the change of coordinates $i_{G,G'}$ (defined in Section 4.6.2). This implies that all Hamiltonians are also invariant under the change of coordinates. In fact, the map $i_{G,G'}$ is a unique rational transformation of face weights preserving the partition function, given a graph mutation from G to G'.

Theorem 4.44 ([GK13, Theorem 4.7])**.** *Given an urban renewal, there is a unique rational transformation of the weights preserving the partition function P_a. This transformation is a Y-seed mutation.*

By counting the number of Hamiltonians and Casimirs, we can conclude on the integrability of the system.

Theorem 4.45 ([GK13, Theorem 1.2])**.** *Let M_0 be a reference perfect matching obtained from a circular-order-preserving map. The Hamiltonian flows of $H_{M_0,a}$ commute, providing an integrable system on $\mathcal{X}_N$. Precisely, we get integrable systems on the generic symplectic leaves of $\mathcal{X}_N$, given by the level sets of the Casimirs.*

Remark 4.46. We notice that the integrable system described in this section is a classical dynamical system where the evolutions are Hamiltonian flows. This system also contains a discrete dynamical system whose evolution is a change of coordinate $i_{G,G'}$ (Y-seed mutation on loop weights).

For a graph G periodic (up to a relabeling of vertices) under a sequence of urban renewals and shrinking of 2-valent vertices, we take the change of loop weight under such sequence to be the dynamic of a discrete system. Since the graph is periodic, the dynamic is a Poisson map with respect to the Poisson bracket in Section 4.6.2. The Casimirs and Hamiltonians return to the same form under such sequence. Since they are also invariant by Theorem 4.44, they are conserved quantities of the system. By Theorem 4.45, the quantities form a maximal set of Poisson-commuting invariants, hence the system is discrete Liouville integrable.

4.7 Conclusion and discussion

In this chapter, we studied a discrete dynamic on a weighted bipartite torus graph. The weight is defined differently from [GK13]. The evolution is a mutation sending one weighted graph to another weighted graph. The mutation is an urban renewal and shrinking of 2-valent vertices on the graph, and is a cluster transformation on the weight. The graph can be any bipartite graph on a torus, not necessarily obtained from an integral polygon. The Hamiltonians are defined and proved to be invariant under the mutation.

For a Q-system of type A, we constructed a weighted bipartite torus graph which is periodic under a sequence of mutations up to a face relabeling. The weight changes according to the Q-system relation. So the Hamiltonians are conserved quantities of the system. We also showed that the Hamiltonians can be written as hard-particle partition functions on a certain graph, which coincides with the result in [DFK10]. A nondegenerate Poisson bracket is defined, and the Hamiltonians Poisson commute.

For a Q-system of type B, a bipartite torus graph is constructed. Each face has another face with the same weight. The graph is periodic, up to a face relabeling, under a sequence of mutations. The weight are transformed according to the Q-system relation. The Hamiltonians are conserved quantities of the system. They can also be interpreted as hard-particle partition functions on a certain graph.

For types C, D and other exceptional types, the sequence of mutations in [DFK09, Theorem 3.1] contains a mutation at a vertex of degree greater than 4. Recall that an urban renewal corresponds to a mutation at a vertex of degree 4 which has exactly two incoming and two outgoing arrows. Although some mutations in type A and B happen at a vertex of degree less than 4, we fixed this issue by adding a frozen vertex. However this technique is not applicable when the degree of a mutating vertex is greater than 4.

Chapter 5

Conclusion and discussion

We have seen a connection between two important discrete integrable systems: A_∞ T-systems and (higher) pentagram maps in Chapter 2. One important feature the two systems have in common is that they both can be realized as mutations in cluster algebras. The (higher) pentagram maps are Y-patterns, while the T-systems are cluster patterns. A solution of an A_∞ T-system with certain quasi-periodic boundary conditions gives rise to a solution of a (higher) pentagram map, via Y-systems. This map of solutions is basically the map τ for the $\tau-$coordinates.

It is necessary to introduce coefficients to the T-systems in order to obtain all the solutions of the (higher) pentagram maps. One important choice of coefficients is the principal coefficients, in the sense that every other choices of coefficients can be written in terms of the principal coefficients. We studied this in Chapter 3 and have shown that solutions to the T-systems with principals coefficients can be written in terms of combinatorial objects such as perfect matchings, nonintersecting paths and networks.

One important reduction of the T-systems are Q-systems. They are obtained from T-systems by forgetting the $j-$parameter. We have explicitly computed conserved quantities for Q-systems of type A and B, in terms of partition functions of perfect matchings on graphs in Chapter 4. A question which is still left open is to investigate whether the Q-systems of other types are integrable, and to find machineries to compute conserved quantities of such systems.

It will be the topic for further research to see how far the machinery in Chapter 4 can be applied to compute conserved quantities of other systems. The examples of such systems include recurrence relations from mutation-periodic quivers [FM11], quivers from quiver gauge theories [FHH01, MR04], $\ell-$restricted T-systems [KNS11], T-systems with quasi-periodic boundary conditions [KV15] which include cluster dynamics on higher pentagram map quivers [GSTV12, GSTV16], and cluster dynamics related to Y-meshes [GP15].

Furthermore, the discrete systems we are interested are the systems whose dynamics are mutations in cluster algebras. There are two common features in all of the known examples of discrete integrable systems in this family. First, the evolution is basically a sequence of mutations at nodes having exactly two incoming and two outgoing arrows. Second, their quivers can be embedded on a surface (especially on a torus) and has a dual bipartite surface graph. In this case, the evolution can be realized as a sequence of urban renewals on the graph, and we can apply our machinery to compute conserved quantities of the systems. So we expect that all discrete systems having the two features are integrable.

Everything we have studied so far lies on the assumption that all variables are commutative. The quantum cluster algebras are introduced in [BZ05]. So it is a big question whether the whole story of discrete integrable systems obtained from cluster algebras can be upgraded to a quantum version in the same spirit as [BZ05, FG09, DF11, DFK11, DFK12, GK13]. In particular, we expect combinatorial solutions of the quantum T-systems with principal coefficients, similar to what was done in the commutative case. Also, the canonical Poisson bracket [GSV03] has a canonical quantization. There are examples when the Poisson-commuting conserved quantities of a commutative system can be upgraded to commuting conserved quantities of the associated quantum system [GK13]. We expect that the quantities obtained from our machinery also have this property. This will give a rough criterion for identifying integrability of quantum systems.

References

[BBT03] Olivier Babelon, Denis Bernard, and Michel Talon. *Introduction to classical integrable systems*. Cambridge Monographs on Mathematical Physics. Cambridge University Press, Cambridge, 2003.

[BZ05] Arkady Berenstein and Andrei Zelevinsky. Quantum cluster algebras. *Adv. Math.*, 195(2):405–455, 2005.

[Ciu98] Mihai Ciucu. A complementation theorem for perfect matchings of graphs having a cellular completion. *J. Combin. Theory Ser. A*, 81(1):34–68, 1998.

[Ciu03] Mihai Ciucu. Perfect matchings and perfect powers. *J. Algebraic Combin.*, 17(3):335–375, 2003.

[DF10] Philippe Di Francesco. The solution of the A_r T-system for arbitrary boundary. *Electron. J. Combin.*, 17(1):Research Paper 89, 43, 2010.

[DF11] Philippe Di Francesco. Quantum A_r Q-system solutions as q-multinomial series. *Electron. J. Combin.*, 18(1):Paper 176, 17, 2011.

[DF13] Philippe Di Francesco. An inhomogeneous lambda-determinant. *Electron. J. Combin.*, 20(3):Paper 19, 34, 2013.

[DF14] Philippe Di Francesco. T-systems, networks and dimers. *Comm. Math. Phys.*, 331(3):1237–1270, 2014.

[DF15] Philippe Di Francesco. Bessenrodt-stanley polynomials and the octahedron recurrence. *Electronic Journal of Combinatorics*, 22(3), 2015. cited By 0.

[DFK09] Philippe Di Francesco and Rinat Kedem. Q-systems as cluster algebras. II. Cartan matrix of finite type and the polynomial property. *Lett. Math. Phys.*, 89(3):183–216, 2009.

[DFK10] Philippe Di Francesco and Rinat Kedem. Q-systems, heaps, paths and cluster positivity. *Comm. Math. Phys.*, 293(3):727–802, 2010.

[DFK11] Philippe Di Francesco and Rinat Kedem. Non-commutative integrability, paths and quasi-determinants. *Adv. Math.*, 228(1):97–152, 2011.

[DFK12] Philippe Di Francesco and Rinat Kedem. The solution of the quantum A_1 T-system for arbitrary boundary. *Comm. Math. Phys.*, 313(2):329–350, 2012.

[DFK13] Philippe Di Francesco and Rinat Kedem. T-systems with boundaries from network solutions. *Electron. J. Combin.*, 20(1):Paper 3, 62, 2013.

[DFSG14] Philippe Di Francesco and Rodrigo Soto-Garrido. Arctic curves of the octahedron equation. *J. Phys. A*, 47(28):285204, 34, 2014.

[EFS12] Richard Eager, Sebastián Franco, and Kevin Schaeffer. Dimer models and integrable systems. *J. High Energy Phys.*, (6):106, front matter+24, 2012.

[EKLP92] Noam Elkies, Greg Kuperberg, Michael Larsen, and James Propp. Alternating-sign matrices and domino tilings. II. *J. Algebraic Combin.*, 1(3):219–234, 1992.

[FG06] V. V. Fock and A. B. Goncharov. Cluster x-varieties, amalgamation, and poisson-lie groups. In *Algebraic geometry and number theory*, volume 253 of *Progr. Math.*, pages 27–68. Birkhauser Boston, Boston, MA, 2006.

[FG09] Vladimir V. Fock and Alexander B. Goncharov. Cluster ensembles, quantization and the dilogarithm. *Ann. Sci. Éc. Norm. Supér. (4)*, 42(6):865–930, 2009.

[FH11] Allan P. Fordy and Andrew Hone. Symplectic maps from cluster algebras. *SIGMA Symmetry Integrability Geom. Methods Appl.*, 7:Paper 091, 12, 2011.

[FH14] Allan P. Fordy and Andrew Hone. Discrete integrable systems and Poisson algebras from cluster maps. *Comm. Math. Phys.*, 325(2):527–584, 2014.

[FHH01] Bo Feng, Amihay Hanany, and Yang-Hui He. D-brane gauge theories from toric singularities and toric duality. *Nuclear Phys. B*, 595(1-2):165–200, 2001.

[FM11] Allan P. Fordy and Robert J. Marsh. Cluster mutation-periodic quivers and associated Laurent sequences. *J. Algebraic Combin.*, 34(1):19–66, 2011.

[FM16] Vladimir V. Fock and Andrey Marshakov. *Loop Groups, Clusters, Dimers and Integrable Systems*, pages 1–65. Springer International Publishing, Cham, 2016.

[For11] Allan P. Fordy. Mutation-periodic quivers, integrable maps and associated Poisson algebras. *Philos. Trans. R. Soc. Lond. Ser. A Math. Phys. Eng. Sci.*, 369(1939):1264–1279, 2011.

[For14] Allan P. Fordy. Periodic cluster mutations and related integrable maps. *J. Phys. A*, 47(47):474003, 44, 2014.

[FR99] Edward Frenkel and Nicolai Reshetikhin. The q-characters of representations of quantum affine algebras and deformations of $\mathcal{W}$-algebras. In *Recent developments in quantum affine algebras and related topics (Raleigh, NC, 1998)*, volume 248 of *Contemp. Math.*, pages 163–205. Amer. Math. Soc., Providence, RI, 1999.

[FZ02] Sergey Fomin and Andrei Zelevinsky. Cluster algebras. I. Foundations. *J. Amer. Math. Soc.*, 15(2):497–529 (electronic), 2002.

[FZ07] Sergey Fomin and Andrei Zelevinsky. Cluster algebras. IV. Coefficients. *Compos. Math.*, 143(1):112–164, 2007.

[GK13] Alexander B. Goncharov and Richard Kenyon. Dimers and cluster integrable systems. *Ann. Sci. Éc. Norm. Supér. (4)*, 46(5):747–813, 2013.

[Gli11] Max Glick. The pentagram map and Y-patterns. *Adv. Math.*, 227(2):1019–1045, 2011.

[GP15] M. Glick and P. Pylyavskyy. Y-meshes and generalized pentagram maps. *ArXiv e-prints*, March 2015.

[GSTV12] Michael Gekhtman, Michael Shapiro, Serge Tabachnikov, and Alek Vainshtein. Higher pentagram maps, weighted directed networks, and cluster dynamics. *Electron. Res. Announc. Math. Sci.*, 19:1–17, 2012.

[GSTV16] Michael Gekhtman, Michael Shapiro, Serge Tabachnikov, and Alek Vainshtein. Integrable cluster dynamics of directed networks and pentagram maps. *Adv. Math.*, 300:390–450, 2016.

[GSV03] Michael Gekhtman, Michael Shapiro, and Alek Vainshtein. Cluster algebras and Poisson geometry. *Mosc. Math. J.*, 3(3):899–934, 1199, 2003. {Dedicated to Vladimir Igorevich Arnold on the occasion of his 65th birthday}.

[GSV11] Michael Gekhtman, Michael Shapiro, and Alek Vainshtein. Generalized Bäcklund-Darboux transformations for Coxeter-Toda flows from a cluster algebra perspective. *Acta Math.*, 206(2):245–310, 2011.

[GV85] Ira Gessel and Gérard Viennot. Binomial determinants, paths, and hook length formulae. *Adv. in Math.*, 58(3):300–321, 1985.

[Her10] David Hernandez. Kirillov-Reshetikhin conjecture: the general case. *Int. Math. Res. Not. IMRN*, (1):149–193, 2010.

[HI14] Andrew N. W. Hone and Rei Inoue. Discrete Painlevé equations from Y-systems. *J. Phys. A*, 47(47):474007, 26, 2014.

[HKO$^+$99] G. Hatayama, A. Kuniba, M. Okado, T. Takagi, and Y. Yamada. Remarks on fermionic formula. In *Recent developments in quantum affine algebras and related topics (Raleigh, NC, 1998)*, volume 248 of *Contemp. Math.*, pages 243–291. Amer. Math. Soc., Providence, RI, 1999.

[HKO$^+$02] Goro Hatayama, Atsuo Kuniba, Masato Okado, Taichiro Takagi, and Zengo Tsuboi. Paths, crystals and fermionic formulae. In *MathPhys odyssey, 2001*, volume 23 of *Prog. Math. Phys.*, pages 205–272. Birkhäuser Boston, Boston, MA, 2002.

[IIK$^+$13] Rei Inoue, Osamu Iyama, Bernhard Keller, Atsuo Kuniba, and Tomoki Nakanishi. Periodicities of T-systems and Y-systems, dilogarithm identities, and cluster algebras I: type B_r. *Publ. Res. Inst. Math. Sci.*, 49(1):1–42, 2013.

[JMZ13] In-Jee Jeong, Gregg Musiker, and Sicong Zhang. Gale-Robinson sequences and brane tilings. In *25th International Conference on Formal Power Series and Algebraic Combinatorics (FPSAC 2013)*, Discrete Math. Theor. Comput. Sci. Proc., AS, pages 707–718. Assoc. Discrete Math. Theor. Comput. Sci., Nancy, 2013.

[Kas63] P. W. Kasteleyn. Dimer statistics and phase transitions. *J. Mathematical Phys.*, 4:287–293, 1963.

[Ked08] Rinat Kedem. Q-systems as cluster algebras. *J. Phys. A*, 41(19):194011, 14, 2008.

[Kel13] Bernhard Keller. The periodicity conjecture for pairs of Dynkin diagrams. *Ann. of Math. (2)*, 177(1):111–170, 2013.

[Ken02] R. Kenyon. The Laplacian and Dirac operators on critical planar graphs. *Invent. Math.*, 150(2):409–439, 2002.

[KNS94] Atsuo Kuniba, Tomoki Nakanishi, and Junji Suzuki. Functional relations in solvable lattice models. I. Functional relations and representation theory. *Internat. J. Modern Phys. A*, 9(30):5215–5266, 1994.

[KNS11] Atsuo Kuniba, Tomoki Nakanishi, and Junji Suzuki. T-systems and Y-systems in integrable systems. *J. Phys. A*, 44(10):103001, 146, 2011.

[KR87] A. N. Kirillov and N. Yu. Reshetikhin. Representations of Yangians and multiplicities of the inclusion of the irreducible components of the tensor product of representations of simple Lie algebras. *Zap. Nauchn. Sem. Leningrad. Otdel. Mat. Inst. Steklov. (LOMI)*, 160(Anal. Teor. Chisel i Teor. Funktsiĭ. 8):211–221, 301, 1987.

[KS12] Boris Khesin and Fedor Soloviev. The pentagram map in higher dimensions and KdV flows. *Electron. Res. Announc. Math. Sci.*, 19:86–96, 2012.

[KS13] Boris Khesin and Fedor Soloviev. Integrability of higher pentagram maps. *Mathematische Annalen*, pages 1–43, 2013.

[KV15] Rinat Kedem and Panupong Vichitkunakorn. T-systems and the pentagram map. *J. Geom. Phys.*, 87:233–247, 2015.

[Lin73] Bernt Lindström. On the vector representations of induced matroids. *Bull. London Math. Soc.*, 5:85–90, 1973.

[Mae87] Shigeru Maeda. Completely integrable symplectic mapping. *Proc. Japan Acad. Ser. A Math. Sci.*, 63(6):198–200, 1987.

[MB13] Gloria Marí Beffa. On generalizations of the pentagram map: discretizations of AGD flows. *J. Nonlinear Sci.*, 23(2):303–334, 2013.

[MB15] Gloria Marí Beffa. On integrable generalizations of the pentagram map. *Int. Math. Res. Not. IMRN*, (12):3669–3693, 2015.

[MP07] Gregg Musiker and James Propp. Combinatorial interpretations for rank-two cluster algebras of affine type. *Electron. J. Combin.*, 14(1):Research Paper 15, 23, 2007.

[MR04] Subir Mukhopadhyay and Koushik Ray. Seiberg duality as derived equivalence for some quiver gauge theories. *J. High Energy Phys.*, (2):070, 22, 2004.

[MS10] Gregg Musiker and Ralf Schiffler. Cluster expansion formulas and perfect matchings. *J. Algebraic Combin.*, 32(2):187–209, 2010.

[Nak03] Hiraku Nakajima. t-analogs of q-characters of Kirillov-Reshetikhin modules of quantum affine algebras. *Represent. Theory*, 7:259–274, 2003.

[OST10] Valentin Ovsienko, Richard Schwartz, and Serge Tabachnikov. The pentagram map: a discrete integrable system. *Comm. Math. Phys.*, 299(2):409–446, 2010.

[OST13] Valentin Ovsienko, Richard Evan Schwartz, and Serge Tabachnikov. Liouville-Arnold integrability of the pentagram map on closed polygons. *Duke Math. J.*, 162(12):2149–2196, 2013.

[Pos06] A. Postnikov. Total positivity, Grassmannians, and networks. *ArXiv Mathematics e-prints*, September 2006.

[RR86] David P. Robbins and Howard Rumsey, Jr. Determinants and alternating sign matrices. *Adv. in Math.*, 62(2):169–184, 1986.

[Sch92] Richard Schwartz. The pentagram map. *Experiment. Math.*, 1(1):71–81, 1992.

[Sch01] Richard Evan Schwartz. The pentagram map is recurrent. *Experiment. Math.*, 10(4):519–528, 2001.

[Sch08] Richard Evan Schwartz. Discrete monodromy, pentagrams, and the method of condensation. *J. Fixed Point Theory Appl.*, 3(2):379–409, 2008.

[Sol13] Fedor Soloviev. Integrability of the pentagram map. *Duke Math. J.*, 162(15):2815–2853, 2013.

[Spe07] David E. Speyer. Perfect matchings and the octahedron recurrence. *J. Algebraic Combin.*, 25(3):309–348, 2007.

[Ves91] A P Veselov. Integrable maps. *Russian Mathematical Surveys*, 46(5):1, 1991.

[Vic16] Panupong Vichitkunakorn. Solutions to the T-systems with principal coefficients. *Electron. J. Combin.*, 23(2):Paper 2.44, 56, 2016.

[Wil15] Harold Williams. Q-systems, factorization dynamics, and the twist automorphism. *Int. Math. Res. Not. IMRN*, (22):12042–12069, 2015.

[Zam91] Al. B. Zamolodchikov. On the thermodynamic Bethe ansatz equations for reflectionless ADE scattering theories. *Phys. Lett. B*, 253(3-4):391–394, 1991.